1127-7

ГЕОХИМИЯ

A Translation of GEOCHEMISTRY

No. 1 1958

CONTENTS

	Page English	Page Russian
Starik, I. E., Yu. V. Kuznetsov, S. M. Grashchenko, and *M. S. Frenklikh.* The ionium method of determination of age of marine sediments	1	3
Savchenko. V. P. The formation of free hydrogen in the earth's crust, as determined by the reducing action of the products of radioactive transformations of isotopes.	16	14
Sidorenko, G. A. X-ray investigations of natural oxides of uranium.	26	22
Marakushev, A. A. Parageneses in boron-bearing magnesium skarns of Taezhnoe deposit in the Archean of the Aldan plate	51	39
Aleksandrov, I. V., and *A. V. Zmeenkova.* Evolution of rocks during progressive metamorphism, as exemplified by the Middle Suite of Krivoi Rog Series	62	47
Bakhmutov, L. A. Distribution of cobalt, nickel, and copper in hydrothermally altered rocks of the Pyshma-Klyuchevskoe deposit	83	60
Yakhontova, L. K. Experimental studies in oxidation of cobalt and nickel arsenides in solutions containing oxygen and carbonic acid	95	70
Studenikova, Z. V., and *V. A. Zolotareva.* Rhenium in molybdenites of the Tyrny-Auz deposit	109	81
Kosterin, A. V., V. N. Zuev, and *I. D. Shevaleevskii.* Zr/Hf ratio in zircons in some igneous rocks of northern Kirgizia.	116	86
Znamenskii, E. B. A contribution to geochemistry of titanium in intrusive process of granitic series	120	90

Chronicle

International Conference on Interplanetary Substance. *E. L. Krinov*	129	96

Published by

The Geochemical Society

GEOCHEMISTRY

A translation of the journal of the Academy of Sciences, U.S.S.R., devoted to geochemistry

A publication of the Geochemical Society, supported financially by a grant from the National Science Foundation.

Officers of the Society:

FARRINGTON DANIELS, *President*
University of Wisconsin
Madison 6, Wisconsin

JOHN F. SCHAIRER, *Vice-President*
Geophysical Laboratory
Washington 8, D. C.

KONRAD B. KRAUSKOPF, *Secretary*
Department of Geology
Stanford University, California

GEORGE T. FAUST, *Treasurer*
U.S. Geological Survey
Washington 25, D. C.

EARL INGERSON, *Past President*
U.S. Geological Survey
Washington 25, D. C.

Councilors

WILLARD F. LIBBY, *1956-1958*
U.S. Atomic Energy Commission
Washington 25, D. C.

HATTEN S. YODER, JR., *1956-1958*
Geophysical Laboratory
Washington 8, D. C.

JOHN A. S. ADAMS, *1957-1959*
The Rice Institute
Houston 1, Texas

ALFRED O. NIER, *1957-1959*
University of Minnesota
Minneapolis 14, Minnesota

E. F. OSBORN, *1958-1960*
Pennsylvania State University
University Park, Pennsylvania

H. G. THODE, *1958-1960*
McMaster University
Hamilton, Ontario

Translation Editor . . . . . . Earl Ingerson
Managing Editor. . . . . . E. Wm. Heinrich

Editorial Assistant: Margaret N. Everett
Board of Associate Editors: Leason H. Adams, F. R. Boyd, Paul E. Damon, Michael Fleischer, Jack Green, E. P. Henderson, T. S. Lovering, A. O. Nier, Jack Vallentyne, O. E. White, Samuel Zerfoss

Subscription Prices

Per year (eight issues) $20.0

To members of the Geochemical Society and to educational institutions $10.0

Subscriptions should be addressed to th Geochemical Society and sent to

Prof. E. Wm. Heinrich
Mineralogical Laboratory
University of Michigan
Ann Arbor, Michigan

TRANSLITERATION

There is no ideal system of translit-erating Russian; each has its advantage and disadvantages. For the translation o *Geokhimiya* we have chosen the syste used by *Chemical Abstracts*, partly be cause of its wide acceptance by othe journals and partly because of certai advantages in alphabetization of names The principal differences between thi system and others in common use are a follows:

Russian	Chem. Abs.	Other
Х	kh	h
Ц	ts	tz
Щ	shch	sch
Ю	yu	iu
Я	ya	ia

THE IONIUM METHOD OF DETERMINATION OF MARINE SEDIMENTS

I. E. Starik, Yu. V. Kuznetsov, S. M. Grashchenko, and M. S. Frenklikh

V. G. Khlopin Radium Institute
Academy of Sciences, SSSR, Leningrad

Abstract

Results of an investigation of the vertical distribution of uranium, radium, ionium and thorium as well as iron, manganese and calcium in 7 cores of marine sediments raised from the bottom of the Indian and the Pacific oceans are given in the article.

The results obtained allow the following conclusions to be drawn:

1. In deep sea sediments radium and ionium are in all experimental points in radio active equilibrium.
2. Ionium and thorium occur in marine sediments in various forms.
3. The thorium and uranium content in all studied sediments does not change by the length of the core, remaining constant in the ranges of the error of measurement.
4. Three types of marine sediments may be distinguished according to the character of distribution of the ionium and radium to them: Littoral sediments, sediments of an intermediate type and typical deep sea sediments.
5. A connection between the vertical distribution of ionium and radium on the one hand and the vertical distribution of calcium on the other hand has been detected in a number of cores.

Pettersson's hypothesis explaining the deficiencies of thorium and radium in sea water by the precipitation of thorium isotopes [1] was employed by Urry and Piggot [2] in the geochronology of deep marine sediments, as studied by the ionium method. According to this method, after secular equilibrium of ionium and radium is established, the changes in the concentration of radium with depth in the sedimentary section serve as indicators of the variations in the concentration of ionium. If the variations in ionium concentration are caused by radioactive decay alone, then the radium-ionium concentrations are a function of the time of deposition of the sediments and the rate of decay of ionium down to the horizon where uranium, ionium and radium are found in radioactive equilibrium. The depth of the sediments in centimeters is an expression of the geologic time-age of the sediments.

Further investigations [3, 4, 5, 6] have shown, however, that the orderly exponential character of the curve representing the distribution of radium in the section of deep-sea sediments in depth is distorted by some secondary maxima which require an explanation.

Materials collected by the Swedish deep-sea expedition in 1947-1948, aboard the Albatross, made it possible to extend the studies of the distribution of radium in the cores of deep-sea marine sediments. On the basis of the radium analysis of 13 cores from the central and the western parts of the Pacific, it was shown by Kroll [3] that the distribution of radium in the sediments is a far more involved problem than one would think it to be, were one to proceed only from the findings of Urey and Piggot. Among the causes responsible for the distortions in the smooth radium curve in the deep-sea cores, the following ones are indicated by Kroll [3]:

1. Changes in the concentrations of ionium in the sediments, in time, because of:
    - a) Differences in the adsorbing capacity of sediments
    - b) Variations in the chemical environments in the sea water responsible for the precipitation of ionium
2. Changes in the rates of sedimentation
3. Diffusion and adsorption of radium in sediments

It is understood that more definite conclusions regarding geochemistry of radium in the ocean may be drawn only from a large number of determinations of uranium, radium, and thorium isotopes both in sea water and in the sediments.

However, there are very few such comprehensive studies on record and even the analytical data on uranium, ionium, and radium in coastal sediments are nearly absent from the literature. Radiochemical studies of coastal sediments are continuing, meanwhile, to be a subject of extraordinary interest, inasmuch as they are concerned with one of the stages in the geochemical cycle of uranium, ionium, and radium prior to their entry into the ocean.

It appeared to be desirable to us therefore to investigate the distribution of uranium, ionium, and radium in coastal sediments to augment such studies in deep sea sediments.

METHODS

Radium and uranium in marine sediments were determined by the procedures described in the literature. Uranium was determined by the luminescent method, first proposed by Karlik and Herrnberger [7]; radium was determined by the vacuum-emanation method [8].

The method for ionium in marine sediments may be accepted as an exact and a reliable procedure, provided it is able to meet the following requirements:

1. In the chemical isolation of thorium isotopes, these isotopes are entirely liberated from non-isotopic α-emitters.
2. Thorium isotopes are isolated without the carrier or with the least amounts of the carrier, in order that, after the deposition of the total bulk of the active sediment onto the target, there would be no self-absorption of alpha-rays.
3. There must be an exact record of the percentage of the α-activity derived from thorium and radio-thorium, so as to afford quantitative estimation of the ionium content of the samples.

The relatively simple and easy method of V. I. Baranov and L. A. Kuzmina [11] fails to meet any one of the foregoing requirements. For this reason, we made no use of their method in our studies.

The low percentage of the recovery of thorium isotopes by the method of Isaak and Picciotto [9] does not permit us to measure the isolated α-activity with a sufficient degree of precision using the apparatus of the DA type. Consequently, this method was not used in our investigations.

Ionium in marine sediments was determined by following the procedure of I. E. Starik, A. S. Starik, and G. S. Lozhkina [10], with certain adaptations to the marine sediments.

It is evident that the measured α-activity depends on four isotopes of thorium: Th^{232}, Th^{230}(Io), Th^{228}(RaTh), and Th^{227} (RaAc).

As shown by Isaac and Picciotto [9], the percentage of α-activity derived from Th^{227} (radioactinium) is extremely small and is disregarded in our estimations, while the percentage of α-activity from Th^{232} and Th^{228} (radiothorium) may prove to be substantial and must be determined with the greatest precision attainable.

Radiothorium is determined by ThX which is separated, together with radium, on the precipitate of barium sulfate in the radium analysis. In order to attain the maximum of accuracy in the measurements of radiothorium, the determination of RaTh by ThX was conducted simultaneously with determination of radium in a 20 gram aliquot of the silt. The error of measurement, in dealing with such quantities of ThX, did not exceed 15%.

Thorium was determined colorimetrically, by the method described by Thomasson, Perry, and Buerly [13]. The measurement error was again not over 15%.

After the determinations of RaTh and Th, the total α-activity was corrected for α-activity due to these constituents and the result obtained was taken for all practical purposes as the α-activity due solely to ionium.

$Th^{234}(UX_1)$, serving as the indicator of thorium isotopes, was prepared from a solution of uranyl nitrate where it was accumulating in the course of one month, after a careful purification of the uranyl nitrate. The purification of uranium from thorium isotopes was performed by the following three methods, in sequence:

1. Extraction of uranium by ether from 1N nitric acid saturated with ammonium nitrate.
2. Separation of thorium isotopes from uranium on iron hydroxide by the soda process.
3. Quantitative adsorption of thorium isotopes on Schott filters, from strongly alkaline media, in the presence of hydrogen peroxide; uranium, as per-uranate, remains in solution, by this procedure.

UX_1, isolated from the solution of uranyl nitrate, after one month's period of its accumulation, was checked by the α-counter and was found to be not higher than the background in its activity.

PROCEDURE

Prior to the determinations of ionium in marine sediments blank tests were performed so as to check the reagents and the chemical glassware for contamination by thorium isotopes. These checks showed that the extent of contamination of the reagents and the glassware does not exceed the background of the α-measurements. The samples were dried in an oven at 105°C to constant weight before their aliquots were taken for the analysis.

5 grams of silt ignited at 800°C were placed in a platinum cup; the UX_1 indicator was added and the sample was treated by a mixture of sulfuric and hydrofluoric acids. The resulting sulfates were washed off with 5% nitric acid into a beaker, dissolved by heating, and the solution was treated by CO_2-free ammonium hydroxide; the precipitated sesquioxides were filtered off and washed with hot water. The precipitate on the filter was dissolved in 5% nitric acid, the solution was evaporated to a small volume, and its acidity was made 0.1N by dilution with water. 50 mg of calcium chloride were added to the hot solution (in the case of samples low in calcium) and the solution was double-diluted with saturated oxalic acid. The precipitated calcium oxalate was filtered off, washed with 1% oxalic acid, ignited to calcium carbonate in a muffle, and dissolved in 20 to 30 ml of 5% nitric acid. The solution was double-diluted with ammonia, with the addition of a few drops of 3% hydrogen peroxide; the small precipitate of the hydroxides was filtered on two Schott filters, joined in series, washed with dilute ammonia, and dissolved in 5% nitric acid. Thorium isotopes were twice co-precipitated with 10 mg of calcium oxalate from a small volume of the solution. After the final separation of ionium from calcium, by passing the solution through a Schott filter, the active residue on the filter was dissolved in 1N nitric acid and the solution was electrolyzed in a platinum cup, which served as the anode, in order to separate polonium from the active residue. The cathode was a platinum plate with the area of 7.2 cm^2. The current was 100 m.a.; the voltage 2.1 v; duration of the electrolysis, 10 hours.

A quantitative separation of polonium on the platinum cathode, unde the conditions of the electrolysis, was attested by control experiments The solution in the platinum cup was evaporated to dryness and the remaining ammonium salts were expelled by heating. The active residu was dissolved in nitric acid and transferred into a cell where its volume was reduced to 0.5 ml by evaporation. The active residue was transferred then onto the target and, after an evaporation under a lamp, the α-measurements of thorium isotopes were made in the DA type apparatus.

After the α-measurements, the active residue was dissolved in nitric acid (1:1) and the percentage of the yield was determined by the β-counter. Yields of the UX_1 indicator varied within the range of 80 to 95%. The background for the α-counter did not exceed two impulse per minute. The accuracy of the ionium measurements was within 8 to 15% for our samples, by the methods here described.

RESULTS AND DISCUSSION

The radiochemical measurements were made by us on a series of cores of marine sediments placed at our disposal by the Institute of Oceanography, Academy of Sciences, USSR. Vertical distribution of uranium, radium, and thorium isotopes, together with the vertical distribution of iron, manganese, and calcium was studied in 7 cores.

Core No. 1 was collected from the southern part of the Indian Ocean (at 3800 meters depth, 60°28'S, 140°21'E) Station No. 51; homogeneous appearance; light gray; 360 cm long. The data on uranium, radium, thorium, and ionium are shown in Table 1. The distribution curves, with the corresponding curves for iron, manganese, and calcium, are represented in Figure 1.

This core does not belong to the typical oceanic deep-water sediments and it is not typical of littoral sediments. More likely than not, the core belongs to sediments of the intermediate type.

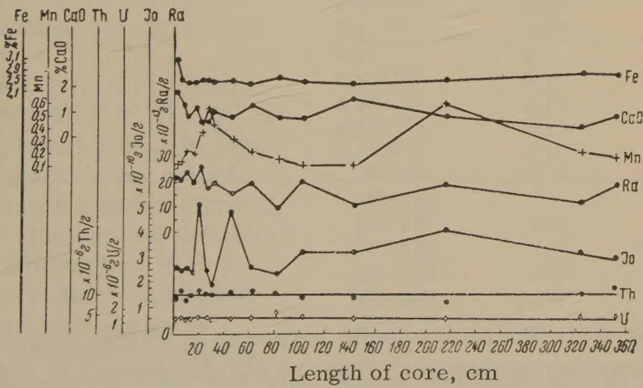

Fig. 1. Distribution curves for chemical elements. Station No. 51. Antarctica.

Inasmuch as we had already shown that thorium and radiothorium are found in radioactive equilibrium, we are reporting only thorium in Tables 1, 2, and 3.

As may be seen from Figure 1, the distribution of thorium and uranium is apparently independent of the depth of the section and is essentially constant. The distribution of radium is more involved and is indicative of several maxima. It is unlikely that these maxima and minima of radium are correlative with the maxima and minima of ionium. Variations in the concentrations of iron, manganese, and calcium in the section are apparently not associated with the distribution of ionium and radium.

Table 1. The Content of U, Ra, Io, and Th in Core No. 1

Horizon cm	U x 10^{-6} g/g	Io x 10^{-10} g/g	Ra x 10^{-12} g/g	Th x 10^{-6} g/g
0-2.5	1.3	2.5	2.2	9
2.5-5.0	1.4	2.5	2.1	8^{4}
7-12	1.2	2.5	2.4	3^{4}
12-17	1.3	2.3	2.0	9^{2}
17-22	1.6	5.2	2.7	9^{2}
22-27	1.5	2.4	1.8	9^{4}
27-32.5	1.2	1.8	1.8	9^{0}
44-49	1.2	4.8	1,6	12^{2}
59-65.5	1.4	2.7	1.9	9
80-85	1.8	2.3	1.0	8^{6}
100-105	1.5	3.3	2.2	11^{4}
140-145	1.3	3.3	1.1	10^{2}
216-223	1.2	4.2	2.0	11^{8}
320-326	1.1	3.3	1.4	12
345-360	1.2	2.9	1.8	12

Core No. 2 (at 90 meters depth; collected in Bering Sea), Station No 990; homogeneous appearance; gray; no abrupt changes in colors note length 260 cm. The data on the distribution of radium, uranium, ionium, and thorium in this core are presented in Table 2.

The distribution curves for uranium, radium, thorium, and ionium are presented in Figure 2.

Like in core No. 1, the distribution of uranium and thorium is remarkably constant throughout the length of the core. The concentratio of radium rises abruptly, beginning with the 80 cm horizon, but falls back almost to its surficial levels toward the bottom of the core. The concentration of ionium decreases somewhat, downward in the core (to the 80 cm horizon), holds constant for a while, and then increases rapidly toward the bottom of the core. There is no apparent connecti

Table 2. The Content of U, Io, Ra, and Th in Core No. 2

Horizon cm	$Ux10^{-6}$ g/g	$Iox10^{-10}$ g/g	$Rax10^{-12}$ g/g	$Thx10^{-6}$ g/g
0-10	1.2	1.4	0.8	6.3
10-15	1.2	0.5	1.1	6.0
15-20	1.6	0.4	1.2	6.0
25-32.5	1.4	0.4	1.1	6.3
37-44	1.8	0.4	1.0	6.0
56-60	1.1	0.4	1.6	---
66-72	1.3	0.2	1.1	---
78-86	1.1	0.2	4.7	7.5
105-111	0.9	0.6	3.0	6.6
152-157	1.2	2.1	5.3	6.4
212-220	1.1	2.0	1.3	6.5
230-239	1.1	4.6	2.0	6.4
248-253	1.0	4.1	1.5	6.4

between the distribution of radium and of ionium. Their distribution is not reflected by the changes in the concentrations of manganese, iron, and calcium.

Core No. 3 (at 221 meters depth; at 57°47.8' N, 161° 21'E); clayey diatomaceous silt; light greenish-gray; some rolled gravel, unrolled gravel, grains of quartz. Ionium and uranium were not determined in this core. The results on radium and thorium are shown in Table 3. Distribution curves for radium and thorium, and iron, manganese, and calcium are given in Figure 3.

Table 3. The Content of Ra and Th in Core No. 3

Horizon cm	$Rax10^{-12}$ g/g	$Thx10^{-6}$ g/g
0-13	0.9	6
13-24	1.1	5
24-34	1.1	5
44-54	1.1	6
71-83	1.2	-
105-112	0.8	5
130-137	0.8	-
166-172	1.6	5
181-190	1.1	-
202-210	1.6	6

As in the previously reported cores, the concentrations of thorium are practically constant throughout the length of this core.

The suppositions offered by Urry and Piggot [2] regarding the constancy of radium concentrations with depth in littoral cores, appear to be justified in this particular case. It appears also that, in this core, the distribution of manganese reflects the distribution of radium.

The concentrations of radium in cores Nos. 1 and 2 exceed significantly the equilibrium concentrations corresponding to the determined amounts of uranium. The radium/ionium ratio is below the equilibrium value throughout the entire length of core No. 1. This ratio varies within a wide range in core No. 2 (Fig. 4).

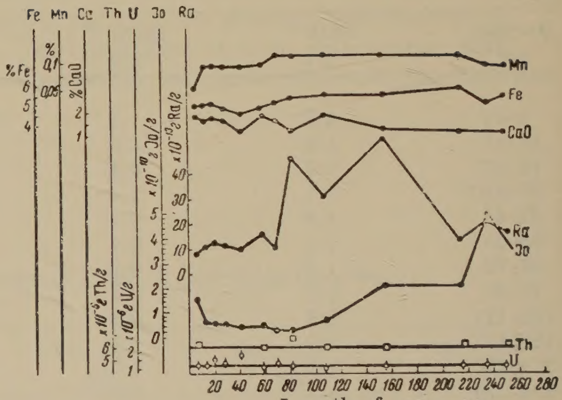

Fig. 2. Distribution curves of chemical elements. Station No. 990.

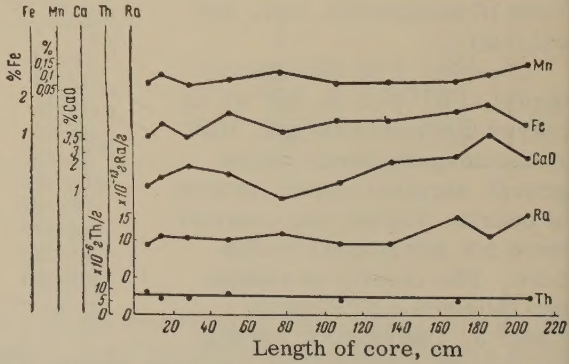

Fig. 3. Distribution curves of chemical elements. Station No. 1817. Okhotsk Sea.

The unlike distribution of ionium and thorium in marine sediments, as established by our studies, is a very interesting fact: while the thorium content remains constant through the entire length of the core, the ionium content shows some highly significant variations. This may be due to external causes (differences in the accessions of ionium and thorium from rivers or differences between sedimentation environments leading to the settling of ionium and thorium at the sea floor) as well as internal ones (migration of ionium in the sedimentary section). Migration of ionium along the length of the sedimentary core, resulting in an irregular distribution of ionium and thorium in depth, is possible only if both ionium and thorium are present in different forms. The Th/U ratio in the cores we had examined is the same as in continental materials. This leads to a suggestion that thorium and uranium are present in marine sediments chiefly as mineral grains. The form of ionium in the sediments is apparently not the same; most probably, ionium is adsorbed by particles of which the sediment is composed.

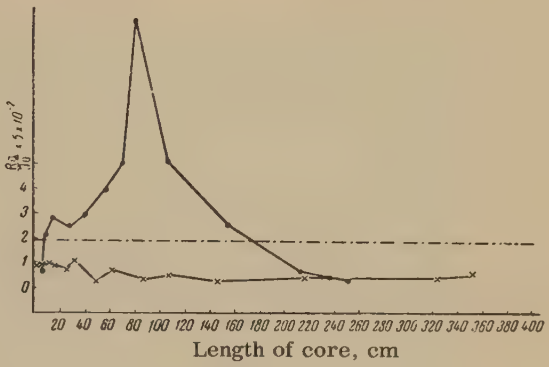

Fig. 4. Distribution of Ra/Io ratio in cores from stations No. 990 and No. 51.

The unlike forms in which ionium and thorium are present in marine sediments should be conducive to the possibility of a vertical migration of ionium. We think, however, that a suggestion of this kind would be premature. It seems more probable that the vertical variations in the concentration of ionium are due to variations in the accession rates, for ionium in the sediments, in different geologic epochs.

Core No. 4, Station No. 97; at 4864 depth; length of core 200 cm; at 40° 32'S, 120°35°E.

The core appears homogeneous; gray color. Figure 5 shows empirical curves of the distribution of radium, uranium, ionium, thorium, manganese, iron, and calcium. As seen in Figure 5, the radium content decreases with depth, from 5×10^{-12} g Ra/1 g of silt to 8×10^{-12} g Ra/1 g of silt at the lower part of the core.[*] 40 cm below the top of the core, there is a definite peak of Ra; the curve runs nearly flat from 70 to 140 cm, whereupon the concentration of radium begins to rise again, reaching 1.6 g Ra/1 g silt in the lower part of the core. Vertical distribution of ionium follows that of radium, in this particular core.

The concentration of thorium is practically independent of depth, in core No. 4, and is constant at 8×10^{-6} g Th/g.[†] The same is the case also for radiothorium which is present in the radioactive equilibrium with thorium in all of the cores we had examined.

The concentration of uranium changes with depth, to some extent.

We could find no relationship between the distribution of radium and ionium on one hand and the distribution of manganese and iron on the

---

[*] The figures do not agree with the diagram or the context. According to the diagram, Ra near the top of the core is about 4.8×10^{-12} g/g silt and about 1.5×10^{-12} g/g silt at the bottom of the core. The range is, roughly, 1 to 5 ($\times 10^{-12}$) g Ra/g silt. VPS

[†] "8×10^{-12}" in the original—a misprint. The diagram's Th scale is not legible. "10^{-6}" is right. VPS

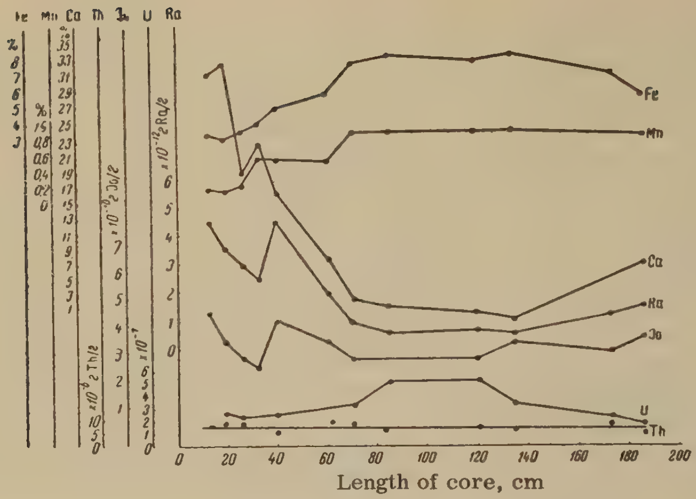

Fig. 5. Distribution of chemical elements. Station No. 97, core No. 4, Indian Ocean.

other. There is a definite association in the distribution of ionium, radium, and calcium: calcium is distributed symbasically with ionium and radium.

Core No. 5. Station No. 129. Depth of sampling 4700 meters; at 30°07'S, 60°35'E; length of core: 200 cm.

The core appears homogeneous; brown color. Figure 6 illustrates the distribution of uranium, radium, ionium, thorium, iron manganese, and calcium in core No. 5.

The concentration of radium decreases with depth, from 16.5 g × 10^{-12} g Ra/g silt to 0.7 × 10^{-12} g Ra/g silt; the latter figure represents the equilibrium with uranium.

The vertical distribution of ionium in this core, as in core No. 4, is entirely the same as the distribution of radium.

There are practically no changes in the concentrations of uranium and thorium in depth.

There is no relationship between the distribution of radium and ionium on one hand and the distribution of iron, manganese, and calcium on the other.

Core No. 6. Station No. 36. Collected at 3820 meters depth; at 60°15'S, 120°50'N. The core appears homogeneous; gray color.

Distribution curves for radium, iron, manganese, and calcium in core No. 6 are shown in Figure 7.

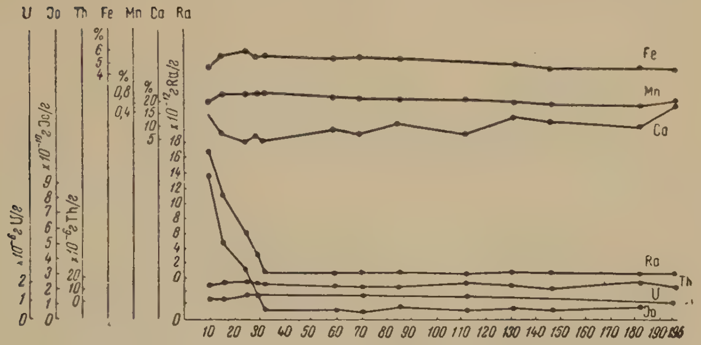

Length of core, cm

Fig. 6. Distribution curves of chemical elements. Station No. 129, core No. 5, Indian Ocean.

The distribution of radium has a complex character, showing several maxima and minima. Uranium, ionium, and thorium were not determined in this core.

We could find no relationship between the distribution of radium on one hand and the distribution of iron and manganese on the other.

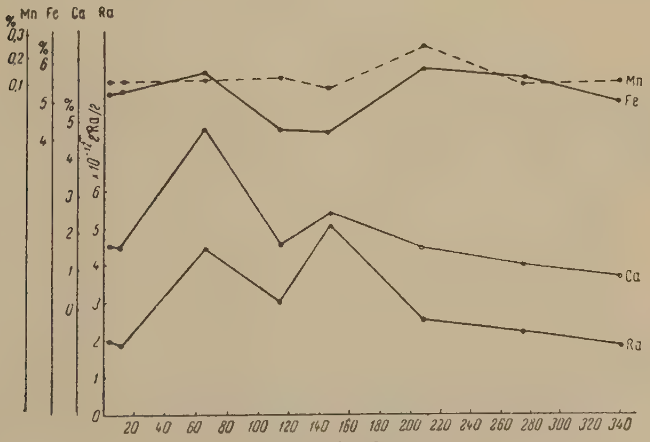

Length of core, cm

Fig. 7. Distribution of chemical elements. Station No. 36, core No. 6.

The distribution of calcium replicates the distribution of radium.

Core No. 7. Station No. 2463. Depth of sampling 3803 meters. At 57°23'N, 167°45'E. The core appears homogeneous; clayey diatomaceous; gray color. Figure 8 shows the distribution curves for radium, manganese, iron, and thorium. The distribution of radium has a complex character. The concentration of radium in the upper part of the core is 3.5×10^{-12} g Ra/g silt, decreasing to 1×10^{-12} g Ra/g silt downward and rising again to 3×10^{-12} g silt, beginning with the 85 cm horizon.

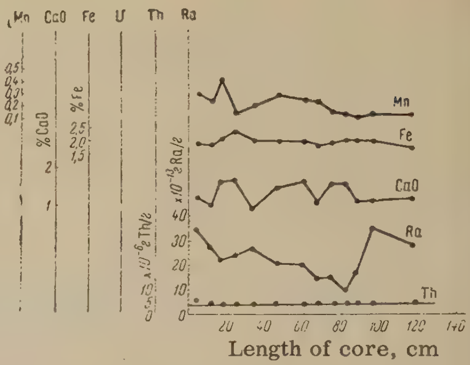

Fig. 8. Distribution curves of chemical elements. Station No. 2463, core No. 7, Pacific Ocean.

The concentration of thorium is constant throughout the core: 5×10^{-6}g Th/g silt. The distribution of calcium, iron, and manganese is unrelated to the distribution of radium, as may be seen in Figure 8.

Table 4 gives an example of the results on radium, ionium, uranium, and thorium in core No. 5 (Station No. 129). Table 5 is an example of the ionium/uranium and radium/ionium ratios in the same core. As it

Table 4

Sample No.	Horizon cm	Ra x 10^{-6} g/g	Th x 10^{-10} g/g	Io x 10^{-10} g/g	U x 10^{-6} g/g
1	8 - 12.5	16.5	13	9.3	1.0
2	12.5 - 17.5	11.0	15	5.0	1.0
3	17.5 - 22	5.9	16	3.3	-
4	22 - 27	2.9	15	1.5	1.3
5	27 - 35	0.6	14	0.4	1.3
6	54 - 64	0.6	13	0.4	-
7	64 - 73	0.7	13	-	1.5
8	73 - 81	0.7	12	0.4	-
9	81 - 89	0.5	1.6	0.8	-
10	107 - 119	0.7	11	0.3	1.6
11	127 - 136	0.6	14	0.5	-
12	143 - 151	0.6	11	0.5	-
13	177 - 187	0.6	14	0.4	-
14	199 - 209	0.5	12	0.4	1.6

is evident from Table 5, the Ra/Io ratio is about the same throughout the length of the core and its magnitude is representative of the radioactive equilibrium between ionium and radium. The Io/U ratio falls from 93×10^{-5} in the upper part of the core to 1.9×10^{-5} in the lower part, which is an indication of the radioactive equilibrium between ionium and uranium in the 35 cm horizon.

The fact of the radioactive equilibrium between ionium and radium in the cores examined by us shows that there is no vertical migration of the radium in the core.

The absence of any relationship between the distribution of ionium and of iron and manganese suggests the absence of any vertical migration of ionium in the core.

We may suggest therefore that the ionium maxima and minima are due to external causes which may be sought in the alterations in the adsorbing properties of the sediments in time.

The parallelism in the distribution of ionium and calcium, as observed in cores Nos. 4 and 6, came as a surprise.

Our results on the distribution of uranium, radium, and ionium in cores Nos. 4, 5, and 7 enabled us to calculate the average rates of the accumulation of sediments represented by these cores.

The average rate of sedimentation for core No. 4 amounts to 5 mm for 1000 years; this rate is somewhat lower for core No. 5, corresponding to about 2 mm per 1000 years. The average rate of sedimentation for core No. 7 is 1.3 cm per 1000 years.

Three types of sediments may be recognized, on the basis of our findings, characterized by certain definite relationships in the vertical distribution of the radioactive elements:

Table 5

Sample No.	Horizon, cm	$(Ra/Io) \times 10^{-2}$ (theoretically 1.9×10^{-2})	$(Io/U) \times 10^{-5}$ (theoretically 1.8×10^{-5})
1	8 - 12.5	1.8	93
2	12.5 - 17.5	2.2	50
3	17.5 - 22	1.9	-
4	22 - 27	1.9	12
5	27 - 35	1.4	3
6	54 - 64	1.4	-
7	64 - 73	-	-
8	73 - 81	0.8	-
9	81 - 89	-	-
10	107 - 119	2.2	1.8
11	127 - 136	1.2	-
12	143 - 151	1.8	-
13	177 - 187	1.5	-
14	199 - 209	1.3	2.5

1. Littoral marine sediments at shallow depths (cores Nos. 2 and 3). The distribution of radium and ionium has a complex character showing several maxima and minima. The distribution of radium is unrelated to the distribution of ionium. The concentrations of thorium and uranium are constant throughout the core, with thorium in radioactive equilibrium with radiothorium.

The complicated character of the vertical distribution of ionium and radium depends apparently on a number of external factors among which we must emphasize the effects of the continental run-off which are subject to variations in time, beyond any doubt.

2. Sediments of intermediate type. An example of this type is core No. 1, described in full, with the radio-chemical analytical results presented in Table 1 and Figure 1. This core was taken at 3800 meters depth at no great distance from the shore.

The effects of the continental run-off are not as conspicuous here as they are in sediments of type 1.

The distribution curves for radium and ionium have a fairly complicated character, although the distribution of radium is somehow related to the distribution of ionium. The concentrations of uranium and thorium are constant throughout the entire length of the core.

3. Deep-water marine sediments (cores Nos. 4, 5, and 7). The concentration of radium decreases vertically in the cores, from the upper horizons to the lower. Several maxima and minima in this distribution, noted in several cases, are due to some possible variations in the accession rates for ionium, in time. The vertical distribution of ionium replicates the vertical distribution of radium. The concentrations of uranium and thorium remain constant throughout the length of the core.

One may reach the conclusion on the basis of our results, that the ionium method of determining the geologic age of marine sediments may be suited for sediments in the deeper parts of the oceanic floor, farthest from the continent.

Distance from the shore serves to minimize the effects of the continental run-off, in the distribution of uranium, radium, and ionium in marine sediments, and accordingly becomes a decisive factor on which the suitability of the ionium method depends.

CONCLUSIONS

1. Vertical distribution of uranium, radium, isotopes of thorium, Fe, Mn, and Ca was investigated in seven cores of marine sediments.

2. The first data were obtained on the vertical distribution of uranium, radium, and isotopes of thorium in sediments of the Indian Ocean.

3. Three distinctive groups of the sediments were recognized by the character of the distribution of ionium and radium in the cores: coastal, intermediate, and deep-marine—farthest from the coast.

4. There is much variation in the ionium content of coastal sediments with the depth of the core. There is no radioactive equilibrium between ionium and radium. The amounts of ionium and radium are far in excess of their equilibrium amounts, as against the amounts of uranium present in the samples.

5. The distribution of ionium and radium in deep-water marine sediments indicates the existence of the radioactive equilibrium between ionium and radium in all of the cores here examined and at all points of the experimental comparison.

6. The forms of occurrence of ionium and thorium in deep-water marine sediments are apparently not the same.

7. There was little change with time in the rate of sedimentation in the areas of the oceanic floor represented by cores Nos. 4 and 5.

8. The concentrations of uranium and thorium in marine sediments represented by the cores here examined are constant throughout the length of the cores.

9. A definite relationship between the vertical distribution of Ra and Io on one hand and of calcium on the other was observed in several cores.

In conclusion, the authors consider it their pleasant duty to offer their profound thanks to P. L. Bezrukov for the samples of the marine sediments he had placed at our disposal.

Received for publication
July 22, 1957

REFERENCES

1. Pettersson, H. Mitteil. Inst. Radiumforschung, 400a, 1938.
2. Piggot, C. S., and W. D. Urry. Bull. Geol. Soc. Am. *53*, 1187, 1942.
3. Kroll, V. St. Reports of the Swedish Deep-Sea Exped. *10*. Special Invest. No. 1, 1-32, 1955.
4. Bernert Traude. Mitteil. Inst. Radiumforschung. N 483, 100, 1951.
5. Kroll, V. St. Nature *171*, 1953.
6. Kroll, V. St. Deep Sea Res. *1*, No. 4, 211. London 1954.
7. Herrnegger, F., and V. Karlik. Medd. Ocean. Inst. 12, 1935.
8. Starik, I. E., and A. S. Smagina. Trudy GRI * *2*, p. 104, 1933.
9. Isaac, N., and E. Picciotto. Nature *171*, 742, 1953.
10. Starik, I. E. *Primenenie Mechenykh Atomov v Analiticheskoi Khimii* (Application of radioactive tracers in analytical chemistry). Izd. Akad. Nauk SSSR. Moscow, 1955.
11. Baranov, V. I., and L. A. Kuzmina. Doklady Akad. Nauk SSR *97*, No. 3, p. 483, 1954.
12. Picciotto, E., and S. Wilgein. Nature *173*, 632, 1954.
13. Thomasson, Perry, and Buerly. Analyt. Chem. *21*, No. 10, p. 1239, 1949.

---

* Geologo-Razvedochnyi Institut (Institute of Geologic Research). VPS

THE FORMATION OF FREE HYDROGEN IN THE EARTH'S CRUST, AS DETERMINED BY THE REDUCING ACTION OF THE PRODUCTS OF RADIOACTIVE TRANSFORMATIONS OF ISOTOPES

V. P. Savchenko

All-Union Research Institute of Natural Gas, Moscow

Abstract

The summary reactivity of the final products of isotope radioactive transformation more than by 50% exceeds the summary reactivity of the initial isotopes. This excess if chiefly caused by the accumulation of Ca^{40} and Sr^{87} being formed at the radioactive transformation in accordance to K^{40} and Rb^{87}.

The free Ca^{40} and Sr^{87} atoms, acting on the water must decompose it in liberating hydrogen. The fact of the occurrence of this process in nature is confirmed by the presence of free hydrogen in deposits of potassium salts, where along with the K^{40} isotope the Rb^{87} isotope is found in greater amounts.

Computations have shown that the hydrogen content of the origin under consideration in gases of sedimentary rocks must be in the same range as the helium content, though in some cases there may be divergences.

As we know, the valence of elements created in radioactive transformations is different from the valence of their predecessors.

The sum of the reaction capacities of the end-products of such transformations exceeds the sum of the reaction capacities of the original isotopes by more than 50%, as may be seen from the balance sheet of the reaction capacities of the isotopes.

Table 1 shows the content of radioactive isotopes in the earth's crust, the kind of their radioactive transformations, and the decay constants, according to A. P. Vinogradov [1] and E. K. Gerling [3]. The Table also shows the calculated amounts of every isotope decayed in 10^9 years as grams and gram-atoms per 1 gram of the earth's crust materials. As shown in Table 1, calculations of the reaction-capacity balance require only the data on the first five isotopes, K^{40}, Rb^{87}, Th^{232}, and U^{235} and the data on the remaining isotopes may be disregarded, in view of their relatively very small magnitudes.

According to present-day opinion, 11% of decayed K^{40} is converted into A^{40} and the remaining 89% into Ca^{40}. Rb^{87} is converted into Sr^{87} quantitatively.

As to Th^{232}, U^{238}, and U^{235}—the following relationships proceeding from their radioactive transformations appear to be probable in the environments of the earth's crust:

$$Th^{232}O_2 - Pb^{208}O + 6He + O$$
$$U^{238}O_2 - Pb^{206}O + 8He + O$$
$$U^{235}O_2 - Pb^{207}O + 7He + O$$

The balance of the reaction-capacity for these five isotopes per 10^9 years, together with concurrently accumulated products of their decay, is presented in Table 2, in accordance with the transformations here visualized. It is shown by the data in Table 2 that the reaction-capacity of the end-products of K^{40}, Rb^{87}, Th^{232}, U^{238}, and U^{235}, in their radioactive transformations exceeds the reaction-capacity of the original isotopes by 53.1%.

This excess of the reaction-capacity of the end-products is due to the accumulations of Ca^{40} and Sr^{87}, both of which are active reducers. Reducing effects due to the products of the radioactive transformations of the isotopes should be conspicuous therefore in the earth's crust. Decomposition of water by free atoms of Ca^{40} and Sr^{87}, with the consequent formation of free hydrogen, is an example of the reducing action of the radioactive transformations.

The presence of free hydrogen in deposits of potassium salts is a convincing evidence of the effectiveness of this process in nature.

The presence of gas, including hydrogen, in potassium salts was studied in the Stassfurt (Germany) and in the Upper-Kama potash deposits. The findings were confirmed by A. A. Cherepennikov and co-

Table 1. Characteristics of the Disintegration of Radioactive Isotopes of the Earth's Crust

Element	Radioactive Isotope	Character of Decay	End-Products of Decay	Amount of Element in Earth's Crust, %	Content of Radioactive Isotope		Constant of Radioactive Decay of the Isotope 10^{-1} years	Amount of Decayed Isotope in 10^9 years	
					In Element %	In Earth's Crust, %		grams per gram	gram-atoms per 1 gram of rock
K	K^{40}	β, E	Ca^{40}, Ar^{40}	2.5	$1.19 \cdot 10^{-2}$	$2.98 \cdot 10^{-6}$	$5.5 \cdot 10^{-10}$	$2.18 \cdot 10^{-6}$	$5.45 \cdot 10^{-8}$
Rb	Rb^{87}	β	Sr^{87}	$2.8 \cdot 10^{-2}$	27.85	$7.8 \cdot 10^{-5}$	$1.16 \cdot 10^{-11}$	$9.12 \cdot 10^{-7}$	$1.05 \cdot 10^{-8}$
Th	Th^{232}	α, β, γ	He^4, Pb^{208}	$1.3 \cdot 10^{-3}$	100	$1.3 \cdot 10^{-5}$	$4.99 \cdot 10^{-11}$	$6.5 \cdot 10^{-7}$	$2.80 \cdot 10^{-9}$
U	U^{238}	α, β, γ	He^4, Pb^{206}	$2.6 \cdot 10^{-4}$	99.28	$2.58 \cdot 10^{-6}$	$1.54 \cdot 10^{-10}$	$4.30 \cdot 10^{-7}$	$1.81 \cdot 10^{-9}$
U	U^{235}	α, β, γ	He^4, Pb^{207}	$2.6 \cdot 10^{-4}$	0.71	$1.85 \cdot 10^{-8}$	$9.81 \cdot 10^{-10}$	$3.07 \cdot 10^{-8}$	$1.30 \cdot 10^{-10}$
Sm	Sm^{147}	α	He^4, Nd^{143}	$4 \cdot 10^{-4}$	15.7	$6.0 \cdot 10^{-7}$	$5.33 \cdot 10^{-12}$	$3.25 \cdot 10^{-9}$	$2.21 \cdot 10^{-11}$
La	La^{138}	E	Ba^{138}	$4 \cdot 10^{-3}$	$8.9 \cdot 10^{-2}$	$3.56 \cdot 10^{-8}$	$5.78 \cdot 10^{-12}$	$2.07 \cdot 10^{-10}$	$1.50 \cdot 10^{-12}$
Lu	Lu^{176}	β, E	He^{176}, Yb^{176}	$\sim 1 \cdot 10^{-4}$	2.60	$\sim 2.6 \cdot 10^{-8}$	$2.88 \cdot 10^{-11}$	$\sim 7.6 \cdot 10^{-10}$	$\sim 4.32 \cdot 10^{-12}$
Re	Re^{187}	β	Os^{187}	$\sim 1 \cdot 10^{-7}$	62.93	$\sim 6 \cdot 10^{-5}$	$1.17 \cdot 10^{-13}$	$\sim 1 \cdot 10^{-13}$	$1 \cdot 10^{-14}$
In	In^{115}	β	Sn^{115}	$\sim 1 \cdot 10^{-5}$	95.77	$\sim 9.6 \cdot 10^{-8}$	$1.15 \cdot 10^{-15}$	$\sim 1.1 \cdot 10^{-12}$	$\sim 8.7 \cdot 10^{-15}$
Sn	Sn^{124}	β	Te^{124}	$3.2 \cdot 10^{-3}$	6.0	$1.92 \cdot 10^{-6}$	$1.15 \cdot 10^{-16}$	$2.2 \cdot 10^{-14}$	$1.77 \cdot 10^{-16}$
Bl	Bl^{209}	α	He^4, Tl^{206}	$\sim 1 \cdot 10^{-5}$	100	$\sim 1 \cdot 10^{-7}$	$2.32 \cdot 10^{-18}$	$\sim 2.4 \cdot 10^{-17}$	$\sim 1.15 \cdot 10^{-19}$

Table 2. Reaction-Capacity of Isotopes Decayed and Formed per 1 Gram of Earth's Crust per 10^9 Years

Decayed		Formed	
Isotope	Gram-Equivalents	Isotope	Gram-Equivalents
K^{40}	5.45×10^{-8}	Ar^{40}	0
Rb^{87}	1.05×10^{-8}	Ca^{40}	9.80×10^{-8}
		Sr^{87}	2.10×10^{-8}
Th^{232}	1.12×10^{-8}	He^4	0
		Pb^{208}	0.56×10^{-8}
U^{238}	0.724×10^{8}	He^4	0
		Pb^{206}	0.36×10^{-8}
U^{235}	0.052×10^{-8}	He^4	0
		Pb^{207}	0.02×10^{-8}
		He^4	0
Total	8.40×10^{-8}	Total	12.84×10^{-8}

The ratio of reaction-capacity of "formed" to "decayed":

$$\frac{12.84 \times 10^{-8}}{8.40 \times 10^{-8}} = 1.53$$

workers in the Solikamsk Mine, Upper-Kama [4, 5] and by Z. N. Nesmelova in the Bereznikovsaya Mine in the same district [6].

The red color of carnallites and sylvinites in the district is due to dispersed iron oxides amounting to 0.07 - 0.33%, according to E. E. Razumovskaya [8]. The red color of the Stassfurt carnallites is due to the same cause.

The salt beds have been subjected to severe deformations. It is believed that the B, V, and G beds are products of a recrystallization of carnallites under the influence of a dynamo-metamorphism.

Gas-filled bubbles and vacuoles are common in carnallite and sylvite Extremely small bubbles are particularly abundant in the milky-white sylvinite.

It should be noted that yellow and brown colors of some carnallite grains may be explained by the presence of some gas, as solid solution, according to E. E. Razumovskaya [8], inasmuch as no iron could be detected in such grains and the recrystallized carnallite, derived from the colored grains, was colorless.

Eruptions of gas containing hydrogen were noted already in the exploratory boreholes by which the Verkhnekamsk potash beds were first exposed. After the exploitation of this deposit was begun, the composition of gas evolving in boreholes and in spurs* cutting the salt beds directly from the mining workings* of the Solikamsk Mine, was studied by A. A. Cherepennikov and his co-workers. They found 30 to 50% hydrogen, and more, in the gas from boreholes and spurs passing through carnallite. The gas from boreholes and spurs through mottled sylvite does not always† contain hydrogen and, moreover, the hydrogen-bearing gas is found characteristically only in the top parts of the salt beds. There is no hydrogen in the gas from boreholes and spurs through banded and red sylvinite.

---

*Rus. "shpur" is German "Spur", an inclined borehole. VPS

A. A. Cherepennikov and co-workers studied also the composition and the amounts of gas locked directly in the salts. The gas was extracted by dissolving the salts in water [4]. Table 3, based on A. A. Cherepennikov's data, shows the amounts of the individual components of the gas extracted from the salts. The results presented in this Table are to the effect that hydrogen is found not only in the gas extracted from carnallite but also in the gas from sylvinite. Consequently, there are striking differences, in the case of sylvinites, in the hydrogen content of the gas evolving in boreholes and spurs and the gas extracted from the very same salts by water.

The same differences between the gas evolving in boreholes and spurs and the gas in the micro-inclusions in the salts extractable by water were observed also by Z. N. Nesmelova [6] in the salt beds of the Bereznikovskaya Mine. Composition of these gases is reported in Table 4.

The volume of hydrogen per 1 kg of potassium salts, carnallites as well as sylvinites, is approximately 2 cm^3, as reported in Table 3. Somewhat smaller amounts of hydrogen were found by A. A. Cherepennikov [4]: the average H_2 - 1.7 cm^3 per 1 kg of carnallite and 0.7 cm^3 per 1 kg of sylvite. The markedly lower hydrogen content of sylvinites, in this particular case, may be explained as due to the inclusion of many gas analyses of hydrogen-free salts among the tabulated results.

The foregoing data show that the average hydrogen in carnallite and sylvite is close to 2 cm^3 per 1 kg of the salts.

The following hypotheses were advanced, as explanations of the presence of hydrogen in potassium salts.

Prekht [8] supposes that iron, as douglasite, $2KCl \cdot FeCl_2 \cdot 2H_2O$, was an original constituent of carnallite. The ferrous iron was subsequently oxydized, in the presence of the water of crystallization: $6FeCl_2 + 3H_2O = 4FeCl_3 + Fe_2O_3 + 3H_2$.

The average amounts of iron oxide in the Verkhnekamsk carnallite are calculated as 2g Fe_2O_3 per 1 kg carnallite, with the total hydrogen calculated as 855 cm^3 per 1 kg carnallite, on the basis of the assumed transformation of $FeCl_2$.

---

*"Gornye vyrabotki" - pits, trenches, etc. VPS

†Misprint in the original, "no vsegda", instead of "ne vsegda" ("but always" instead of "not always"). VPS

Table 3. Composition of Gas Extracted from Potassium Salts, Solikamsk Mine

		Extracted, cm^3 gas per 1 kg of K salts				
	Wt. of salt sample, kg	Total	CH_4	C_2H_6 + higher hydrocarbons	H_2	N_2 + rare gases
Carnallite						
Bed G, Borehole 268	15	7.5	0.5	0.05	2.6	3.8
Bed V, Horizon 6, top	21	19.1	1.0	1.9	2.0	10.2
Bed V, Horizon, middle	17	4.8	0.2	0.04	1.1	2.7
Bed V, Horizon, bottom	18	14.1	0.7	0.2	4.4	7.3
Bed V, Horizon 4	12.3	10.2	1.6	0.09	2.4	4.3
Bed V, Horizon 2	12.2	12.9	0.9	0.3	4.2	5.9
Bed V, Horizon 1	17	28.6	0.5	0.5	-	3.0
Average		13.9	0.82	0.43	2.4	5.3
Mottled Sylvinite						
Bed V, Horizon 6	3.0	142	6.7	1.4	0.7	126
Bed V, Horizon 5	4.5	120	7.3	1.6	-	108
Bed V, Horizon 2	2.4	135	4.5	1.5	3.6	124
Bed V, Horizon 1	8.6	90	2.9	1.4	3.1	78
Bed VI, H	7.4	56.3	3.5	1.0	1.3	48
Average		109	5.0	1.4	1.4	97
Banded Sylvinite						
Bed A, top; chamber 17	8.1	46	2.2	1.3	0.6	40.3
Bed A, top; chamber 108	9.7	66.7	6.2	1.5	3.1	50.8
Bed A, bottom; chamber 17	9.3	52.0	5.0	0.8	1.3	42.5
Bed A, bottom; chamber 108	12.2	41.0	2.3	1.9	5.1	29.8
Bed A, chamber 31	10.0	54.3	6.2	1.9	-	41.4
Average		52	4.4	1.5	2.0	41.0
Red Sylvinite						
Bed I	12.7	39.6	2.8	1.3	2.9	32.1
Bed II	18.6	14.5	0.7	0.6	2.5	10.5
Bed III	10.2	21.6	1.6	0.3	2.0	22.6
Average		25.2	1.7	0.7	2.5	21.7
Sylvinite bed average		-	-	-	1.9	-

Erdman [8]* performed many experiments with heating of ferrous chloride together with water and carnallite but was not able to observe any formation of Fe_2O_3 and free hydrogen. Taking into account the presence of up to 0.17% He in the free gas of Stassfurt potassium salts, Erdman suggested that, as a consequence of a radioactive decay of some element accompanied by the formation of helium, a decomposition of water into hydrogen and oxygen also taking place and that hydrogen remained as a free gas while oxygen was used up in the oxidation of ferrous to ferric iron.

---

*This and other citations under [8] refer probably to articles by authors other than Razumovskaya [8] in the same issue of the publication which is probably of the "Collected Papers" type. VPS

Yu. V. Morachevskii and A. A. Cherepennikov [5] believe that the hydrogen and the hydrocarbon gases in potassium salts had originated from organic residues in the basin where the salts were being deposited and that these gases were captured by the crystallizing salts. A part of the captured gases was liberated at some later time and accumulations of the free gases were developed accordingly.

All of the enumerated hypotheses are essentially unfounded.

There is no doubt whatsoever, on the other hand, that free hydrogen must be produced in deposits of potassium salts as the result of the decomposition of water by calcium and strontium formed in the radioactive transformations of potassium and rubidium respectively.

It is possible to represent the relationships of the participating substances as follows:

$$100K^{40}Cl \rightarrow 50Ca^{40}Cl_2 + 39Ca^{40} + 11A^{40}$$

$$39Ca^{40} + 78H_2O = 39Ca^{40}(OH)_2 + 39H_2$$

$$2Rb^{87}Cl \rightarrow Sr^{87}Cl_2 + Sr^{87}$$

$$Sr^{87} + H_2O = Sr^{87}(OH)_2 + H_2$$

Sylvite contains 52.4% K and carnallite 14.1% K, as we know.

According to the available data [7], the average content of rubidium

Table 4. Average Composition of Gases in Potassium Salts from Bereznikovski Mine. Per Cent by Volume

	Free Gases							Gases Extracted from Salts					
	CO_2 + H_2S	CH_4	C_2H_6 + higher hydroc.	H_2	N_2 + rare gases	A + Kr + Xe	He + Ne	CO_2 + H_2S	CH_4 + higher hydrocarbons	H_2	N_2 + rare gases	A + Kr + Xe	He + Ne
Carnallite	0.06	31.0	3.8	7.8	57.5	0.077	0.003	22.0	7.0	32.6	38.3	0.954	0.003
Mottled sylvinite, Bed V	-	-	-	-	-	-	-	14.5	1.9	4.6	78.5	-	-
Milky-white sylvinite	-	-	-	-	-	-	-	10.3	1.6	1.1	87.0	0.360	0.001
Mottled sylvinite, Bed B	0.5	33.2	7.5	0.0	45.5	0.180	0.004	12.7	1.2	2.9	83.4	0.322	0.003
Banded sylvinite, Bed A	0.75	43.1	10.5	0.0	45.8	0.182	0.007	5.5	1.9	3.3	89.2	0.476	0.001
Red sylvinite, Bed P	0.0	31.4	13.3	0.0	55.0	0.196	0.008	7.1	5.3	9.6	85.6	1.724	0.001

in carnallite is 0.02% and the average rubidium in sylvite is smaller by one order of magnitude.

The age of the Verkhnekamsk salt beds is approximately 200 million years. Taking into account this period of time and the radioactive transformations of K^{40} and Rb^{87}, the amounts of argon and free hydrogen formed in the processes are as follows:

Per 1 kg of sylvite:

from K^{40} A^{40} ------ 0.42 cm^3
H_2 ------ 1.50 cm^3

Per 1 kg of carnallite:

from K^{40} A ------ 0.113 cm^3
H_2 ------ 0.395 cm^3
from Rb^{87} H_2 ------ 0.015 cm^3
Total H_2 0.410 cm^3

There is a certain discrepancy between the calculated quantity of hydrogen per 1 kg of potassium salts and the empirical results. Thus there should be more hydrogen in sylvinite than in carnallite, according to our calculations, while in reality the reverse is the case. There is also a discrepancy between the calculated and the observed total amounts of hydrogen. These discrepancies are not highly important, however.

They may be explained by a redistribution of hydrogen between the salts, and possibly in part by analytical errors.

It is possible also that less than 50 out of 89 atoms of Ca^{40} are combined with the chloride. If we assume that all of the radiogenically produced Ca^{40} reacts with water, the calculated amounts of the resulting hydrogen must be multiplied by 2.28. If so, the empirically established hydrogen content of the Solikamsk potassium salts will come closer to the calculated magnitude. The liberated chlorine, in this particular case, may replace from their compounds bromine and iodine, whose presence was already established in the potassium salts here discussed [5]. It is possible that the peculiar colors of carnallite grains previously noted may be due to the liberated bromine and iodine.

The fact that the gas evolved from sylvinites contains no hydrogen, while the gas extracted from sylvinites by water contains appreciable proportions of hydrogen, may be easily accounted for by a reference to our suggestions regarding the origins of hydrogen in potassium salts. The cause of this phenomenon is to be found probably in the fact that, inasmuch as sylvinite is anhydrous, the decay of its K^{40} does not result in the formation of hydrogen and its radiogenically formed Ca^{40} remains free. When sylvinite is dissolved in water, free hydrogen is produced in the reaction between Ca^{40} and H_2O.

The presence of free calcium in sylvinites offers a possible explanation also of the blue color of halite crystals. We know that these halite crystals are in contact with sylvinite. One may assume that free calcium may rob NaCl of some of its chloride, whereupon the liberated sodium may render the halite crystals blue.

Data on the presence of gas in the Verkhekamsk deposit indicate that the presence of free hydrogen in these salts may be explained most convincingly by the decomposition of water, in its reaction with the Ca^{40} and Sr^{87} isotopes which are the products of the radioactive transformations of K^{40} and Rb^{87} isotopes respectively.

Table 5 shows the amounts of He and A forming in rocks of the earth's crust through the radioactive decay of Th^{232}, U^{238}, U^{235}, and K^{40} The amounts of free H_2 and O_2 that may be formed in the radioactive transformations of the same isotopes and from Rb^{87} are also shown in the same Table, on the assumption that only 39 out of 89 atoms of Ca^{40} produced in the transformations of K^{40} are reacting with water.

The amounts of hydrogen that may be formed in the rocks of the earth's crust, in consequence of the radioactive transformations of K^{40} and Rb^{87}, are relatively small, as may be seen in Table 5, even in the course of a very long geologic time. However, if we take into account large volumes of the rocks, the amounts of hydrogen of radioactive origin may attain substantial magnitudes. For example, approximately 1.5×10^6 cubic meters of H_2 may be formed per 1 cubic kilometer of rock per 10^9 years and about 5×10^6 cubic meters per 1 cubic kilometer per 2×10^9 years.

The amounts of K, Rb, Th, and U in sedimentary rocks (clays and shales) are 2.28, 4×10^{-2}, 1.1×10^{-3}, and 3.2×10^{-4}% respectively, on the average [2]. It has been calculated that the amounts of He and A forming in such rocks and the amounts of free H_2 and O_2 that may be forming there, by the considerations here discussed, may not be significantly different from their amounts estimated in the rocks of the earth's crust.

Both He and H_2 should be released by mineral particles of sedimentary rocks to the pore space of these rocks with about the same degree of facility, as one may well imagine. The volume of H_2 in the pore space, moreover, cannot exceed the volume of He released to the same space, as is evident from the results in Table 5. Inasmuch as the helium content of natural gases is rarely higher than 1% and is generally only hundredths or tenths of one per cent, on account of the foregoing considerations, the hydrogen content of these gases, originated in the processes here discussed, may be expected to be also within the same limits, although there may be departures from these magnitudes, in some isolated cases.

Received for publication
December 2, 1957

Table 5

Possible Maximum of Ar and H_2 in Consequence of Radioactive Decay of K^{40} and Rb^{87} Cubic Centimeters of Gas per 1 Kilogram of Earth's Crust

Time for accumulation, years	A from K^{40}	H_2 from:		
		K^{40}	Rb^{87}	Total
5×10^{7}	5.12×10^{-3}	1.83×10^{-2}	0.55×10^{-2}	2.38×10^{-2}
1×10^{8}	1.03×10^{-2}	3.70×10^{-2}	1.11×10^{-2}	4.81×10^{-2}
2×10^{8}	2.11×10^{-2}	7.55×10^{-2}	2.19×10^{-2}	9.74×10^{-2}
3×10^{8}	3.27×10^{-2}	0.116	3.32×10^{-2}	0.149
4×10^{8}	4.49×10^{-2}	0.161	4.42×10^{-2}	0.205
5×10^{8}	5.75×10^{-2}	0.205	5.62×10^{-2}	0.261
1×10^{9}	0.134	0.477	0.117	0.594
2×10^{9}	0.366	1.32	0.237	1.55
3×10^{9}	0.765	2.72	0.358	3.08

Possible Maximum of He in Consequence of Radioactive Decay of Th^{232}, U^{238}, and U^{235}. Cubic Centimeters of Gas per 1 Kilogram of Earth's Crust

Time for accumulation, years	He from:			
	Th^{232}	U^{238}	U^{235}	Total
5×10^{7}	1.87×10^{-2}	1.50×10^{-2}	0.62×10^{-3}	3.43×10^{-2}
1×10^{8}	3.76×10^{-2}	3.00×10^{-2}	1.3×10^{-3}	6.87×10^{-2}
2×10^{8}	7.50×10^{-2}	6.02×10^{-2}	2.7×10^{-3}	0.138
3×10^{8}	0.113	9.12×10^{-2}	4.5×10^{-3}	0.209
4×10^{8}	0.150	0.124	6.0×10^{-3}	0.280
5×10^{8}	0.187	0.155	7.9×10^{-3}	0.350
1×10^{9}	0.376	0.325	0.021	0.721
2×10^{9}	0.780	0.704	0.070	1.55
3×10^{9}	1.23	1.16	0.220	2.61

Possible Maximum of O_2 in Consequence of Radioactive Decay of Th^{232}, U^{238}, and U^{235}. Cubic Centimeters of Gas per 1 Kilogram of Earth's Crust

Time for accumulation, years	O_2 from:			
	Th^{232}	U^{238}	U^{235}	Total
5×10^{7}	1.56×10^{-3}	0.94×10^{-3}	4.43×10^{-5}	0.25×10^{-2}
1×10^{8}	3.13×10^{-3}	1.87×10^{-3}	0.09×10^{-3}	0.51×10^{-2}
2×10^{8}	6.26×10^{-3}	3.76×10^{-3}	0.19×10^{-3}	1.02×10^{-2}
3×10^{8}	9.39×10^{-3}	5.70×10^{-3}	0.32×10^{-3}	1.54×10^{-2}
4×10^{8}	1.25×10^{-2}	7.75×10^{-3}	0.43×10^{-3}	2.07×10^{-2}
5×10^{8}	1.56×10^{-2}	9.70×10^{-3}	0.56×10^{-3}	2.59×10^{-2}
1×10^{9}	3.13×10^{-2}	2.03×10^{-2}	0.15×10^{-2}	5.31×10^{-2}
2×10^{9}	0.065	0.044	0.005	0.114
3×10^{9}	0.103	0.103	0.016	0.181

REFERENCES

Vinogradov, A. P. *Geokhimiya Izotopov* (Geochemistry of isotopes). Izv. Akad. Nauk SSSR, Ser. Geol. No. 3, 1954.

Vinogradov, A. P. *Zakonomernosti Raspredeneniya Khimicheskikh Elementov v Zemnoi Kore* (Regularities in the distribution of chemical elements in the earth's crust). Geokhimiya, No. 1, 1956.

Gerling, E. K. *Argonovyi Metod Opredeleniya Vozrasta i Ego Primenenie dlya Raschleneniya Dokembriiskikh Obrazovanii Baltiiskogo i Ukrainskogo Shchitov* (The Argon Method of age measurements and its application in the differentiation of Precambrian formation of the Baltic and of the Ukranian shields). Geokhimiya, No. 5, 1956.

Morachevskii, Yu. V., A. G. Samartseva, and A. A. Cherepennikov. *Gazonosnost' Tolshchi Kalievykh Solei Verkhnekamskogo Mestorozhdeniya* (Presence of gas in potassium salt beds of the Upper-Kama deposit). Kalii, No. 7, 1937.

Morachevskii, Yu. V., pri uchastii (with the participation of) A. G. Bezdenezhnykh, T. B. Polenova, M. M. Tikhomirova, and A. A. Cherepennikov. *Ocherki Geokhimii Verkhenekamskikh Solyanykh Otlozhenii* (Essays in geochemistry of the Upper-Kama deposits of salts). Trudy Vsesoiuzn. Inst. Galiergii, Vyp. XVIII, 1939.

Nesmelova, Z. N. *Gazonosnost' Solyanoi Tolshchi Bereznikovskogo Kaliinogo Rudnika* (The presence of gas in the salt beds of Bereznikovskoe potash mine). *Avtoreferat na soiskanie uchenoi stepeni kandidata geologo - mineralogicheskikh nauk* (Author's abstract of thesis for the Degree of Candidate of Geologic-Mineralogical Sciences), VSEGEI, 1956.

Plyuschov, V. E., and I. V. Shchakhno. *Rubidii i Tsezii; Oblasti Primeneniya i Metody Polucheniya* (Rubidium and Caesium; fields of use and methods of production). Khim. Nauka i Promyshl. *1*, No. 5, 1956.

Razumovskaya, E. E. *Prichiny i Kharakter Krasnoi Okraski Kalievyh Soedinenii Solikamskogo Mestorozhdeniya* (Causes and character of the red color of potassium compounds in Solikamsk deposit). Materialy po obshchei i Prikladnoi Geologii. Vyp. 105, 1927.

X-RAY INVESTIGATIONS OF NATURAL OXIDES OF URANIUM

G. A. Sidorenko

All-Union Scientific Research Institute of
Economic Minerals (VIMS), Moscow

Abstract

By means of investigation it has been established that the structure of the CaF_2 type is the only crystalline form in which uranium oxides occur in natural conditions. As the tetravalent uranium oxide is oxidizing into a hexavalent, the size of the elementary cell of the oxide is changing. The character of dependence of the elementary oxide cell on the degree of its oxidation state, expressed by the value of the hydrogen coefficient X has been shown. It has been ascertained that the chief reason for the diffusivity of the diffraction lines of the x-ray patterns of highly oxidized uranium pitchblendes and uranium sooty pitchblende is the high degree of their dispersivity which increases as the mineral is further naturally oxidized. The study of these transformations which the natural uranium oxides are undergoing in the process of their oxidation and ignition in the air, has shown that their initial crystalline structure is more stable than the structure of the synthesized uranium oxides and that the course of phase transformations differs from the course of the latter. Among the ignition products of the mineral uranium oxides a new phase, named the phase Y, has been detected.

1. VARIATIONS IN SIZE OF UNIT CELL IN NATURAL OXIDES OF URANIUM

Three morphologic varieties of uranium oxides are found in natural environments: definitely crystalline uraninite; crypto-crystalline collomorphic pitchblende; powdery sooty uranium black [2, 4, 18, 21]. The composition of uranium oxides is changing, in time, in the direction governed by the radioactive decay of uranium, with the result that lead of radiogenic origin makes its appearance in natural uranium oxides, and in the direction conducive to the oxidation of tetravalent uranium to its hexavalent state. The composition of natural uranium oxides, as a whole, is commonly expressed by the formula: $(U,Th)O_2 \cdot mUO_3 \cdot nPbO$. The $UO_3 : UO_2$ ratio in the oxide of uranium indicates the state of its oxidation which is generally expressed as a magnitude "x", the oxygen coefficient. The oxygen coefficient shows the number of oxygen atoms for each atom of uranium in the given sample of the oxide [5]. The magnitude of "x" is found from the analytical chemical data on UO_2 and UO_3* in the sample. No mineral corresponding to the formula UO_2 has been found in nature. Uranium in its minerals is always more or less oxidized.

---

*Independent determinations of UO_2 and UO_3 by chemical methods are made difficult by the presence of elements that may have more than one valence (Fe, Mn, V, etc.) and of organic matter in the sample.

Gradual changes in composition and properties of uranium oxides undergoing oxidation were observed by Ellsworth [10] in a crystal of uraninite with a clearly defined zonal structure, in consequence of the oxidation taking its course from the periphery toward the center of the crystal. Depending on the oxidation, there are changes in color, hardness, specific gravity, and chemical composition of the mineral: an increase in U^{6+} and a decrease in U^{4+}, together with a decrease in the total U and a relative increase in Th and in the rare earth elements. According to Ellsworth, the UO_3:UO_2 ratio provides exact information regarding the degree of the decay (alteration) of the mineral.

A question presents itself: what are the crystal-chemical changes in the natural uranium oxides with time? The earliest crystal-chemical study of uranium oxides was the research by Goldschmidt and Thomassen [12] who showed that uraninite has a structure of the fluorspar type (Fig. 1): a cube, with uranium atoms at the centers of its faces and at the corners and with oxygen atoms at the center of every octahedron. Length of the side of the cube: 5.46 Å. The same investigators expressed a view, to the effect that "natural uraninite, containing much UO_3, on account of oxidation, is apparently identical in its structure with uranium dioxide, UO_2". Subsequent studies by Arnott [6] demonstrated that the length of the side of the cube is not constant, nor is the size of the unit cell of uraninite or pitchblende. The same phenomenon was noted by Brooker and Nuffield [18] for Canadian pitchblende. They also called attention to differences in the character of x-ray patterns of the pitchblende, without determining the reason of this phenomenon, however.

Wasserstein [23, 24] sees the fundamental cause of the variations in the size of the unit cell of uranium oxides in the different proportions of radiogenic lead contained therein, as such lead persists in the crystal structure of the oxide, where it replaces tetravalent uranium, with the resulting change in the a_0, the unit cell, by 0.0035 Å per 100 million years, which fact, according to this author, offers a possibility of determining the age of the mineral by its a_0. However, this thesis is controversial [15, 17]. On the one hand, there is an opinion to the effect that radiogenic lead does not enter the structure but is distributed at the boundaries of the blocks; on the other hand, even on the assumption that all of the radiogenic lead is indeed in the crystal structure, the replacement of U^{4+} by Pb is overbalanced by the replacement of tetravalent uranium by thorium, the rare earths, and the hexavalent uranium derived from tetravelent uranium by oxidation.

The present investigation was carried out with natural uranium oxides from several domestic and foreign deposits of different origins. Since most of our test materials are found in nature as polycrystals or as fragments of monocrystals (in the case of uraninites), the x-ray analysis had to be performed by the Debye-Scherrer method. The

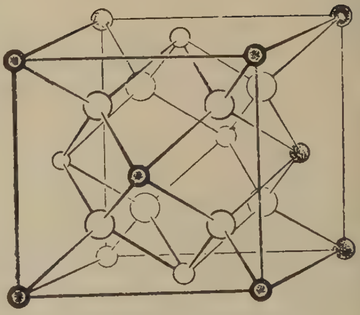

Fig. 1. Crystal structure of uranium dioxide. Black circles - uranium; white circles - oxygen.

diffraction patterns were obtained at different radiations, with the BCV tubes (chromium, copper, iron) under the following standard conditions: 25, 34, 45, kv and 8, 10, 16 m.a. respectively, in cameras with the diameter of 57.6, 86.0, and 114.0 mm respectively. The reflection angles were corrected by means of the simultaneous recording with the standard rock salt (a_0 = 5.6285 Å).

It was shown even by a preliminary examination of the x-ray patterns of natural uranium oxides that most of them have a structure of the CaF_2 type and that the diffraction patterns are not the same for different oxides. Comparisons of the patterns with the degree of oxidation of the minerals enabled us to draw the following conclusion: the greater the degree of oxidation of the pitchblende—the more diffuse are the diffraction lines of its pattern. It is possible to distinguish four types of patterns: the first one has characteristically sharp lines at all reflection angles. This first type is produced by uraninites. The second type yields sharp reflections at small angles (theta up to 45°) and broad ones at larger theta. Patterns of this type are produced by weakly or moderately oxidized pitchblende. The third type is a diffuse diffraction pattern at any angle. It is produced by strongly oxidized pitchblende. The fourth type—broad rings against a strong background—is given by the uranium black. The latter material is often indicated as amorphous, in the x-ray patterns.

If the degree of oxidation of natural uranium oxides is characterized by the magnitude of "x", the oxygen coefficient, it may be said that the first two types of the patterns are produced by the oxides whose "x" is 2.5 or lower. The remaining two types are the oxides whose "x" is higher than 2.5. Experience shows that the best x-ray patterns of the oxides were produced with copper radiation. Patterns so obtained mad it possible qualitatively to appraise the degree of oxidation of a natural uranium oxide. There is no clear-cut boundary between the types of patterns, of course, even as there is no such boundary between natural uranium oxides whose composition embraces the whole gamut of the $UO_3:UO_2$ ratios, i.e. whose "x" ranges from two to three. The x-ray powder photographs of all four types (the oxide group) are presented in Figure 2.

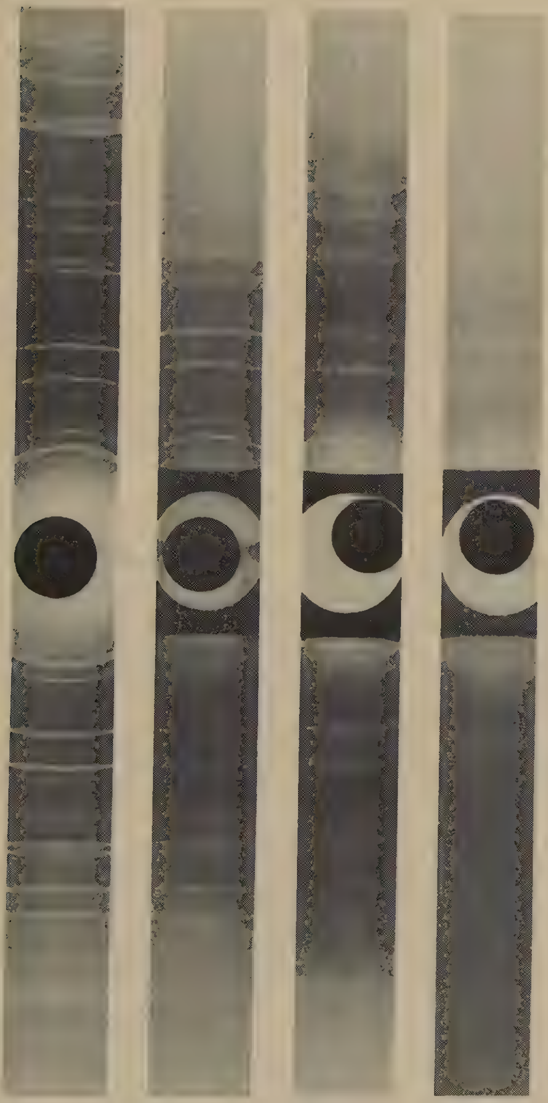

Fig. 2. X-ray powder patterns of the four groups of natural uranium oxides. Character of the diffraction lines permits a qualitative estimation of the degree of oxidation of the oxide (Cu radiation).

Table 1. Spectrographic Analysis of Uraninites

Sample No.	More than 1%	ca. 1%	ca. 0.1%	ca. 0.01%	ca. 0.001%
1	U, Pb, Si Fe	Na	Al, Mg, Ca Mn, P	Ni, Co, Mo, Cu, Sb	Bi?
2	U, Pb, Si, Fe	Ca, Na	Al, Mg, P, Mn, Cu	Ni, Co, Ag, Sb	-----
3	U, Pb	Ca	Si, Al, Mg, Y, Yb, Na	Fe, Mn, Cu, Sc	Ag
4	U, Pb	------	Al, Y, Yb	Si, Mg, Fe	Mn, Cu
5	U, Pb, Si, Fe, Mg	Ca, Na	Al, Mn, P	Ni, V, Mo, Cu, Sb	Ag
6	U, Pb	Th	Y, Yb	-----	-----
7	U, Pb, Fe	Si, Mg, Ca, Mn	Al, Zn, Sn	Ti, Zr	Cu, Ag, Bi
8	U, Pb	------	Si, Al, Fe, Th, Y, Yb	Mg, Ca, Mn, Cu, Bi	Ag
9	U	Ca, Cu, Pb, Na	Si, Al, Fe, Y, Yb	Mg, Mn, Ag	Sn

We know from the studies of synthetic uranium oxides that within the $UO_{1.75}$ to $UO_{2.50}$ composition range a crystal structure of the CaF_2 type is characteristic of the oxides and that the size of the unit cell becomes smaller, depending on the oxidation of tetravalent uranium to hexavalent uranium. We know also that the dimensions of the unit cell of natural uranium oxides are not constant [1, 3, 13, 14, 16]. It is natural therefore to relate the unit cell sizes to the degree of oxidation for the natural uranium oxides. Comparisons of this type were undertaken in the present study.

Table 2. Microchemical Analysis of Uraninites

Sample No.	UO_2, %	UO_3, %	ThO_2, %	PbO, %
1	32.23	18.19	--	very high
2	34.32	19.69	--	very high
3	39.79	26.00	--	17.38
4	41.78	28.92	--	20.28
5	28.73	24.91	--	very high
6	42.64	37.83	present	19.53
7	32.04	31.11	--	18.64
8	37.80	37.46	1.62	19.05
9	27.07	35.32	--	high

The objects of our study were specimens of uraninite, pitchblende, and uranium black. Spectrographic and microchemical determinations of their principal constituents are reported in Tables 1, 2, 3, and 4. Their mineralographic examinations (in polished sections) showed inclusions of pyrite, galena, chalcopyrite, and some other sulfides. These specimens were selected chiefly from samples which were analyzed chemically and by x-rays, so that the x-ray patterns showed only the oxides of uranium in the samples.

Size of the unit cell, a_0, for all of the natural uranium oxides was investigated in the present study. Table 5 is a comparison of the oxygen coefficients of the uraninites with the size of their unit cell. The oxygen coefficient, "x", was calculated from the chemical analysis.

A phenomenon analogous to the previously noted phenomenon, in the case of synthetic materials, may be now seen in the uraninites, as is

Table 3. Spectrographic Analysis of Pitchblende (Groups 2 & 3)

Sample No.	More than 1%	ca. 1%	ca. 0.1% *	ca. 0.01%	ca. 0.001%
10	U, Al	Ca, Si, Na, Pb, Mg, Ba	Co, P, Tl, Cu, As, Zn, Ni	Fe, Y, Yb, Mn, Bi, Sb, Ag	----
11	U, Pb	------	Sl†, Si, Al, Ca	Na, Fe	----
12	U, Pb	Si, Al, Ca, Fe, Bi, Mn	Mg, V, W, As, Na	Mo, Cu, Ag, Sb, Sn, Be	Ge?
13	U, Pb	Si	Mn, Co, Cd, W, Sb, Tl, Zn	As, V, Cs, Cu, Y, Yb, Ag	Sn, Be, Ga, Ge
14	U, Ca	Si, Al, Mg	Fe, Ti	Mn, V, Zr, Pb, Na	Cu
15	U, Pb	------	Si, Ca	Al, Fe	----
16	U, Ca, Fe, Pb, As	Al, Ag, Sb, Na	Si, Mg, Mn	V, Mo, W, Cu, Y	Ni, Bi
17	U, Pb	Ca, Sb, As, Na	Al, Mn, Mo	Si, Mg, Fe, Zn	Cu, Ge
18	U	Al, Si, Mg, Pb, As	Fe, Cu, Sb, Bi	Ca, Mn, Ti, Zr, Ag, Y, Yb	Ni
19	U	Pb, Si	Al, Ca, V, Bi, As	Mg, Fe, Mn, Y	Cu, Ag, Be
20	U	Ca, Zn, Si	Al, Be, Mn	Mg	Cu, Ge, Pb?
21	U	Si	Al, Ca, As	Pb, Be, Y, Yb	Fe, Mn
22	U, Ca	Si, Zn, Be	Al, Mn, Sb	Mg, Fe, Cu	Pb?
23	U	Ca	Si, Al, As, Sc	Mg, Fe, Pb, Mn, Y, Yb	Ni, Ti, Cu

* "0.01" in the original; a misprint. VPS

† "Sl" - a misprint for Se? Sc? Sb? VPS

illustrated by the foregoing comparison: a decrease in the size of the unit cell, depending on the extent of the oxidation of tetravalent to hexavalent uranium, i.e., the fact that uraninites, at the higher degree of their oxidation, have a smaller unit cell without any change in its symmetry. In contrast with synthetic crystals preserving their CaF_2 type structure within a narrow range of the oxygen coefficient, "x" from 2.00 to 2.25, the natural crystals retain this structure within a much wider range of the "x". In the present study, we had uraninites whose oxygen coefficient ranged from 2.32 to 2.53, with the parallel and gradual decrease of the unit cell from 5.480 to 5.455 Å. Individual samples (Nos. 4 and 8) show certain departures from this relationship. However, spectrographic analysis demonstrated presence of small amounts of thorium and of the rare earths in such samples. As we know, thorium may substitute isomorphously for tetravalent uranium.

Table 4

Microchemical Analysis of Pitchblende (Groups 2 & 3)

Sample No.	UO_2, %	UO_3, %	PbO, %
Group 2			
10	35.19	17.00	0.63
11*	22.57	7.79	6.86
12	59.16	27.59	1.00
13	55.93	29.00	10.19
14	36.20	27.56	low
15	38.67	28.03	19.68
16	42.19	33.15	2.18
17	43.46	47.63	very high
18	32.10	44.30	none
Group 3			
19	34.91	38.58	high
20	32.03	41.87	none
21	37.43	42.27	0.31
22	28.78	50.29	none
23	33.00	57.52	low

*The low U-content of this sample is explained by an insufficiently careful sorting of the test material from the admixtures.

Existence of the complete isomorphous series, from UO_2 to ThO_2, was proved for synthetic compounds [22]. Sabina and Robinson [20] demonstrated the existence of different members of this series in natural environments, from uraninites to thorianites, in a confirmation of natural replacements of uranium by thorium. Inasmuch as the ionic radius of thorium is larger than the ionic radius of tetravalent uranium

Table 5

	Sample No.								
	1	2	3	4	5	6	7	8	9
"x"	2.32	2.36	2.38	2.40	2.45	2.46	2.48	2.48	2.53
a_0, Å	5.480	5.479	5.472	5.460	5.470	5.459	5.458	5.455	5.456

the replacements of this type cause an increase in the size of the unit cell of uraninite. The isostructural relation of UO_2 and CeO_2 gives us a reason to suppose that the rare earths also may enter the crystal structures of uraninite, by way of the isomorphous replacement of tetravalent uranium. It is this mechanism that is responsible for the departures from the norm, in the relationship between the unit cell size and the degree of oxidation of uraninite.

Table 6 is a comparison of the unit cell size with the oxygen coefficient for pitchblende in groups 2 and 3, indicating that the relationship between these two variables, already observed in uraninite, is apparent also in the case of pitchblende. Pitchblende,* as a rule, contains no thorium or rare earths, and any departures from the direct relationship should be rare accordingly. Such departures could be more easily ascribed to errors in chemical analysis to which we had to resort, in the absence of a more reliable method, unaffected by the admixtures, of appraising the degree of oxidation of uranium. As the "x" varies from 2.16 to 2.62, the unit cell edge of pitchblende varies from 5.46 to 5.37 Å.

Table 6

Group 2

Sample No.

	10	11	12	13	14	15	16	17	18
"x"	2.16	2.25	2.31	2.33	2.37	2.43	2.43	2.50	2.56
a_0, Å	5.46	5.45	5.43	5.43	5.42	5.42	5.41	5.41	5.41

Group 3

Sample No.

	19	20	21	22	23
"x"	2.51	2.52	2.52	2.62	2.62
a_0, Å	5.39	5.38	5.37	5.37	5.37

The unit cell size of pitchblende decreases with the transition from the less to the more oxidized samples. However, this is not a simple extension of the relationship observed in uraninites, at the increasing "x", as is evident from the graphical representation of the x = f(a) relationship shown in the same system of the coordinates. As illustrated in Figure 3, we are dealing here with two parallel relationships between the unit cell size and the oxygen coefficient. The cause of this phenomenon is hidden probably in the genetic peculiarities of the morphologic variants in question.

---

*This sentence is garbled in the original. VPS

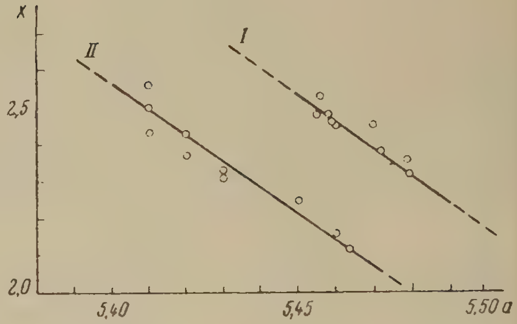

Fig. 3. The x = f (a) relationship for uraninites (I) and pitchblende (II).

The manifested relationship enables us to ascertain the state of oxidation of uraninites, poor in thorium and in rare earths, by the sizes of the cube edge of their unit cells. This appraisal requires the use of 5 to 10 mg of the substance. Reliability of unit cell measurements is not the same for uraninite and for pitchblende, because pitchblende produces diffuse lines at large reflection angles. Experience shows that, if the magnitude of a_0 is determined with the reliability of 0.001 Å (for uraninite), the reliabilit of "x" is ± 0.02; if the reliability of a_0 is ± 0.005 to 0.01 Å (for pitchblende), the accuracy of "x" is ± 0.05 of its absolute magnitude, which is equivalent to ± 2%, absolute, in the separate chemical determinatior of UO_2 and UO_3. Mineralogists may be entirely satisfied by such accuracy, especially if only small quantities of the test material are available.

Natural uranium oxide has a crystal structure analogous to syntheti uranium dioxide and thus is of the fluorspar type. As the state of oxidation increases crystallization becomes less perfect.

The cause of the decrease in the unit cell size of natural uranium oxides with oxidation could reasonably be ascribed to the isomorphous replacements of tetravalent uranium (ionic radius 0.89 Å) by hexavale uranium (ionic radius believed to be 0.78 Å). The resulting increase i the valence of uranium is compensated by the entry of supplementary oxygen atoms into the crystal structure, into the octahedral interstice of the uranium pocket (i.e. the oxygen atoms are placed in the centers of the sides of the unit cube) or into the center of the cell. The latter alternative is less probable, however, from the crystal-chemical poin of view, inasmuch as, in a case like this, the nearest neighbors of oxygen would be other oxygen atoms. The settling of the supplementary oxygen atoms and the row (the side) of the cell, on the other hand, wou be in keeping with the CaF_2 type structures, on the whole (for exampl CaF_2 + YF_3). Another consideration in favour of such distribution of oxygen atoms is the gradual transition of the isometric into the tetragonal phase, observed in synthetic uranium oxides, as a possible consequence of the distribution of the supplementary oxygen atoms not only on the horizontal but also on the vertical rows of the unit cube.

The penetration of oxygen into the structure does not push the uranium atoms apart because the octahedral cavities are already sufficiently large (the length of the row of the cube is 5.46 Å and the sum of two ionic radii of U^{4+} is 1.78 Å). Consequently, the isomorphous replacement of U^{4+} by U^{6+}, which may be thought of as governed by the Vegard Rule, is really definitive of the unit cell size. The slow oxidation of uranium in natural environments does not upset the symmetry of the unit cell, as happens in synthetic oxides, and only large proportions of U^{6+} may disturb the crystal structures, as reflected in the character of the lines in the x-ray patterns.

2. DIFFUSENESS OF DIFFRACTION PATTERNS OF PITCHBLENDE AND URANIUM BLACK IN X-RAY POWDER DIAGRAMS

Strongly oxidized pitchblende and uranium black produce diffuse diffraction lines in their x-ray powder diagrams, as we stated. This diffuseness increases for samples with high oxygen coefficients.

It is known that the diffraction lines are diffuse for highly dispersed substances, i.e. where the crystallites are smaller than 0.1 micron, and also if the crystal structures of the test material carry strains of some other kind, sufficient to affect distances between the parallel planes or between some individual planes, in consequence of which there are reflections from the planes, within a certain range of the angles, whose interplanar distances, $d + \Delta d$, are of similar magnitudes. The mechanism responsible for the broadening of the diffraction lines may be surmised on the premises to the effect that the expansion caused by the strains of the second kind increase progressively at increasing reflection angles, proportional to $\tan\theta$, while the expansion which depends on the state of dispersion of the sample is proportional to $\lambda \sec\theta$, i.e. is determined by the wave length of the x-ray spectrum employed in the analysis.

In order better to understand the diffuseness of the diffraction lines of strongly oxidized pitchblende and uranium black, we took x-ray powder patterns of a series of samples at different wave lengths of the radiations: chromium, iron, and copper (λ 2.287, 1.934, and 1.539 Å respectively) at the following routine conditions for the tubes: voltage 25, 30, and 40 kv; current 8, 10, and 16 m.a. respectively; diameter of cameras 57.3 and 86.0 mm; diameter of samples 0.3 to 0.4 mm. An internal standard was used. Broadening of the diffraction lines was estimated with the aid of the Johns nomogram; the x-ray patterns were taken microphotometrically, with the MF-4 microphotometer and the estimations were made with the IZA-2 comparator. It was found that the diffuseness of the lines depends on the wave length of the radiation (Fig. 4) and that the relationship between the broadening of the lines and the angle of reflection, $\beta = f(\theta)$, may be taken as evidence confirming that the diffuseness of the diffraction lines of strongly oxidized pitchblende and uranium black is due to the degree of dispersion of

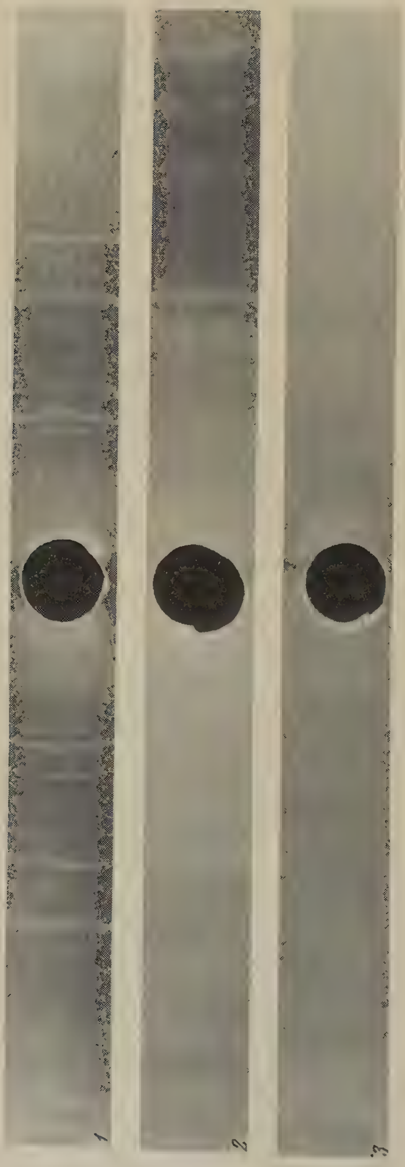

Fig. 4. X-ray powder patterns of pitchblende obtained at different wave lengths (Cr, Fe, Cu radiations).

ıese minerals which increases with the degree of their oxidation. his conclusion justifies the use of the Seliakov-Bragg Equation in esmations of the size of the crystallites of pitchblende and of uranium lack:

$$\beta = \frac{C \times \lambda}{\epsilon \times \cos\theta}$$

here β is the diffraction broadening of the lines in the x-ray pattern, . - the wave length of the radiation employed, ϵ - the length of a row ı the cubic crystallite, θ - the angle of reflection, C - constant, ssumed to be 1.0 to 0.9.

The size of crystallites of strongly oxidized pitchblende and of ranium black, at "x" larger than 2.5, is within the 150 to 300 Å range. he ϵ decreases at increasing magnitudes of the oxygen coefficient, ith a concurrent decrease of the size of the unit cell. (A more detailed tudy of the dispersion of uranium oxides is to be reported in a separate ıblication.)

3. CHARACTER OF PHASE TRANSFORMATIONS OF NATURAL URANIUM OXIDES OF IGNITION

We know from the studies of synthetic and natural uranium oxides ıat synthetic uranium oxides preserve their crystal structure of the aF_2 type within a narrow range of the "x" (1.75 to 2.24); oxidation by nition in the air causes a recrystallization of the cubic phase into the tragonal, at x = 2.24 and 175°C. The hexagonal oxide, U_3O_8, begins be formed at 300°C. Natural uranium oxides preserve their crystal ructure of the CaF_2 type in natural environments within a much wider ınge of variation of the "x", practically from 2 to 3; the course of idation is slow in natural environments and the oxidation is likewise nducive to changes in the size of the unit cell, while leaving its symetry unaffected. Goldschmidt and Thomassen [7], who were the first vestigators of uraninite crystal structures, reported that "Ignition in e presence of oxygen causes a partial or a complete conversion of aninite into U_3O_8, while pure UO_2 remains unaffected." This thesis d Conybeare and Ferguson [6] to their investigations of the ignition oducts of pitchblende from Saskatchewan and to their classification pitchblende which was based on comparisons of x-ray powder patrns (more specifically of the phase composition) of the original and e ignited samples. According to Conybeare and Ferguson, such comrisons may be the means of tentative appraisals of the degree of idation of uranium, in the given pitchblende:

"1. Crystalline pitchblende; unoxidized; strong UO_2 pattern, before d after ignition.

2A. Metamict pitchblende; unoxidized; UO_2 pattern weak before the nition; stronger afterwards.

2B. Metamict pitchblende; partially oxidized; weak UO_2 pattern bere ignition; moderately strong pattern of UO_2 and U_3O_8 afterwards.

2C. Metamict pitchblende; strongly oxidized; weak UO_2 before ignition; weak UO_2 pattern after ignition, together with moderately strong U_3O_8 pattern.

3. Crystalline pitchblende; strongly oxidized; strong UO_2 pattern before ignition; strong U_3O_8 and insignificant UO_2 after ignition."

The authors of the pitchblende classification ascribe the difference in the behavior of pitchblende on ignition to differences in the oxygen content of pitchblende of different kinds, since oxygen "reacts chemically with uranium, on ignition", on their assumption that oxygen of th air is neutral. Some other investigators see the cause of the differences in question among the mechanical admixtures of other minerals in the pitchblende. However, before we may talk about the causes of different behavior of natural uranium oxides on ignition, we must lear experimentally the details of the phase transformations suffered by natural oxides of uranium on ignition. Investigations presently to be discussed were carried out by the groups: uraninites; pitchblende; uranium black. The test materials were the samples whose spectrographic and chemical analyses were reported earlier in this article (with regard to their principal constituents).

The artificial oxidation of the samples was carried out in a muffle furnace and in open porcelain crucibles. The temperature routine wa regulated by the mercury thermostats of the muffle. Moreover, the temperature inside the muffle was controlled by a millivoltmeter wit a platinum-palladium thermocouple, with the reliability of ± 5°C. 3 t 5 mg aliquots of the samples were pulverized in an agate mortar, ignited for 30 minutes, at a definite temperature, whereupon they were re-ground in the mortar and were readied for the x-ray analysis, by having their powder pasted onto a glass thread, 0.25 to 0.30 mm in diameter, with the aid of the tzapon-lac. Individual portions of every mineral were ignited at 50°C intervals, i.e. at 300, 350, 400, 450°C, etc., within the 300 to 1000°C temperature range. X-ray patterns of the ignition products were taken, using unfiltered copper radiations a 45kv, and 16 m.a. current, in cameras with 57.3 mm diameter (RKD). The ignition products were identified by the standard x-ray powder patterns. Whenever there was evidence of a new phase in crystal structures, such phase was re-photographed with large-diameter can eras (86.0 or 114 mm). Additional recordings of the new phase were made with the use of the internal standard (NaCl), so as to obtain cor rected values for the interplanar distances. We were aware of the fa that, in the analysis of the ignition products, a recrystallized phase may be detected by the x-ray powder method only if its crystallites a larger than 0.01 micron in diameter and when they constitute 5 to 10 of the sample, by volume, i.e. that there is a delay in recording tran formations of the phases by the method here employed. Ignition curv for natural uranium oxides were recorded by the F. V. Syromiatniko pyrograph.

RESULTS

Table 7 is a generalized record of the phase transformations in raninites during ignition.

It follows from Table 7 that: 1) The crystal structure of the CaF_2 ype, inherent in all uraninites, in their natural environments, is reained by them up to 500 to 550°C; there is a general weakening of the iffraction pattern and an intensification of the background at temperaures exceeding this threshold; this is indicative of a partial destrucion of the crystal structure, although a complete transition into the morphous state is not observed. 2) A new phase, designated here as , is formed at 550 to 600°C; this new phase is retained by most urannites on ignition up to 1000°C (this phase is described later).) Strongly oxidized uraninites pass through phase X before they enter hase Y, which was observed by Brooker and Nuffield [8], in their tudies of ignited pitchblende from Canada. The Y phase was formed t 800 C, in that particular case. 4) Formation of the hexagonal phase $_3O_8$ was observed only in two instances. This phase originates at 600 o 700°C; it co-exists with phase X, for some time, becoming independnt only at 800 to 1000°C. Phase X is not found together with phase Y.

Table 7.* Characteristics of Phases Developed in Ignition of Uraninites

Key: C - cubic phase; CaF_2 type structure. C_f[†] - the same phase but with diffuse diffraction lines; Y - the Y phase (see below); X - the X phase of Brooker and Nuffield [8]; H - the hexagonal phase U_3O_8.

t°C x	450	500	550	600	650	700	750	800	850	900	950	1000
2.32	C	C	Cd	Y	Y	Y	Y	Y	Y	Y	Y	Y
2.36	C	C	Cd	Y	Y	Y	Y	Y	Y	Y	Y	Y
2.38	C	C	Cd	Y	Y	Y	Y	Y	Y	Y	Y	Y
2.40	C	C	Cd	CH	CH	CH	H	H	H	H	H	H
2.46	C	C	X	X	X	X	X	← not determined →				
2.48	C	C	Cd	Cd	Cd	CdH	CdH	CdH	CdH	CdH	HCd	HX?
2.48	C	C	C	Y	Y	Y	Y	Y	Y	Y	Y	Y
2.48	C	C	X	X	X	X	X	X	X	Y	Y	Y
2.53	C	C	Cd	X	X	X	X	Y	Y	Y	Y	Y

* The Cyrillic letters in the Key including Y and X which are used as Latin Y and X, are transliterated here as follows:
К as C; Г as H; Х as X;
Д as d; У as Y; Ф as f. VPS

[†] "Cd" does not appear in the original Key but is shown in the original Table; "Cf" is explained in the Key but is not used in the Table. The two mean probably the same thing. VPS

Temperatures of transition of one phase into another and the charac ter of the phase transformations in uraninites, on the whole, are not related either to the degree of their oxidation or to their composition or to the size of their unit cell.

It was observed that the size of the unit cell of the cubic phase is diminished by ignition in open air. There is no such diminution on ignition in hydrogen; this casts a doubt on the thesis of Conybeare and Ferguson [9] to the effect that the phase transformations in natural uranium oxides, on ignition, are due to the interaction between U^{4+} anc the excess of oxygen contained in the oxide structures.

Thermal analysis of three samples, by the Syromyatnikov pyrograp were performed in parallel with the x-ray studies of the phase transformations in uraninites. The thermograms are shown in Figure 5. A of them are characterized by a single exothermal effect at 325 to 350° Referring our thermograms to the results of the x-ray analysis, we may draw the following conclusions: 1) The smooth endothermal effect is related to a partial destruction of the uraninite crystal structure through oxidation of U^{4+} to U^{6+} which is expressed as an intensificatic of the background and of the diffuseness of the diffraction pattern in th x-ray diagram. 2) The exothermal peak (325 to 350°) is associated with the formation of a new phase, Y or X. Inasmuch as there is a del in the x-ray recording of this new phase, we refer this event to the 50

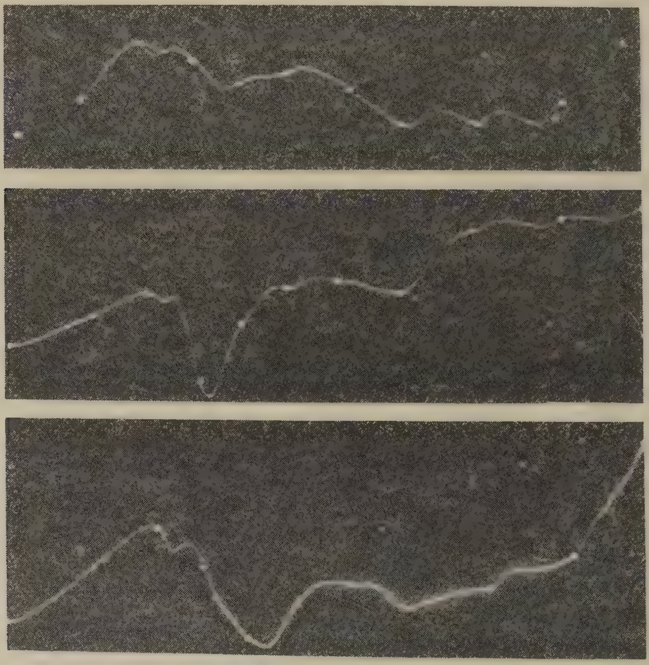

Fig. 5. Thermograms of uraninites (Syromyatnikov pyrograph).

550°C range. 3) The fluctuations in the thermogram at temperatures
oove 350°C may be treated as a super-imposition of the recrystalli-
ation effects, because neither the Y nor the H phase remain constant
n subsequent ignition (see below).

PITCHBLENDE

Behavior of pitchblende on ignition is more uniform than the be-
avior of uraninites and is rather different. The cubic phase of the
aF_2-type structure is retained up to 500 to 700°C by weakly and
oderately oxidized pitchblende but only to 400 to 500°C by strongly
xidized ones. The hexagonal phase U_3O_8 originates abruptly at these
mperatures and it co-exists at first with the cubic phase. The tem-
erature of the formation of the hexagonal phase is inversely propor-
onal to the oxygen coefficient ("x") of the original pitchblende: the
reater the "x" - the lower is the temperature of the origin of U_3O_8.
he hexagonal phase at its inception is characterized by one single
large" unit cell, according to Milne [19]; a smaller unit cell is de-
eloped in all pitchblende at 700°C; both phases remain co-existent
rom then on.

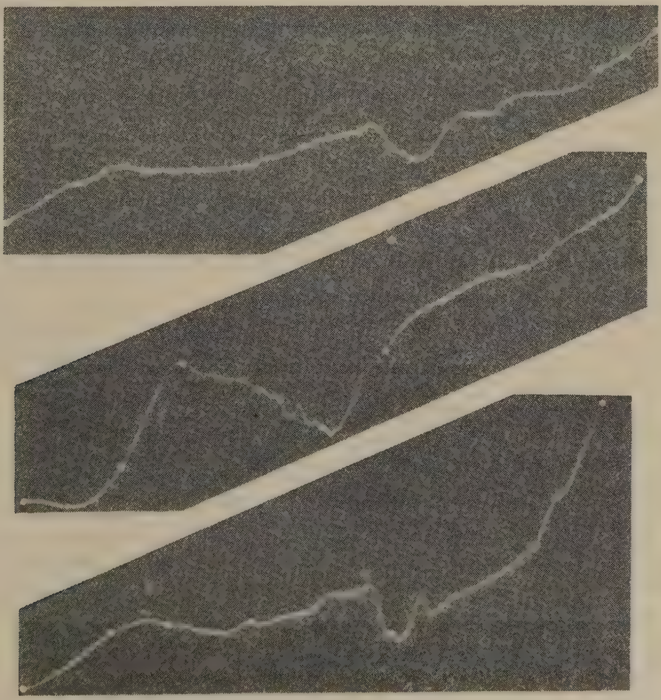

Fig. 6. Thermograms of uranium pitchblende (Syromyatnikov pyrograph).

Phase Y is observed very rarely in the ignition of pitchblende.

The tetragonal phase is not observed.

Thermograms of pitchblende (Fig. 6) are fairly uniform and are characterized by one major exothermal peak within the 450 to 700°C range, followed by minor fluctuations at higher temperatures. This peak may be naturally referred to the crystallization of U_3O_8; the fluctuations—to the appearance of hexagonal phases of different kinds. A small endothermal peak at 100 to 300°C is related apparently to the loss of adsorbed water and to a partial destruction of the crystal struc ture by the artificial oxidation.

URANIUM BLACK

The test materials, in this case, were represented by isolated samples of small weight and we are not entitled to make any generalizations for that reason. Nevertheless, certain peculiarities in the behavior of uranium black during ignition seem to be indicated: the lines of the x-ray powder diagrams corresponding to the crystal struc ture of the CaF_2 type are broadened and weakened progressively and disappear in the end, at about 400 to 500°C; the background increases in its intensity concurrently and the oxide passes into its amorphous state. The amorphous oxide becomes recrystallized, with the formati of the Y phase or, more rarely, of the hexagonal phase, at 500 to 700° temperature of the crystallization depends on the degree of oxidation the original sample. Formation of crystalline UO_3 is not observed during ignition of uranium black.

DEPENDENCE OF TEMPERATURE OF RECRYSTALLIZATION OF NATURAL OXIDES INTO HEXAGONAL PHASE ON DEGREE OF THEIR OXIDATION

It was observed by different investigators on several occasions tha the transition temperature at which natural uranium oxides pass into U_3O_8 is not constant. The cause of this phenomenon was generally se in various mechanical admixtures to the oxides. However, it is not possible for us to share this view, on comparisons between recrystall zation temperatures of the oxides with their spectrographic and chem cal analyses as well as with the mineralographic characteristics of th minerals (paragenesis). A clear-cut relationship between the recryst lization temperature and the degree of oxidation of the original sampl exists within the group of minerals in which both pitchblende and urar um black are included. Table 8 presents a comparison between the transition temperatures (to U_3O_8) and the oxidation coefficients of the original samples, for a series of pitchblendes and uranium black.

Even a relative appraisal of temperatures at which the oxides pass into U_3O_8 (we cannot call these temperatures "absolute", because the x-ray analysis records appearance of a new phase only after a certai

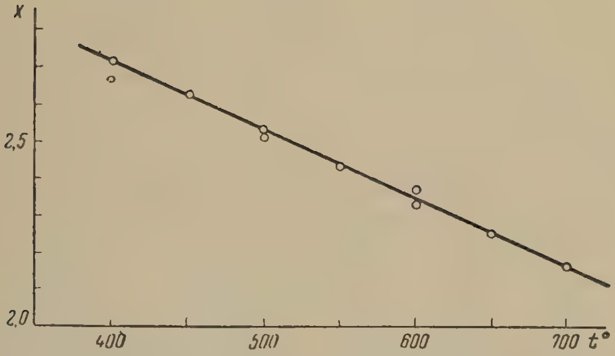

Fig. 7. Relationship between transition temperatures into the hexagonal phase U_3O_8 for pitchblende and uranium black and the degree of their oxidation.

ay and because the temperature grid is relatively sparse in the igni-
n of our samples) permits us to maintain that the reason for the in-
ıstancy of the recrystallization temperature at which natural uranium
des are converted into U_3O_8 is found in the differences between their
grees of oxidation in their natural state. The oxidation of U^{4+} to U^{6+}
a natural uranium oxide loosens the crystal structure and facilitates
reorganization. The higher is the proportion of U^{6+} in the natural
de—the lower is the temperature of its transition into U_3O_8; the
it here is 300°C, i.e. the crystallization temperature of synthetic
O_8. This limiting temperature should be specific for a natural
nium oxide, although ignition up to 700°C is required for the re-
stallization of a weakly oxidized pitchblende. Figure 7 is a graphic
resentation of the relationship of the temperature of the transition
U_3O_8 and the degree of oxidation, in the case of pitchblende and
nium black.

Table 8

	Sample No.											
	10	11	12	13	14	15,16	19	20,21	24	22	25	26
"x"	2.16	2.25	2.31	2.33	2.37	2.43	2.51	2.53	2.53	2.62	2.66	2.71
t,°C.	700	650	600	600	600	550	500	500	500	450	400	400

HEXAGONAL PHASE

Milne [19], in his x-ray studies of single-crystal structures of
thetic U_3O_8, showed that this oxide has a hexagonal symmetry, in

its atomic distribution, and that it consists of two phases of a single structural type, in the majority of the cases, the unit cells of which differ one from another only by their size (a_0 3.86 and 3.93 Å) and that the orientation of these two phases, in single crystals, is parallel to each other.

X-ray investigations of the products of ignition of natural uranium oxides enabled us to establish that, in the case in question, the "one-cell" phase, with a large unit cell, is formed first, while further ignition leads invariably to the formation of the "two-cell" U_3O_8. The cubic phase "jumps" into the first hexagonal phase but the first hexagonal phase passes into the second one gradually: the images of the first hexagonal phase are split and parted, while the a_0 of the smaller unit cell is going through its change. Individual samples at temperatures in the vicinity of 900° produce an oxide containing several phases with different unit cell sizes a_0. The result of this is an involved diffraction pattern in which the reflections hkl, h00, 0k0 are replaced by groups of sharp reflections corresponding to several phases within a single structural type. Estimations of the parameters for every phase are made difficult by this particular complexity of the pattern. Table 9 reports the interplanar distances of the phases—the products of ignition of natural uranium oxides: the "one-cell", the "two-cell", and the "multi-cell" hexagonals. The character of the changes in the hexagonal phase is the same, whether the initial material is uraninite or pitchblende.

Y PHASE

A new phase, here designated as Y, is formed on ignition of uraninites, strongly oxidized pitchblende, and uranium black. This phase is the end-product of the ignition, as if it were a replacement of the hexagonal phase. Transition from the cubic to the Y phase is gradual: there is a gradual weakening of the (311) reflection of the cubic phase accompanied by its broadening, a growing intensity of the (220) reflection, together with a progressively increasing general diffuseness of all reflections at the larger magnitudes of the angle. The exact temperature at the inception of the Y phase could not be registered, because of the superimpositions of every one of the clear reflections at small angles on the reflections of the cubic phase at the first moment of the existence of the new phase. At increasing temperature of ignition, reflections of the Y phase became clearer, whereupon they began to split, with the formation of complex groups which could be interpreted by analogy with the hexagonal phase, as the result of an imposition of the diffraction patterns belonging to several phases resembling one another in their crystal structures. The number of the phases is not the same in different stages of the ignition, with the resulting differences in the complexity of the diffraction patterns. The "one-cell" phase is formed first; the "two-cell" is next; finally come the

Table 9. Interplanar Distances in Hexagonal Phases - Products of Ignition of Natural Uranium Oxides

“one-cell”		“two-cell”		“multi-cell”		“one-cell”		“two-cell”		“multi-cell”	
d/n	I	d/n	I	d/n	I	d/n	I	d/n	I	d/n	I
--	--	--	--	6.87	2	--	--	1.324	5	1.331	1
--	--	--	--	5.86	3	--	--	1.312	2	1.319	1
--	--	5.16	2	5.07	1	--	--	1.300	2	--	--
4.61	2	4.58	4	4.62	5	--	--	1.282	7	1.285	8
4.14	7	4.14	10	4.11	5	1.266	2	1.264	1	--	--
3.77	2	3.79	4	3.76	2	--	--	1.252	5	1.255	2
--	--	3.69	1	3.50	3	--	--	1.224	5	1.231	2
3.42	10	3.44	10	3.41	10	--	--	1.209	4	1.217	1
--	--	3.33	7	3.32	6	--	--	1.197	1	1.196	1
--	--	--	--	3.23	10	--	--	1.147	3	1.147	3
2.914	1	2.926	4	3.024	2	--	--	1.139	3	--	--
--	--	2.878	1	--	--	--	--	1.126	5m	--	--
--	--	--	--	2.731	5	--	--				
--	--	--	--	2.703	5	--	--	1.089	4	--	--
2.632	9	2.645	10	2.652	8	--	--	1.078	6	--	--
--	--	2.591	7	2.608	2	--	--	1.062	1	--	--
--	--	--	--	2.516	5	--	--	1.036	3	--	--
--	--	2.293	2	--	--	--	--	1.003	4	1.016	1
--	--	2.214	1	2.208	4m	--	--	--	--	1.002	1
--	--	2.148	2	--	--	--	--	0.9928	6m	0.9907	1
2.070	3	2.073	6	2.086	4	--	--	0.9764	2	--	2
--	--	2.004	5	2.017	8	--	--	--	--	0.9696	--
1.945	6	1.941	7	1.986	8	--	--	0.9604	1	--	--
--	--	--	--	1.960	8	--	--	0.9520	3	0.9567	1
--	--	1.903	2	1.896	6	--	--	0.9358	2	0.9445	1
--	--	1.868	1	1.843	6	--	--	0.9221	3	0.9334	1
--	--	1.835	1	--	--	--	--	0.9170	3	--	--
--	--	1.806	5	1.815	7	--	--	0.9051	3	--	--
--	--	1.776	8	1.785	7	--	--	0.8915	3	--	--
1.756	8	1.758	9	1.769	7	--	--	0.8838	4	--	--
--	--	1.715	5	1.724	5	--	--	0.8753	2	0.8678	2m
--	--	--	--	1.691	6	--	--	0.8616	4	--	--
--	--	1.664	4	1.666	1	--	--	0.8473	4	0.8564	2m
--	--	1.588	6	1.605	8	--	--	0.8180	4	--	--
1.579	2	1.570	1	1.551	1	--	--	0.8107	5	--	--
--	--	1.544	5	1.524	1	--	--	--	--	--	--
--	--	--	--	1.485	2	--	--	--	--	--	--
--	--	1.441	6	1.452	5	--	--	--	--	--	--
1.409	3	1.418	8	1.422	6	--	--	--	--	--	--
--	--	1.382	4	1.407	3	--	--	--	--	--	--

ulti-cell” phases. The Y phase is most characteristic for strongly idized varieties of the minerals: such minerals contain large propor- ns of U^{6+} and their transition into Y phase is gradual; if there is not ough U^{6+} from the start, to bring about such gradual transition into Y ase, the supplementary oxidation of U^{6+} to U^{4+} caused by the ignition leads to the formation of the hexagonal phase.* Uraninites are an exception to this generalization: although they are not strongly oxidized, they pass into the Y phase, on ignition, possibly because of the greater resistance to oxidation on the part of their crystal structures. The Y phases—the ignition products—in uraninites, pitchblende, and uranium black are identical. Y phase has a brilliant orange color, indicative possibly of the high degree of oxidation of the original substance. Table 10 gives the interplanar distances for the Y phase at different levels of oxidation. Figure 9 is an x-ray pattern of the "multi-cell" phase Y.

X PHASE

This phase was first observed by Brooker and Nuffield [8] in their ignition studies of Canadian pitchblende. This phase was observed in our studies only on the ignition of uraninites whose oxygen coefficient was from 2.45 to 2.53. The X phase is formed at 500 to 600°C and is a predecessor of the more strongly oxidized phases (the hexagonal or the Y). Phase X is tetragonal. Dimensions of the unit cell of this phase were found to be as follows, by the analysis of its x-ray powder pattern with the aid of the Hull curves: $a_0 = 5.31 \pm 0.01$; $c_0 = 5.52 \pm 0.01$ Å; $c/a = 1.04$. This phase is different from the synthetic tetragonal phase. Transition of the cubic phase into X phase is gradual: first, the reflections from the cubic phase are broadened in the x-ray pattern, then split and sharpened, as the tetragonal phase X forms. Unlike the synthetic oxides, natural uranium oxides produce only one tetragonal phase on ignition. The x-ray pattern of this phase is shown as Figure 10. Table 11 gives the interplanar distances, the relative intensities, and the refraction indices for the tetragonal phase X, in comparison with the data by Brooker and Nuffield [5].

CONCLUSIONS

1. The multiplicity of crystal structures of synthetic uranium oxides, corresponding to different degrees of oxidation of the contained uranium, has no analogies in nature, where uranium oxides maintain their cubic structure of the CaF_2 type, identical with synthetic UO_2, and where there is no constancy in the composition and properties of the oxides.

---

*The original is poorly intelligible here. It reads: "supplementary oxidation U^{4} to U^{6+} which leads to the formation, if the amount of U^{6+} is insufficient for the formation of the Y phase, there is the hexagonal phase." The translation of this sentence, "if there is not enough" is the translator's wording, in harmony with the context. VPS

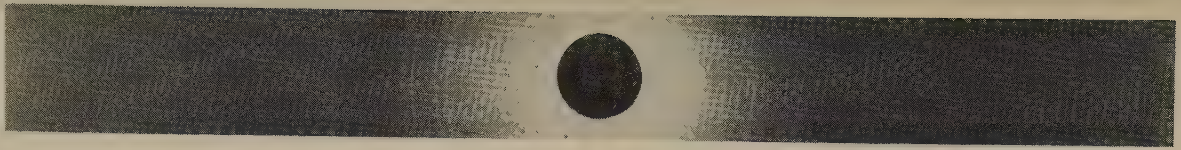

Fig. 8. X-ray powder patterns of ''multicell'' hexagonal phase, the product of ignition of a natural uranium oxide ($CuK_{\alpha\beta}$, diameter of camera 86.0 mm).

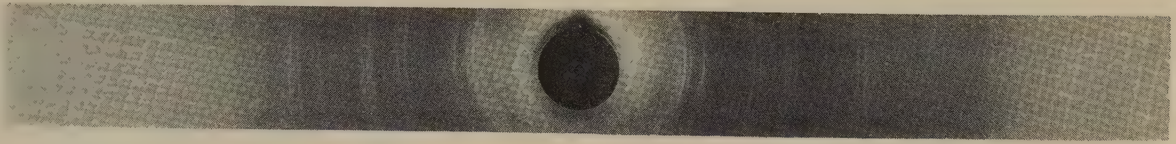

Fig. 9. X-ray powder pattern of ''multicell'' phase Y, the product of ignition of natural uranium oxides ($CuK_{\alpha\beta}$, diameter of camera 57.3 mm).

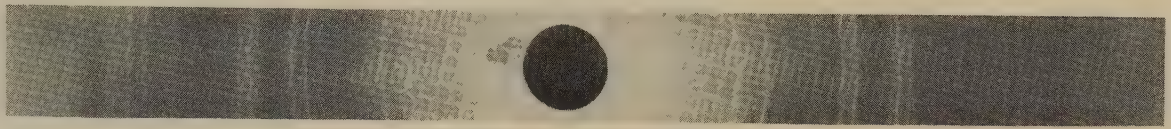

Fig. 10. X-ray powder pattern of phase X, the product of ignition of uraninites ($CuK_{\alpha\beta}$, diameter of camera 86.00 mm).

Table 10. Interplanar Distances in Y Phases - Products of Ignition of Natural Uranium Oxides

"one-cell"		"two-cell"		"multi-cell"		"one-cell"		"two-cell"		"multi-cell"	
d/n	I	d/n	I	d/n	I	d/n	I	d/n	I	d/n	I
--	--	6.02	5	5.86	9	--	--	--	--	1.376	4
--	--	--	--	3.74	3	--	--	1.355	2	1.349	5
--	--	3.56	5	3.56	4	--	--	--	--	1.332	3
3.34	10	3.40	7	3.38	9	--	--	--	--	1.295	4
3.16	6	3.22	10	3.22	10	1.268	6	1.278	5	1.280	5
2.91	3	3.03	6	2.932	7	--	--	--	--	1.252	2
--	--	2.723	8	2.705	8	1.227	3	1.236	5	1.239	4
2.64	7	--	--	--	--	--	--	1.133	3	1.139	1
--	--	2.524	6	2.540	5	1.105	3	1.114	3	1.116	7
--	--	--	--	2.236	2	--	--	--	--	1.097	4
2.19	5	2.198	5	2.201	4	--	--	1.062	2	1.060	3
--	--	--	--	2.149	1	--	--	1.047	2	1.041	6
--	--	2.078	1	2.095	1	--	--	1.010	1	1.024	2
--	--	--	--	2.024	3	--	--	--	--	0.9896	5
1.96	8	1.982	9	1.983	9	0.9781	3	0.9828	1	0.9882	3
--	--	--	--	1.943	6	--	--	--	--	0.9702	3
--	--	1.882	6	1.883	6	--	--	0.9511	1	--	--
1.861	4	1.843	4	1.846	7	--	--	--	--	0.9439	3
1.766	5	1.773	1	--	--	0.9384	2	0.9386	2	--	--
1.693	4	1.692	7	1.707	3	--	--	--	--	0.9262	2
--	--	--	--	1.685	6	--	--	0.9236	1	--	--
--	--	1.651	6	1.649	7	--	--	--	--	0.9199	2
--	--	--	--	1.620	2	--	--	0.8993	1	0.8990	5
--	--	1.601	7	1.599	3	--	--	0.8873	1	0.8899	4
--	--	--	--	1.563	5	--	--	0.8710	3	0.8712	6
1.547	2	--	--	1.542	1	--	--	--	--	0.8535	4
--	--	1.480	6	--	--	--	--	0.8481	1	0.8483	4
--	--	1.448	6	1.457	3	--	--	0.8320	3	--	--
--	--	--	--	1.419	2	--	--	0.8106	1	--	--
1.408	3	1.411	2	--	--	--	--	--		0.7820	2
--	--	--	--	1.387	4	--	--	--			

2. Depending on the degree of natural oxidation of uraninite and pitchblende, both of which may be regarded rationally as oxides of tetravalent uranium only, in their initial state, a part of their uranium becomes hexavalent, while remaining in their crystal structures and replacing isomorphously the tetravalent uranium. This replacement leads to a diminution in the size of the unit cell of uraninite and pitchblende. The well-defined relationship between a_0 and the degree of oxidation makes it possible to estimate "x" roentgenographically for the crystallized fraction of the oxide.

3. Conversion of the bulk of uranium into its hexavalent state cause a gradual increase in the degree of the dispersion of its oxide, a decomposition of the structures, and the formation of the powdery varieties o uranium oxides—the uranium black.

Table 11. Interplanar Distances in Tetragonal Phases of the X-product of Ignition of Natural Uranium Oxides

Uraninite Ignition Products			Brooker and Nuffield		Uraninite Ignition Products			Brooker and Nuffield	
hkl	d/n	I	d/n	I	hkl	d/n	I	d/n	I
-	-	-	5.95	6	040β	-	-	1.528	1
111β	3.443	4	3.36	4	1.32,123	1.742	1	-	-
-	3.254	5	-	-	004	1.443	1	-	-
111	3.105	10	3.21	10	040	1.375	2	1.377	1
-	-	-	3.17	2	-	1.330	3	1.341	1
-	-	-	3.04	2	133,330, 141	-	-	1.290	1
200β	2.919	5	2.95	1	331	1.251	6	1.252	1
-	-	-	2.75	5	240,142	1.214	7	-	-
200	2.644	9	2.65	1	005	1.174	3m	-	-
-	-	-	2.49	1	224,034	1.116	1	-	-
120	2.410	2	2.44	1	143	1.099	5m	-	-
022β	2.113	4	2.23	1	155β	1.048	3	-	-
220β	2.017	3	2.07	1	125	1.034	2	-	-
-	-	-	1.989	5	351β	1.011	1	-	-
022	1.925	9	1.949	2	251	0.9976	1	-	-
-	-	-	1.892	4	026	0.9728	3	-	-
220	1.833	8	1.852	3	252,441, 334	0.9587	1	-	-
131β	1.788	1	-	-	006	0.9272	4m	-	-
222β	1.725	1	1.687	2	351	0.9145	2	-	-
113	1.637	5	1.662	3	026	0.8996	4m	-	-
131	1.609	8	1.612	2	-	0.8650	3m	-	-
-	-	-	-	-	335,162	0.8414	1m	-	-
222	1.559	6	1.568	1	-	0.8308	1	-	-

4. Artificial oxidation of natural uranium oxides, by ignition in air,
ows that they are more stable than synthetic oxides: the original
ystal structure of the CaF_2 type is maintained by them up to 400 to
0°C, as against 175°C, in the case of synthetic oxides. Natural
anium oxides pass into the X, the Y or the U_3O_8 phases at 400 to
0°C. The Y phase is formed on ignition of uraninites and of strongly
idized pitchblende and uranium black. The temperature of recrys-
llization of pitchblende and uranium black into U_3O_8 depends on the
gree of oxidation of the original material. Inasmuch as our studies
monstrated the formation of several crystalline phases during igni-
n of natural uranium oxides, the method of Conybeare and Ferguson
], previously suggested for determining the degree of oxidation of
ural uranium oxides, on the basis of the single-phase or the two-
ase characteristics of their ignition products, has only a limited
efulness, in the case of weakly or moderately oxidized pitchblende.
e dark brown color of the U_3O_8 phase and the bright orange color of
Y phase justify qualitative appraisals of the degree of oxidation of

pitchblende or uranium black, without resorting to the x-ray analysis of the phases.

Received for publication
June 6, 1957

REFERENCES

1. Bokii, G. B. *Vvedenie v Kristallokhimiyu* (Introduction to Crystal Chemistry). Izd. MGU* 1954.
2. Dana, J. D., H. Berman, C. Palache, and C. Frondel. *Sistema Mineralogii* (System of Mineralogy). t.1, p/t 2, 1951.
3. Katz, J. J., and E. Rabinovich. *Khimiya Urana* (Chemistry of Uranium). Izd. IL† 1954.
4. Soboleva, M. V., and I. A. Pudovkina. *Mineraly Urana* (Uranium Minerals). Gosgeoltekhizdat, 1956.
5. Melkov, V. G. *Poiski Uranovykh Mestorozhdenii* (Prospecting for Uranium Deposits). Gosgeoltekhizdat, Izd. Akad. Nauk SSSR, 1956.
6. Arnott, R. J. Am. Mineral. *35*, 386, 1950.
7. Biltz, W., and H. Muller. Z. anorg. Chem. *163*, 257, 1927.
8. Brooker, E. J. and E. W. Nuffield. Am. Mineral. *37*, 363, 1952.
9. Conybeare, C. E. B., and R. B. Ferguson. Am. Mineral. *35*, 401, 1950.
10. Ellsworth, J. E. Am. Mineral. *15*, 455, 1930.
11. Graham, A. R. Am. Mineral. *40*, 560, 1955.
12. Goldschmidt, V. M., and L. Thomassen. Videnskapsselskapets Skrifter (I), 2, 12, 1923.
13. Gronvold, F. Nature, *162*, 70 1948.
14. Gronvold, F., and H. Haraldsen. Nature, *162*, 69, 1948.
15. Hoekstra, H. R., and J. J. Katz. Nature, *175*, 4475, 605, 1955.
16. Hoekstra, H. R., S. Siegal, L. H. Fuchs, and J. J. Katz. Journ. Phys. Chem. *59*, 136, 1955.
17. Hoekstra, H. R. Nature, *176*, 4478, 1955.
18. Kerr, P. F. Science *114*, 91, 1951.
19. Milne, J. H. Am. Mineral. *36*, 5-6, 415, 1951.
20. Robinson, S. C., and A. P. Sabina. Am. Mineral. *40*, 7, 624, 1955.
21. Rogers, A. F., and A. P. Sabina. Am. Mineral. *32*, 90, 1947.
22. Slowinski, S., and N. Elliott. Acta Crystallogr., *5*, 768, 1952.
23. Wasserstein, B. Nature, *174*, 1004, 1955.
24. Wasserstein, B. Nature, *176*, 4473, 159, 1955.
25. Jones, F. W. Proc. Roy. Soc. *166*, 16, 1938.

---

* Moscow University Press. VPS
† Foreign Literature Press. VPS

PARAGENESES OF BORON-BEARING MAGNESIUM SKARNS AT TAEZHNOE DEPOSIT IN THE ARCHEAN OF THE ALDAN PLITA *

A. A. Marakushev

Institute of Geology, Ore Deposits, Petrography, Mineralogy,
and Geochemistry
Academy of Sciences, USSR, Moscow

Abstract

The mineralogy and paragenetic history of magnesium skarns of the Taezhnoe iron ore deposit, Aldan region, Yakutiya, Siberia, is presented from the standpoint of relative elemental mobilities during post-magmatic replacement of dolomite and aluminosilicate rocks. Boron mineralization is associated with hese skarns. Formation of magnesium skarns and associated magnetite ore s related to the highest temperature phase of post-magmatic hydrothermal ctivity. This activity is dated as contemporaneous with intrusion of Archean laskite dikes into dolomite marbles and related aluminosilicate rocks. Principal skarn minerals of the dolomite marble include phlogopite, pargasite, diopside, ludwigite, magnetite, forsterite, and humite or clinohumite. Principal karn minerals of the aluminosilicate rocks include phlogopite, hornblende, diopside, tourmaline of the draviteschorlite series, calcite, and plagioclase or scaplite. Accessory minerals are fluoborite, warwickite, sinhalite, serendibite, phene, and apatite. Relict minerals include dolomite and spinel; moderate to ow temperature minerals are dravite, epidote, albite, plagioclase, serpentine, scharite, and szaibelyite.

Mineral parageneses are studied from the standpoint of elemental mobilities uring skarn formation. In decreasing order of mobility, these elements are: $_2$O, CO_2, Na_2O, K_2O, CaO, O_2, B_2O_3, Fe, P_2O_5, MgO, SiO_2, Al_2O_3 and TiO_2. lthough MgO, SiO_2, and Al_2O_3 are relatively inert during metamorphism, i.e., o not migrate, their proportions in host rocks determine mineral associations volving the mobile elements of magnesium skarns.

Mineral parageneses in post-magmatic magnesium skarns in dolomites and ssociated aluminosilicate rocks are detailed. The high degree of paragenetic ariations in skarns depends upon the variable activity of boron and iron in the eacting solutions. A diagram involving mineral triads and iron and boron ctivities illustrates mineral parageneses. Low iron environments with modrate activities of boron are characterized by plagioclase-phlogopite-diopside arageneses. With increasing iron content, hornblende appears and with critical oron content hornblende may associate with tourmaline. A higher boron con-

---

'Plita'' (''plate'') is a Russian geotectonic term that has no equivalent in English. Plita is a part of a platform where the crystalline case of the platform is overed by a thick horizontally bedded mass of sedimentary rock which may or ot be very gently folded. VPS tent produces a tourmaline-diopside assemblage. The tourmaline-diopside-hornblende paragenesis represents the environment with the highest activity of both iron and boron in the reacting solutions. Suitable conditions of desilication can lead to formation of a practically monomineralic fine and equal grained tourmalinite which commonly borders earlier skarn mineralization.

Magnesium skarns containing borates in dolomite-granitoid contacts, in both young and geologically ancient complexes, have been described in the literature on many occasions (Geijer [5], Tilley [6], Shannon [7]). This paper is a presentation of our results on the study of their parageneses in the Taezhnoe deposit of iron ore in magnesium skarns (Aldan Region, Yakutiya, ASSR) in the Archean of the Aldan Plita. Presence of borates in these skarns was discovered and described by L. I. Shabynin [4].

The Taezhnoe deposit is associated with a mass of dolomite marbles underlain by diopside-hypersthenes and overlain by biotite-sillimanite gneisses and quartzites. This mass is approximately 200 meters thick and is interbedded with para-amphibolites and leucocratic gneisses, alongside the marble sequences. This mass is strongly faulted and is intruded by alaskites. Migmatization phenomena and granitization of crystalline schists and dolomite-marbles are widely distributed in the area and are associated with the intrusion of alaskites. In addition to the alaskites, diopside granites are common at the site, found, as a rule, near the dolomite-marbles and the products of their replacement.

Formation of the magnesium skarns in question, and also of the magnetite ores, is related to the highest temperature stage of the post-magmatic hydrothermal activity which was associated with the intrusion of alaskites. The dolomite marbles and, to a lesser degree, the adjoining aluminosilicate rocks (gneisses, migmatites, etc.), are replaced by postmagmatic skarns. Moreover, spinel-diopside, spinel-forsterite, and other rocks, whose parageneses are outside the scope of this report, the products of an earlier replacement of the marbles during the magmatic stage, were also subjected to the post-magmatic high-temperature mineralization and to the reception of the magnetite ore.

The principal minerals in the post-magmatic skarns are shown in the following table.

It should be noted that minerals like forsterite and diopside also enter the composition of some relatively high-temperature rocks of the magmatic stage in their characteristic paragnesis with spinel, in the deposit here discussed. This paragenetic relationship is unstable in the post-magmatic stage, because of the alkalinity of the environment. Forsterite and diopside are paragenetic with pargasite, phlogopite, etc., in the post-magmatic stage.

The following minerals are found in skarns and in skarnized rocks, in addition to the minerals here enumerated:

Skarns in Dolomite Marbles	Skarns and Near-Skarn Rocks in Aluminosilicate Rocks
Phlogopite (f = 8-15)	Phlogopite (f = 19-28)
Pargasite (f = 10-20)	Hornblende (f = 35-50)
Diopside (f = 5-20)	Diopside (f = 20-40)
Ludwigite	Tourmaline of the dravite-schorl series (f = 65-75)
Forsterite (f = 5-10) or humite and clino-humite	Plagioclase (36-65% An) or scapolite (50-70% Me)
Magnetite	Calcite

NOTE: The degree of iron-impregnation of minerals, $f = \frac{f \times 100}{Fe + Mg}$ (as per cent) is determined by their optical properties, by the means of the Winchell diagram (diopside, forsterite, tourmaline) and of the diagrams based on the available chemical analyses of the Taezhnoe minerals (phlogopite, pargasite, hornblende).

1) Relict minerals, dolomite and spinel, replaced by phlogopite, ludwigite, etc.

2) Relatively rare and accessory, contemporaneous, on the whole, with the skarn minerals: fluoborite, warwickite, sinhalite, serendibite, sphene, apatite.

3) Post-intermediate-temperature minerals: dravite, epidote, and albite replacing scapolite and plagioclase, tremolite, etc.

4) Low-temperature minerals: serpentine (chiefly after forsterite), ascharite (szaibelyite) replacing ludwigite, hydrotalcite, etc.

Paragenetic studies of magnesium skarns had led to the establishment of the following relative mobility series of their components: *

---

*This article makes use of the methods and the analytical concepts of the paragenesis of minerals treated systematically in D. S. Korzhinskii's book [3]. A certain group of the components behave as if they were ''inert,'' in the given zone of metasomatic processes, in the sense that they do not migrate, for all practical purposes, while the other components act as if they were almost ''entirely mobile,'' so that the given amounts of the given component in the rock are no longer reflected in the composition of the replacement product. Mineral composition of a metasomatic rock depends therefore on the proportion of the inert components therein as well as on the chemical potentials (or activities) of the entirely mobile components in the reacting solution. The number of minerals present in the equilibrium associations during metamorphism does not exceed the number of inert components and does not depend on the number of the entirely mobile components. In the case of metasomatism at a constant volume, the number of synchronous minerals may exceed the number of the inert components by one. By applying the methods of systematic paragenetic analysis to a sufficiently abundant test material, it is possible to ascertain the inertness of the entire mobility of the participating components for any ''metasomatic facies.'' The more intensive the metasomatism, the greater is the number of the components passing into the ''entirely mobile'' state. Consequently, it is possible to establish the relative mobility of the components, in the given process, by comparisons of rocks subjected to different degrees of replacement.

Editor of Geokhimiya

H_2O, CO_2, Na_2O, K_2O, CaO, O_2, B_2O_3, Fe/P_2O_5, MgO, SiO_2, Al_2O_3, TiO_2. The five latter ones are inert. The not uncommon admixtures of sphene and apatite in skarns depend on the presence of titanium and phosphorus. The other 3 of the 5 (MgO, SiO_2, Al_2O_3) are virtually inert and their mineral associations in magnesium skarns are determined as single values. The alkalies, next to H_2O and CO_2, are the most highly mobile constituents, among the entirely mobile ones. According to D. S. Korzhinskii [1], all post-magmatic skarns are classified under Group II (sub-groups A-4, A-5), with the ordinary or slightly above-the-ordinary alkalinity characterized by the phlogopite-plagioclase (scapolite) association and by the instability of the spinel-diopside association.

The observed diopside-spinel parageneses belong to an earlier magmatic stage; in the stage here discussed, this association is replaced by phlogopite, pargasite, serendibite, etc. The phlogopite-plagioclase (scapolite) paragenesis is not uniformly stable throughout the deposit and is replaced locally by the associations of diopside or of hornblende with tourmaline which is due not to any change in alkalinity of the solutions, but, as it will be shown later, with the increased activity of boron in the solutions.

Iron and boron are the least mobile constituents, among the "entirely mobile" ones and a large number of parageneses may be identified almost entirely on the basis of these two elements.

Let us consider now separately skarns in dolomites and the near-skarn rocks replacing the aluminosilicate rocks. Magnesium skarns by which the beds of dolomite marble were replaced during the post-magmatic stage are preponderant in their distribution at the site here discussed. These skarns form large bodies whose dip and strike may extend for hundreds of meters without any interruptions. The replacement of dolomites by magnesium skarns was accompanied by a magnetite mineralization. Structural relationships between magnetite and skarn minerals (ludwigite, phlogopite, post-magmatic forsterite) indicate, on the whole, their synchronous origin: the primary magnetite is cementing the skarn minerals without any signs of their corrosion. Elsewhere, one may observe replacements of the skarn minerals by magnetite as well as the converse replacements. One may see, for example, veinlets of phlogopite cutting through magnetite. Alongside magnetite, calcite is found not uncommonly in the parageneses of the dolomite-replacing magnesium skarns. Both of these minerals are made up of the entirely mobile constituents and their formation is contingent upon the volume constancy during the replacement of the marbles, as their precipitation from the solution serves to "compensate for the decrease of the volume brought about upon the replacement of the primary minerals by the reacting ones," according to D. S. Korzhinskii [2]. Paragenetically, the post-magmatic magnesium skarns in dolomite are divided into three groups (Fig. 1).

The parageneses of Group I are exceptionally common. Contacts of these skarns with aluminosilicate rocks show generally the following

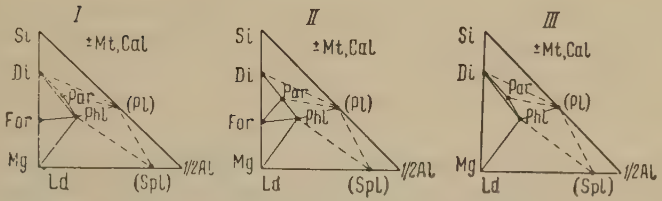

Fig. 1. Paragenetic diagrams of post-magmatic magnesium skarns replacing dolomite marbles (marked off by the solid lines).

zonations: phlogopite-forsterite skarns with magnetite → phlogopite-diopside skarns — hornblende skarns. Phlogopite-forsterite skarns are associated not uncommonly with forsterite-clinohumite-ludwigite skarns containing magnetite and phlogopite. Locally, they may form isolated lenses or clusters in magnetite-bearing forsterite skarns or else they may be between the latter and the dolomite marble, as if they were a "forefront" of replacement of the dolomite by infiltration: Dolomite marble (Dol + Cal ± For ± Spl) → ludwigite skarn (Ld + Mt ± For ± Cal ± Phl) → forsterite skarn (For + Mt ± Phl ± Cal). The "zones" of ludwigite skarns separating forsterite skarns from dolomite marble may attain appreciable thickness (up to 30-40 meters).*

Skarns belonging paragenetically to Group II (Fig. 1) are not particularly abundant in their distribution. The forsterite-pargasite paragenesis is observed in small clusters within skarns in the marbles and in some forsterite-magnetite ores where large poikiloblastic grains of pargasite associated with phlogopite and magnetite compose the fillings between idiomorphic grains of forsterite. Characteristically, the relatively more highly ferruginous silicates, by comparison with Group I, are associated here with magnetite, as it may be seen from the following reaction by which they are bound:

$$12.1\ \mathrm{Di}_{f=15} + 2.95\ \mathrm{Phl}_{f=10} + (0.9\ \mathrm{FeO}) \rightarrow 5.9\ \mathrm{Par}_{f=15} + 0.6\ \mathrm{For}_{f=5}{}^{*}$$

The increased chemical potential of FeO should be conducive to the foregoing reaction, in accordance with the Mass Action Law.

The skarns of Group II were formed therefore in environments where the chemical potential of iron was high. Taking into account the presence of magnetite in both parageneses, we may suppose that the Group II skarns also represent a relatively low oxygen potential,

---

*Ap - apatite
Cal - calcite
Di - diopside
Dol - dolomite
For - forsterite
Hb - hornblende
Ld - ludwigite
Mt - magnetite
Ort - orthoclose
Par - pargasite
Phl - phlogopite
Pl - plagioclose
Q - quartz
Sc - scapolite
Sph - sphene
Spl - spinel
Tu - tourmaline

inasmuch as the increasing chemical potential of iron is a possibility only when there is a lowering of the oxygen potential:

$$\mu_{Fe} = K - \frac{3}{4}\mu_O$$

Iron enters ludwigite chiefly as ferric oxide. Consequently, a lowering of the oxygen potential in the reacting solutions must have an adverse effect on the ludwigite mineralization. There is no evidence of the presence of ludwigite scarns associated with magnetite-bearing pargasite-forsterite skarns of a higher iron-content; parageneses of ludwigite with relatively iron-high minerals (for example, pargasites) are also absent. Phlogopites in ludwigite parageneses are represented only by their iron-low varieties:

Sample No.	Color of sample	α	β	γ	$\gamma-\alpha$	f
2636	Pale green	1.543	1.578	1.585	0.042	10
3282	Pale brown	1.548	1.581	1.586	0.038	11

The ludwigite-phlogopite paragenesis is relatively rare in this deposit.

Relatively more ferruginous phlogopites (f = 14 to 15) are found in the dolomite-forsterite parageneses in the absence of ludwigite.

The ludwigite-diopside paragenesis in the presence of calcite (Group III) is representative of environments with a very high activity of boron* in the reacting solutions, sufficiently high to make forsterite unstable, as it is shown in Figure 1, with the resulting decomposition of forsterite into diopside and ludwigite: 4 For + (2.85 Fe + 2.25 B) = 2.0 Di + 2.95 Ld. This is a rarity in the deposit under consideration, although there are descriptions of magnesium skarns on record [7] in which the paragenesis of this type is preponderant.

Let us pass now to a discussion of the magnesium replacement of aluminosilicate rocks in contact with the dolomite marbles. The following groups may be here recognized:

Magnesium skarns (phlogopite, hornblende, clino-pyroxene); near-skarn quartz-free rocks; the products of the desilicification of the aluminosilicate rocks; quartz-bearing metasomatically altered rocks (partially replaced by hornblende, tourmaline, scapolite, ferruginous phlogopite, etc.).

Let us limit our discussion to the magnesium skarns and to the directly adjoining near-skarn quartz-free (desilicified) rocks. In addition to the previously enumerated principal minerals (Phl, Hb, Di, Tu, Pl, Sc, Cal), these rocks may also contain magnetite, but in contrast with the previously considered skarns replacing the dolomites, the magnetite here is not contemporaneous with the silicates but is formed by replacement of the silicates. The imposition of magnetite mineralization on the near-skarn rocks (very much like the subsequent sulfide mineralization) has a clear structural expression: The magnetite forms veinlets, forms a cement between fragments of its host rocks, develops along cleavage planes of the other minerals and corrodes their grains. It is not possible therefore to regard magnetite as a paragenetic member of the near-skarn rocks.

---

*By the activity, in the present report, we understand ordinary chemical activit (concentration times the activity coefficient).

The skarn parageneses in the aluminosilicate and in the near-skarn rocks show a high degree of variation. It becomes evident on comparing them that their greatest differences are in the amounts of boron and iron they contain, while the amounts of the other entirely mobile constituents show a significantly more narrow range of variation. The observed high degree of paragenetic variations in the near-skarn rocks depends apparently on the variable activities of boron and iron in the reacting solutions.

Figure 2, a diagram constructed by the Korzhinskii Method [3], illustrates the paragenetic dependence of the rocks in question on the

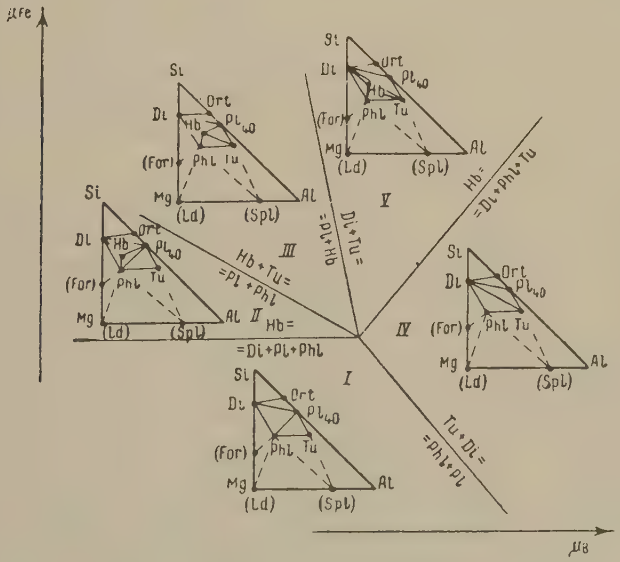

Fig. 2. Diagram of chemical potentials of iron and boron for near-skarn rocks and for post-magmatic magnesium skarns replacing aluminosilicate rocks (gneisses, migmatites, etc.). Their parageneses are shown by solid lines in the triangular diagrams.

chemical potentials of boron and iron. This diagram is built on the assumption that temperature, pressure, and chemical potentials of the rest of the entirely mobile constituents remain constant. The following possible reactions between the already listed principal minerals of the near-skarn rocks serve as the premises of the diagram (the inert constituents, MgO, SiO_2, Al_2O_3, are equalized):

1. 137.52 Di + 18.24 Phl + 8.52 Tu + (42.624 Fe) = 81.12 Hb + (51.12B)
2. 11.46 Pl + 3.558 Phl + (11.8128 Fe + 6.6 B) = 6.324 Hb + 1.1 Tu
3. 4.56 Pl + 3.78 Hb + (6.594 B + 1.392 Fe) = 10.674 Di + 1.099 Tu
4. 3.78 Phl + 20.28 Pl + (15.024 Fe + 18.732 B) = 3.122 Tu + 18.927 Di

   Di + Pl + Phl + (Fe) $\longrightarrow$ Hb

The algebraic (matrix) calculations of the reacting proportions [3, pp. 134-138] were made on the assumption that the composition of plagioclase No. 40, diopside (f = 30), and tourmaline (f = 70) is represented by their theoretical formulae and that the composition of phlogopite and hornblende corresponds to the chemical analyses of these minerals, as they were made available to me by L. I. Shabynin (the analyses were done at the Chemical Laboratory of the IGEM*).

On the assumption of constant temperature, pressure, and chemical potentials of the entirely mobile components, CaO, Na_2O, K_2O, H_2O, CO_2, O_2, in our particular case, in accordance with the phase rule for a 5-component system, MgO, Al_2O_3, SiO_2, Fe, B_2O_3, the association of all of the five minerals here discussed, Pl, Di, Phl, Hb, Tu, represents an assumed-nonvariant system shown as a point in Figure 2, the diagram of the chemical potentials $\mu_B - \mu_{Fe}$. The associations of any 4 out of the 5 minerals are represented by the lines of the assumed monovariant equilibria originating at the point of the nonvariant association. Directions for these lines of the equilibria may be obtained from the reaction equations already cited, in conformity to the Law of Mass Action. The distinctions between the stable and the metastable parts of the monovariant equilibrium lines are based on the "Schreinemaker's Rule" [3, p. 128, Fig. 73].

The diagram shown as Figure 2 permits a systematization of the observed parageneses, depending on the environments of their development.

As is evident from this diagram, the low-iron environments with moderate activities of boron are characterized by the plagioclase-phlogopite-diopside paragenesis (I). At increasing content of iron, hornblende (II) makes its appearance in the parageneses and, provided that the activity of iron is high, hornblende may form an association with tourmaline (III). Environments with activity of boron are characterized by the tourmaline-diopside paragenesis (IV). The

---

*The Institute of Geology and Mineralogy (Institut Geologii i Mineralogii), Aka
Nauk, SSSR. VPS

tourmaline-diopside-hornblende paragenesis (V) represents environments with the highest chemical activity of both iron and boron in the reacting solutions.

All of the paragenetic groups shown in Figure 2 are found in the Taezhnoe deposit.

The parageneses of Group I are abundant on the flanks of the deposit in the environments where both the magnetite and the borate mineralization play out. These parageneses are relatively rare in the deposit itself. Wherever they are found in the near-skarn zones, the following replacement sequence is traceable, in the course of the desilication:

$$\mathrm{Di} + \mathrm{Pl} \rightarrow \mathrm{Phl} + \mathrm{Pl} \rightarrow \mathrm{Tu}\ (\pm\ \mathrm{Pl})$$

which results in the appearance of peculiar coarsely mottled rocks. Such rocks consist chiefly of diopside-plagioclase and contain fantastically shaped clusters of fine-grained tourmaline with rims of phlogopite-plagioclase rocks.

The parageneses of Groups II and III are more abundant in the deposit.

The following replacements observed in the near-skarn rocks are referred also to Group II:

$$\mathrm{Di} + \mathrm{Pl} \rightarrow \mathrm{Hb} + \mathrm{Pl} \rightarrow \mathrm{Phl} + \mathrm{Pl} \rightarrow \mathrm{Tu}\ (\pm\ \mathrm{Pl})$$

The textures of these rocks have a visual resemblance of the textures already described. Moreover, the diopside-plagioclase rocks are, as a rule, completely replaced by a hornblende-plagioclase rock wherein only their small relicts may be preserved. The fine-grained tourmaline, in its oddly shaped clusters and vein-like formations, replaces the plagioclase-hornblende rock from which it is separated invariably by thin margins of the phlogopite-plagioclase composition generally of the cross-leaf structure. Presence of these rims serves to distinguish these replacements from the other kind, belonging to Group II, which took place in the environments containing highly ferruginous solutions. In this latter case, the tourmaline-hornblende

Minerals	Inert Constituents			Entirely Mobile Constituents*				
	MgO	Al_2O_3	SiO_2	$FeO + Fe_2O_3$	B_2O_3	CaO	Na_2O	K_2O
Plagioclase (Pl_{40}); 40% An	0.0	1.4	2.6	0.0	0.0	0.4	0.6	0.0
Diopside (Di); f = 30%	0.7	0.0	2.0	0.3	0.0	1.0	0.0	0.0
Phlogopite (Phl); chem. anal. No. 1580	5.0	2.4	6.0	1.0	0.0	0.1	1.0	0.0
Hornblende (Hb); chem. anal. No. 2514	2.5	1.8	6.0	1.7	0.0	1.9	0.5	0.3
Tourmaline (Tu); f = 70%	1.8	12.0	12.0	4.2	6.0	0.0	2.0	0.0

---

* The more conventional Fe_2O_3, B_2O_3, Na_2O, etc. were adopted in the translation, as against $FeO_{3/2}$, $BO_{3/2}$, $NaO_{1/2}$, etc., respectively of the original. VPS

paragenesis acquires stability and the desilication of the crystalline schists becomes characterized by the following sequence of the replacements:

$$\mathrm{Di + Pl \rightarrow Hb + Pl \rightarrow Tu\ (Pl)}$$

The parageneses of Groups IV and V are amply represented in the deposit (the environments with the high activity of boron in the solutions) and are typical for the near-skarn rocks in contact with the ludwigite skarn bodies. The tourmaline-diopside association is stable in such environments and the most common replacement sequence for the near-skarn rocks is as follows:

$$\mathrm{Di + Pl \rightarrow Di + Tu \rightarrow Tu\ (Phl\ or\ Hb)}$$

In such a manner, in the Taezhnoe deposit, the desilication of the near-skarn rocks in contact with the skarns, under different conditions with respect to the amounts of iron and the activity of boron in the solutions, leads to the formation of practically single-mineral fine, equigranular tourmaline rocks. The tourmaline forms either isolated clusters or irregular bodies, up to 5-7 meters thick, generally in contact with the skarns by which the dolomite marble was replaced, although narrow zones of these rocks were noted also in the Zahlbands of the cross-cutting veins in gneisses.

Paragenetic studies of boron-bearing magnesium skarns of the Taezhnoe deposit lead us to the conclusion that they were formed in the environments with a fluctuating activity of boron in the solutions. When the activity of boron was moderate, this element was accumulated in the near-skarn rocks, with the formation of tourmaline paragenetically with phlogopite and plagioclase or (while the iron was high) with hornblende. There was no ludwigite mineralization in such environments. As the activity of boron was increasing in the reacting solutions, the tourmaline-diopside paragenesis was becoming stable in the near-skarn rocks, while the ludwigite-forsterite paragenesis was becoming extensive in the skarns in the dolomite. Further increases in the activity of boron were responsible for the instability of forsterite and for the appearance of the ludwigite-diopside paragenesis which is very rare in the Taezhnoe deposit.

Received for publication
December 15, 1956

---

*Zahlbands are the lateral surfaces separating veins from the host rock. In the Russian usage of this German term, the mineralized parts of the host rock, next to the veins, are often included. VPS

REFERENCES

1. Korzhinskii, D. S. *Bimetasomaticheskie Flogopitovye i Lazuritovye Mestorozhdeniya Arkheya Pribaikal'ya* (Bimetasomatic deposits of phlogopite and lazurite in Baikal area). Trudy IGN*, Vyp. 29, Petrograf. Ser. (No. 10), 1947.
2. Korzhinskii, D. S. *Ocherk Metasomaticheskikh Protsessov* (An outline of metasomatic processes). *In sb. Osnovnye Problemy v Izuchenii Magmatogennykh Rudnykh Mestorozhdenii* (In Collected Papers: The Fundamental Problems of Magmatic Ore Deposits), 1956.
3. Korzhinskii, D. S. *Fiziko-Khimicheskie Osnovy Analiza Paragenezisov Mineralov* (The physico-chemical principles of the analysis of the paragenesis of minerals). Izd. Akad. Nauk SSSR, 1957.
4. Shabynin, L. I. *Ob Asharite i dr. Boratah v Magnetitovykh Rudakh Metasomaticheskikh Mestorozhdenii* (In reference to ascharite and other borate minerals in magnetite ores of metasomatic deposits). Doklady Akad. Nauk SSSR, 101, No. 5, 1955.
5. Geijer, P. Some Mineral Associations from the Norberg District. Sveriges Geologiska Undersoking Arsbok, 20, No. 4, 1926. 32 pp.
6. Tilley, C. E. The zoned contact-skarns of the Broadford area, Skye. The Min. Mag., Vol. XXIX, No. 214, pp. 621-666, 1951.
7. Shannon, E. V. Ludwigites from Idaho and Korea. Proc. U. S. Nat. Mus., Vol. 59, pp. 667-676, 1921.

Institute of Geologic Sciences (Institut Geologicheskikh Nauk). VPS

EVOLUTION OF ROCKS DURING PROGRESSIVE METAMORPHISM, AS EXEMPLIFIED BY THE MIDDLE SUITE OF THE KRIVOI ROG SERIES

I. V. Aleksandrov and A. V. Zmeenkova

V. I. Vernadskii Institute of Geochemistry and Analytical Chemistry,
Academy of Sciences, USSR, Moscow

Abstract

During progressive metamorphism of these rocks, alterations of both mineralogical and chemical composition occurred. According to their behavior the chemical elements may be divided into three groups:

(a) elements, the content of which in rocks did not substantially alter (iron)
(b) elements, the content of which was decreasing in some rocks and at the same time increasing in others (silicium, aluminium, magnesium);
(c) elements, the content of which in rocks was either only increasing or on decreasing (sodium, potassium, carbon from carbonates).

The migration of the matter occurred with the assistance of solutions. Ther were conditions near to equilibrium between rocks and solutions. Simultaneous with the alteration of the chemical composition of the rocks the composition of solutions was also changing.

Three rock suites, the Lower, the Middle, and the Upper may be identified within the Precambrian Krivoi Rog Series (which is called some the Saksagan Series). The Lower Suite is composed of arkosic sandstones, quartzites, and phyllites. The Middle Suite is represente by interbedded iron-rich and iron-poor rocks (ferruginous and metamorphosed-shaly horizons). The Upper Suite contains well-developed mica and chlorite schists and carbonate rocks (Fig. 1).

Rocks of the Krivoi Rog Series are crumpled into large isoclinal folds and are traceable, as bands, for distances of about 230 km roughly in a north-south direction. Geologic structures of these ban are described in the reports by N. P. Semenenko, Ya. N. Belevtsev, M. N. Dobrokhotov, and others [1, 2, 3, 4].

Let us consider first changes in the mineralogical composition of the rocks in the course of progressive metamorphism and, later, changes in their chemical composition.

CHANGES IN MINERALOGICAL COMPOSITION

The degree of metamorphism of rocks is not the same in different areas. This enables us to make comparisons between rocks in different stages of metamorphism, by way of a basic approach to the proble of mineralogical variations at different levels of metamorphism.

The weakly metamorphosed ocks may be divided into three roups:

A. Rocks high in aluminum but elatively low in iron

B. Rocks high both in aluminum nd in iron

C. Rocks high in iron but very ow in aluminum

Let us consider now these three roups, in reference to the changes 1 their mineralogical composition aused by the metamorphism.

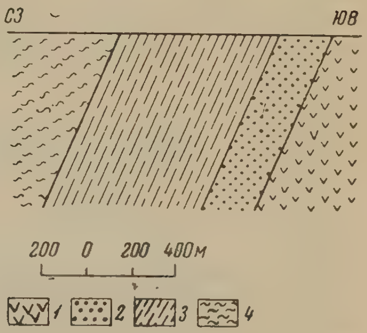

Fig. 1. Profile of Krivoi Rog Series* (vicinity of Krasnaya Gvardiya mine). 1—Greenstone rocks underlying the Krivoi Rog Series; 2—Krivoi Rog Series, Lower Suite; 3—Krivoi Rog Series, Middle Suite; 4—Krivoi Rog Series; Upper Suite.

Group A. Rocks high in aluminum ut relatively poor in iron.

This group is represented by uartz-chlorite-mica microschists, f low grade metamorphism. The iicas are biotite and sericite. arying amounts of carbonates, ore ust, and carbonaceous substance re also present. Pyrite and tour- aline may be found as accessories. uartz and feldspar fragments are resent in some horizons.

A recrystallization of the miner- s took place during the progressive metamorphism. Larger grains biotite and quartz and, later, of muscovite began to appear in the ne-grained mass of the rock. The recrystallization of chlorite was ccompanied by a diminution in its amount in the rock. The carbon- es disappeared. The micro-schists were transformed into musco- te-biotite-quartz or into chlorite-muscovite-biotite-quartz schists. ommonly garnet (almandine) was developed, in the iron-rich varieties schists.

Upon further increases in temperature and pressure, the recrystal- zation of micas and quartz continued, while chlorite disappeared. iere was an increase in the content of quartz, to a certain degree. uring the most advanced stage of the metamorphism, the feldspars ade their appearance (oligoclase, albite-oligoclase, microcline), as ell as sillimanite. The typical paragenetic associations are as llows:

quartz-biotite-muscovite (with or without sillimanite and feldspars);
quartz-biotite-muscovite-garnet (occasionally with sillimanite).

eries and Suites of Krivoi Rog have no generally accepted definitions and are ubject to controversy, according to Stratigraficheskii Slovar SSSR; Gosnauch- ekhizdat, 1956, 1,283 pp., pp. 504-505.

Among the accessory minerals, one may find zircon, apatite, tourmaline, pyrite. The ore dust was partially recrystallized as magnetite

During regressive metamorphism, garnet and micas were chloritiz oligoclase was sericitized and albitized, carbonate made its appearanc and quartz was recrystallized, while schist was silicified to an appreciable degree.

Group B. This group may be broken into two subgroups:

1. Chlorite and quartz-chlorite schists and micro-schists
2. Magnetite-chlorite and magnetite-stilpnomelanite schists and microschists

During progressive metamorphism, a partial recrystallization of chlorite took place in chlorite schists and micro-schists. Nuclei of biotite formed as porphyroblasts, with the subsequent appearance of garnet (almandite) and amphibole (cummingtonite-grunerite). The chlorite content of the rock went down and carbonate disappeared entirely. Garnet-biotite-amphibole-chlorite and biotite-amphibole-chlorite schists were formed.

Later on, amphibole and garnet recrystallized and chlorite disappeared. The results were garnet-amphibolite and amphibolite schists, with or without biotite, containing subordinate quantities of magnetite and quartz and, among the accessory minerals, zircon.

Garnet-amphibole-quartzite and amphibole-quartzite schists were the results of the metamorphism.

During regressive metamorphism, there was chloritization of garnet, replacement of amphibole by biotite and hydrobiotite and development of carbonate and quartz.

Magnetite-chlorite schists and micro-schists are characterized by the following paragenetic associations, in the early stage of their metamorphism:

chlorite-magnetite-quartz;
chlorite-magnetite-carbonate-quartz.

The corresponding associations in stilpnomelane schists and micro schists are:

stilpnomelane-magnetite-quartz;
stilpnomelane-magnetite-carbonate-quartz.

Mica in the foregoing varieties of rock is generally described as biotite, even though the analytical data, however few, are indicative o its low-alkali content, to the point that the mica in question may be stilpnomelane and not biotite. This tentative conclusion must be verified by further studies of magnetite-mica schists.

Progressive metamorphism of these rocks has its early expressio in recrystallization of the minerals, whereupon there begins an intensive development of amphibole (cummingtonite-grunerite) which replac chlorite and carbonate (siderite) quantitatively and also replaces mic to some extent. Stilpnomelane is converted into biotite. The results are quartz-magnetite-amphibole and quartz-mica-amphibole schists. Garnet (almandine) is found more rarely in these schists than in the rocks of the former subgroup.

Group C. Rocks rich in iron but very poor in aluminum.

These rocks are represented by ferruginous quartzites and by iron-arbonate quartzites in the early stage of their metamorphism. They re composed of quartz and hematite in the first case and of quartz, ematite, and siderite in the second.

In the course of the metamorphism, hematite is replaced by magne-ite which is more stable in the new environments. The ore minerals re represented only by magnetite in the highly metamorphosed quartz-tes, with rare exceptions.

The hematite-magnetite sequence is not unidirectional and is merely ndicative of the general trend. As a matter of fact, especially in the arly stages of the metamorphism, there were temporary regressions, oward the precursor environments, and the newly formed magnetite vas undergoing a conversion into martite. Thus magnetite made its ppearance in the ferruginous quartzites in the early stages of the netamorphism, in a metastable environment, wherein it was subjected o martitization, often to a considerable degree. Magnetite was re-ormed afterwards; mica (biotite or stilpnomelane?) also appeared, to-ether with amphiboles (alkali amphiboles and cummingtonite-grunerite) nd with partially recrystallized siderite and quartz. There was an mergence of amphibole-hematite-magnetite and of amphibole-magne-ite-hematite-carbonate-quartzites, with or without mica. Later on, at ncreasing temperatures and pressures, siderite, hematite, and mar-ite disappeared, while amphiboles, mica, quartz, and magnetite were ecrystallized, with the resulting mica-amphibole-magnetite and mphibole-magnetite quartzites.

Appearance of large grains of pyroxene (generally aegirite or egirite-augite), alkali amphiboles, and microcline is typical for side-itic varieties of quartzite which contain dark mica.

These rocks were formed in the following manner:

In the beginning there was a partial recrystallization of quartz, iderite, mica, and magnetite and a formation of microcline, alkali mphibole, and pyroxene. Accessory minerals were represented by patite. The rock became coarser-grained later, because of the growth f pyroxene grains as well as of alkali amphibole, quartz, and magne-ite. There was a complete disappearance of siderite and a decrease n the proportion of mica in the rock. There was a development of nicrocline-mica-pyroxene-amphibole-magnetite quartzites.

During regressive metamorphism, carbonates (dolomite, calcite) vere developed around pyroxene and amphiboles; hydromicas and hlorite appeared; there was a partial martitization of magnetite and, some extent, a silicification.

Let us consider now a concrete example of a change in the mineral-gical composition of rocks during a progressive metamorphism. The hange is to be illustrated by a comparison of four areas in the north-rn part of Saksagan Band and in Annovskaya Band (Fig. 2).

The extent of metamorphism in this area is associated, first of all, ith the growth of temperatures and pressures, increasing from south north, area by area.

Alternations of different rock types are fairly common in the Middle Suite, in the majority of the cases. These alternating rocks were metamorphosed at the same temperatures and pressures.

In the vicinity of the Krasnaya Gvardiya Mine, where the rocks are only weakly metamorphosed, we may observe the following pattern in the lower part of the Middle Suite:

Group A. Micaceous microslates are weakly retrogressive; isolated relatively coarse grains of quartz and biotite are found in the fine-grained matrix.

Group B. (Subgroup 1). Biotite porphyroblasts are present in quartz-chlorite micro-schists. Amphibole and garnet are absent.

Group B (Subgroup 2) and Group C are represented by quartz-mica-magnetite-amphibole schists and by mica-amphibole-magnetite quartzites in which cummingtonite-grunerite is abundantly distributed.

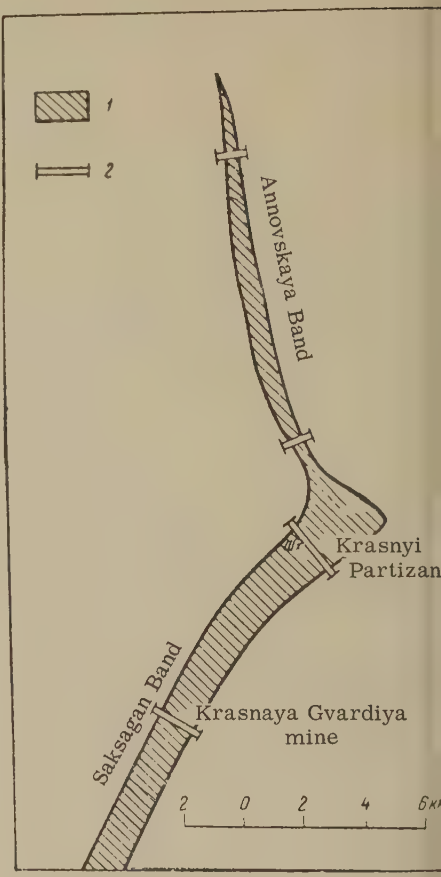

1

Fig. 2. Outline map of test areas. 1-Rocks of the Middle Suite of the Kriv Rog Series; 2—Areas of comparison.

The upper part of the Middle Suite is composed chiefly of the Group C and Group B (Subgroup 2) rocks, including quartz, siderite, magnetite, hematite, cummingtonite-grunerite, mica, and, in one horizon, also aegerite, microcline, and alkali amphibole. Apatite is prese as an accessory mineral. Recrystallization of the minerals is noticeable in the rocks.

In the vicinity of Krasnyi Partizan Mine, the lower part of the Middle Suite is metamorphosed more extensively than it is in the preceding area.

Group A. Alongside biotite and quartz, in mica schists, muscovite ıs also recrystallized; some chlorite remains; zircon may be found.

Group B (Subgroup 1). Alongside chlorite, biotite, amphibole, and .rnet are developed abundantly in the schists.

Group B (Subgroup 2). Magnetite was recrystallized in magnetite-ilpnomelane schists and amphibole (cummingtonite-grunerite) is well eveloped.

Group C. This group is represented by mica-magnetite-amphibole ıartzites. Siderite is rare, although it should be noted that there is ery little siderite, as a rule, in the lower part of the Middle Suite, ıd in the northern part of the Saksagan Band, even in the weakly meta-orphized rocks of this group.

On a comparison of this area with the preceding one, one may see at muscovite was recrystallized in the mica schists (Group A), to-ther with biotite, quartz, and, locally, chlorite. The rocks of Group (Subgroup 1) contain amphibole and garnet, in addition to chlorite and otite.

In the vicinity of the Krasnyi Partizan Mine, rocks in the upper part the Middle Suite, belonging chiefly to Groups C and B (Subgroup 2), e less metamorphosed than the rocks in the lower part of the Suite d it is possible to trace the decrease in the intensity of the metamor-ism in the profile, from the bottom up. It appears that, in this par-ular case, intensity of the metamorphism was seriously affected by granites underlying the Krivoi Rog Series in intrusive contact with amphiboles.

In the vicinity of the southern end of the Annovskaya Band, the fol-ving situation is observed in the lower part of the Middle Suite:

Group A is represented by muscovite-biotite-quartz schists in which rnet is fairly common. Practically no chlorite is left (this does not ply to the chlorite which is replacing micas and garnet and which was med in the regressive metamorphism). The micro-schists are sent.

Group B (Subgroup 1) is represented by garnet-biotite-amphibole l garnet-amphibole schists. Locally, there are schists containing ompletely replaced chlorite.

Group B (Subgroup 2) is represented by magnetite-mica-amphibole ıists.

Group C consists of magnetite-amphibole and magnetite-mica-phibole quartzites.

Mica-magnetite-amphibole quartzites (Group C) are abundant higher ın the profile, together with subordinate quantities of mica-magnetite-ohibole schists (Group B, Subgroup 2). Both cummingtonite-grunerite alkali amphiboles may be found in the rocks of Group C. Siderite is ıd more rarely than in the low-temperature metamorphics and is ent wherever amphiboles are abundant.

Consequently, micro-schists are no longer encountered in the next to the first stage of the metamorphism. Garnet appears in the mica schists (Group A). The amount of chlorite decreases in the schists of Group B, Subgroup 1, although some chlorite is still found. The same applies to siderite in the rocks of Group C.

In the northern part of Annovskaya Band, in the area of most highly metamorphosed rocks, feldspar and, occasionally, sillimanite are present in mica schists of Group A. Group B, Subgroup 1 is represented by garnet-biotite-amphibole and biotite-amphibole schists. Chlorite is replaced completely by the minerals of which the rock is composed. Siderite is replaced completely in mica-magnetite-amphibole and in mica-microcline-amphibole-aegirite-magnetite quartzites (Group C). Only carbonates (dolomite, calcite), which were formed during regressive metamorphism and by which the other minerals were replaced, may be found here, in places.

The following conclusions may be drawn from the foregoing considerations: chlorite disappeared from the schists of Groups A and B (Subgroup 2) in the earlier stages of the metamorphism than from the schists of Group B (Subgroup 1); siderite remained longest in the ferruginous quartzites (Group C); amphiboles in rock groups C and B (Subgroup 2) appeared at an earlier time, in the metamorphism, than in the schists of Group B (Subgroup 1); garnet appeared first in the chlorite schists and later in the mica schists.

Thus one and the same mineral would appear or disappear in different stages of the metamorphism, in rocks of different kinds.

CHANGES IN CHEMICAL COMPOSITION

We shall be making use of the diagrams of Figure 3* in our discussion of changes in the chemical composition of rocks during progressive metamorphism.

PRINCIPLE OF THE DIAGRAM

Percentages by weight are expressed as atomic quantities. [Editor's note: First oxide weight percentages of standard chemical analyses are converted to ionic weight percentages for Si, Al, Fe^{+3}, Fe^{+2}, Mg, Ca, Na, K, and C (from CO_2). Then these ionic weight percentages are divided by their respective atomic weights to give ionic weight proportions. Each ionic weight proportion is finally divided by the sum of the proportions for all nine constituents. This quantity

*In the preparation of these diagrams, we used the data of:

N. F. Anikeeva
Ya. N. Belevtzev
M. N. Dobrokhotov
V. S. Domakev
R. P. Dubinkina
G. V. Zhukov
P. M. Kanibolotskii
K. P. Liaschenko
A. P. Nikolskii
A. S. Pavlenko
R. P. Petrov
Yu. I. Polovinkina
N. I. Polovko
N. P. Semenen
A. I. Tugarinov
M. S. Tsibulska
I. V. Aleksandr
and others

Fig. 3. Diagrams of Chemical Composition of Metamorphic Rocks, Middle Suite, Krivoi Rog Series.

1 - relatively weakly metamorphosed mica schists and micro-schists; 2 - relatively highly metamorphosed mica schists; 3 - chlorite, magnetite-chlorite, and magnetite-stilpnomelane schists and micro-schists; 4 - granite-amphibole and garnet-pyroxene schists; 5 - magnetite-amphibole schists; 6 - hematite quartzites; 7 - iron carbonate quartzites; 8 - magnetite-hematite quartzites; 9 - magnetite-amphibole quartzites and amphibole-pyroxene-magnetite quartzites.

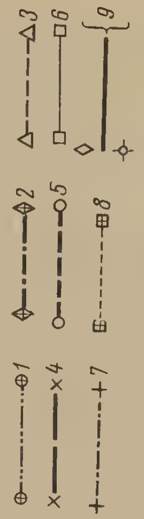

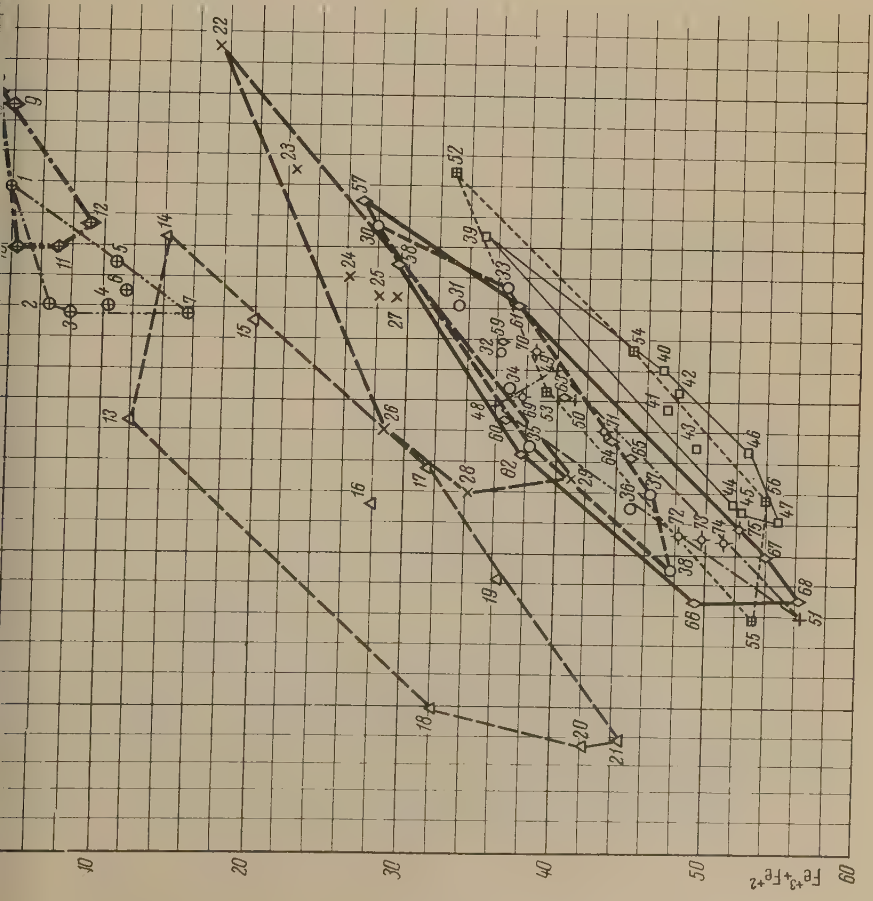

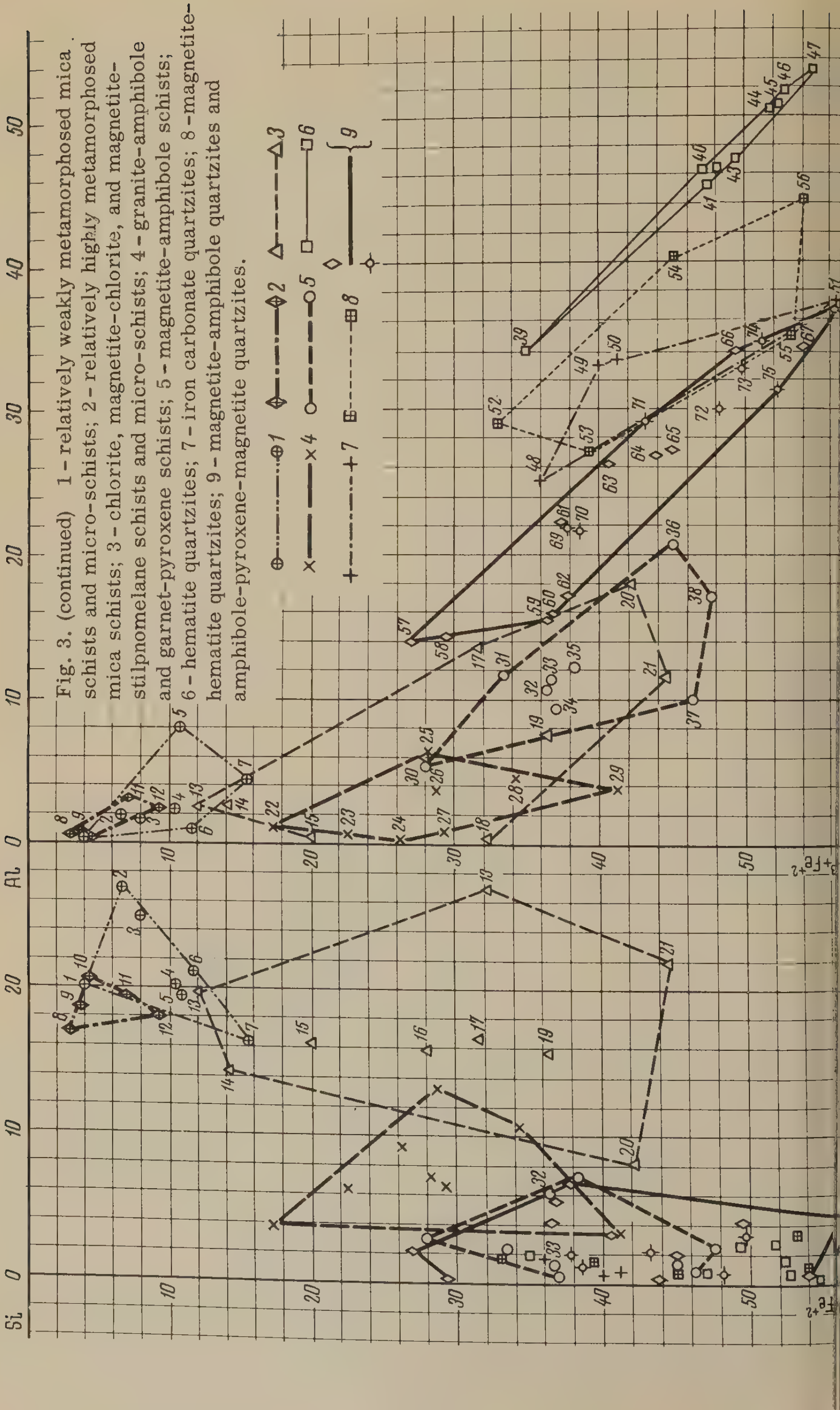

Fig. 3. (continued) 1 – relatively weakly metamorphosed mica schists and micro-schists; 2 – relatively highly metamorphosed mica schists; 3 – chlorite, magnetite-chlorite, and magnetite-stilpnomelane schists and micro-schists; 4 – granite-amphibole and garnet-pyroxene schists; 5 – magnetite-amphibole schists; 6 – hematite quartzites; 7 – iron carbonate quartzites; 8 – magnetite-hematite quartzites; 9 – magnetite-amphibole quartzites and amphibole-pyroxene-magnetite quartzites.

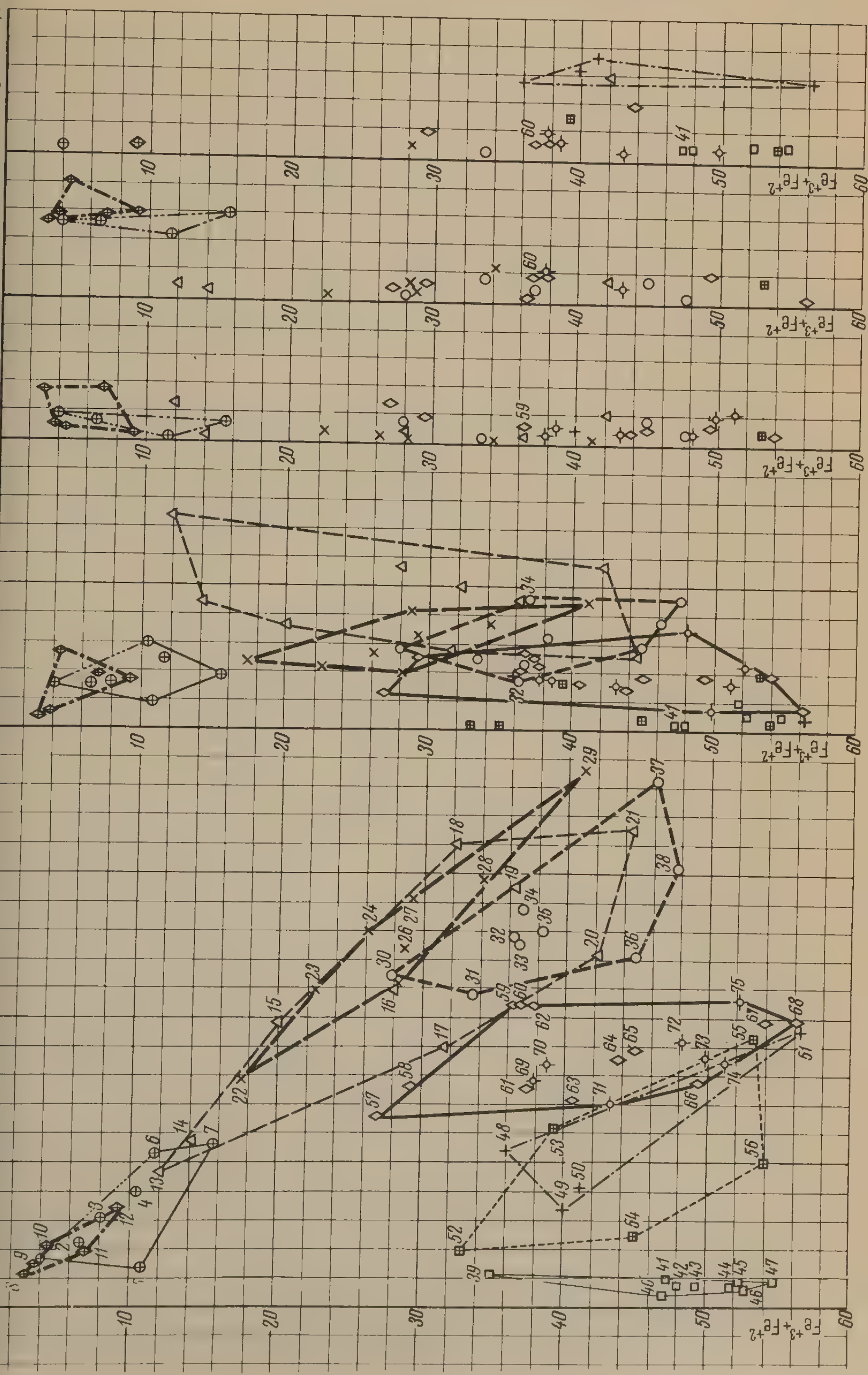
10
20
30
40
50
60
$Fe^{+3}+Fe^{+2}$
60
59
34
32
41
1
2
3
4
5
6
7
8
9
10
11
12
13
14
15
16
17
18
19
20
21
22
23
24
26
27
28
29
30
31
32
33
34
35
36
37
38
39
40
41
42
43
44
45
46
47
48
49
50
51
52
53
54
55
56
57
58
59
60
61
62
63
64
65
66
67
68
69
70
71
72
73
74
75

expressed as per cent is termed "atom per cent" in the following discussion.] The recalculated analytical data are plotted on the diagrams. The ordinate is the sum of the atom per cent of Fe^{3+} and Fe^{2+}; the abscissa, the atom per cent of every one of the elements here listed, including Fe^{3+} and Fe^{2+} individually. Thus the same analysis is always found at one and the same level in all diagrams, on the ordinate, and it is possible therefore to locate analyses in different diagrams fairly easily, and also to ascertain relationships not only between iron and some other single element but between any two of any other elements.

The diagram Ca - (Fe^{3+} + Fe^{2+}) is not included here because calcium content of the rocks is generally less than 2 atom per cent, i.e., is very low. Wherever Ca exceeds 2 atom per cent, the case is treated separately in the text.

The rocks in the diagrams are divided into the groups already described; in some cases the groups are divided into subgroups. Analysis numbers in every subgroup are cardinal numbers arranged in the increasing order of iron content. The lines are boundaries of the areas in which analyses, within the subgroups, are abundant. Names of the rocks are the same as they are in the original sources.

GROUP A

Mica Schists and Micro-Schists (fields 1 and 2, Fig. 3)

This group is represented in the diagrams by quartz-biotite-sericite schists and by micro-schists containing subordinate quantities of chlorite, as well as by their relatively highly metamorphosed analogues: biotite-muscovite-quartz schists containing occasionally plagioclase. The abundantly distributed garnet-mica schists form a separate subgroup for which we could find but a few chemical analyses on record.

The relatively weakly metamorphosed mica schists and micro-schists (Fig. 3) are as follows:

1. Slate schist, sericite-biotite-quartz. Popelnastovskii Uchastok. E. V. Romanishina, analyst [1].
2. Slate schist, quartz-sericite. Popelnastovskii Uchastok. P. P. Makhovka, analyst [1].
3. Quartz-mica schist. Kremenchug Band ($Na_2O + K_2O = 5.85\%$ by wt).
4. Quartz-mica schist. Kremenchug Band ($Na_2O + K_2O = 4.88\%$ by wt).
5. Quartz-mica schist. Kremenchug Band ($Na_2O + K_2O = 5.08\%$ by wt).
6. Quartz-biotite micro-schist. Northern part of Saksagan Band. A. N. Axelrod, analyst [5].
7. Quartz-biotite micro-schist. Northern part of Saksagan Band. M. T. Selyutina, analyst.

As sericite and quartz increase in schists, at the expense of biotite Si increases also, while Fe decreases and Al shows an insignificant increase (analyses 1 through 7); as sericite increases at the expense of biotite and quartz, there is a decrease in Fe, an increase in Al, while Si remains practically unchanged (analyses 2 through 7). Fe^{2+} is higher than Fe^{3+} in most of the schists (biotite, chlorite) with the exception of Analysis No. 5, in which Fe^{3+} is higher than Fe^{2+} because of included dusty hematite. Mg content varies from 2 to 6 atom per cent; K content, from 5 to 6 atom per cent; Na and Ca are low in schists; CO_2 is included in the loss-on-ignition and is not determined separately.

The relatively highly metamorphosed mica schists include:

8.* Muscovite-albite-quartz schist. Zheltorechenskaya Band. A. V. Zmeenkova, analyst.

9.* Biotite-muscovite-quartz schist. Zheltorechenskaya Band. A. V. Zmeenkova, analyst.

10. Quartz-biotite schist. Zheltorechenskaya Band.

11.* Muscovite-biotite-quartz schist with plagioclase. Zheltorechenskaya Band. I. V. Aleksandrov, analyst.

12. Mica schist. Zheltorechenskaya Band. A. N. Axelrod and B. S. Kopelevich, analysts.

During the progressive metamorphism, in Group A, there is a tendency toward an increase in Si and a decrease in Fe and Al. The first tendency is showing in iron-rich schists; the second one, in alumina-rich weakly metamorphosed schists. There is a decrease in Mg, in some cases. As plagioclases make their appearance, Na increases. Development of micas at the expense of chlorite is conducive to higher K.

GROUP B

Chlorite, Magnetite-Chlorite and Magnetite-Stilpnomelane Schists and Micro-Schists (field 3, Fig. 3)

13. Slate schist, quartz-chlorite. Popelnastovskii Uchastok. . Dokhlenko, analyst.

14. Knotty quartz-garnet-chlorite schist. Popelnastovskii Uchastok. . A. Panchenko, analyst.

15. Garnet-chlorite-quartz-biotite micro-schist. Northern part of the Saksagan Band. K. A. Baklanova, analyst (Na_2O absent; 0.10% K_2O by weight. Apparently stilpnomelane and not biotite in the rock - I. A.).

16.* Chlorite schist. Quartz, cummingtonite-grunerite, and magnetite are present in subordinate quantities. Saksagan Band, northern part. A. V. Zmeenkova, analyst.

17. Chlorite schist. Dzerzhinskii Mine.

18. Garnet-chlorite schist. Saksagan Band. K. A. Baklanova, analyst.

19.* Chlorite schist. Quartz, magnetite, and cummingtonite-grunerite are present in subordinate quantities. Saksagan Band,

---

Analyses of the rocks marked by an asterisk are reported in Table 1.

northern part. K. A. Baklanova, analyst.

20.* Magnetite-stilpnomelane schist. Cummingtonite and carbonate are present in subordinate quantities. Saksagan Band, northern part. A. V. Zmeenkova, analyst.

21. Chlorite schist. Inguletz River, left bank [6].

Chlorite, garnet, stilpnomelane, and magnetite increase in the rocks at the expense of quartz, with a concurrent increase in the total iron and a decrease in silica. There is more Fe^{2+} than Fe^{3+} (more ferruginous silicates than magnetite). The more Fe^{3+}, the less Fe^{2+} and Al because magnetite increases at the expense of ferruginous silicates (compare analysis 17 and 20 with 18 and 21 respectively; in each pair of analyses the sum of Fe^{2+} and Fe^{3+} is about the same). Since ferruginous silicates increase at the expense of quartz (and not at the expense of magnetite), the content of Al and Fe^{2+} goes up, as Si goes down (compare analyses 15 and 18, where Fe^{3+} is the same in both).

Mg varies from 5 to 14 atom per cent, depending on its original content. There are no significant variations in the concentrations of other constituents. The alkalies and Ca are low in the schists.

Subgroup. Garnet-Amphibole and Garnet-Pyroxene Schists (field 4, Fig. 3)

22. Garnet-cummingtonite-biotite-quartz schist. Northern part of Saksagan Band. L. N. Chuenko, analyst.

23. Cummingtonite-biotite-quartz schist. Zheltorechenskaya Band. M. I. Makarova, analyst.

24. Garnet-cummingtonite-biotite schist. Northern part of Saksagan Band. O. R. Kolysheva, analyst.

25. Garnet-biotite-amphibole schist. Zheltorechenskaya Band. A. N Axelrod and B. S. Kopelevich, analysts.

26. Garnet-biotite-amphibole schist. Zheltorechenskaya Band. M. P. Chinevoa, analyst.

27. Cummingtonite-garnet ferrohypersthene quartzite. Zelenovskii Uchastok. S. A. Panchenko, analyst.

28. Garnet-biotite-cummingtonite schist. Northern part of Saksaga Band. A. N. Axelrod, analyst.

29. Garnet-pyroxene rock. Zelenovskii Uchastok. S. A. Panchenko analyst [1].

As iron increases, there is a decrease in silica. This is related to the increasing content of ferruginous silicates in the rocks and the decreasing content of their quartz. There is a parallel increase in Fe^{2+} in relation to Fe^{3+}. Aluminum varies from 3.5 to 13 atom per cent.

While iron is increasing, aluminum either increases (there is more garnet, biotite, but less quartz) or remains practically unchanged (there is more pyroxene, amphibole, but less quartz). Mg fluctuates within the range of 4 to 9 atom per cent, with a slight tendency toward igher concentrations in the somewhat more highly ferruginous rocks. a, K, and Na do not exceed 1 to 2 atom per cent.

---

*Analyses of the rocks marked by an asterisk are reported in Table 1.

Judging by rock samples Nos. 27 and 29, pyroxenes are developed referably in the relatively ferruginous varieties of schists.

ıbgroup. Magnetite-Amphibole Schists (field 5, Fig. 3)

30. Biotite-magnetite-amphibole-quartz schist. Zheltorechenskaya and. A. V. Zmeenkova, analyst.
31. Magnetite-amphibolite schist. Zheltorechenskaya Band. A. N. xelrod, analyst.
32. Magnetite-garnet-grunerite schist. Zheltianskii Uchastok. . P. Makhovka, analyst [1].
33. Magnetite-grunerite-ferrohypersthene quartzite. Zelenovskii chastok. E. V. Romanshina, analyst.
34. Magnetite-amphibole schist. Zheltorechenskaya Band. A. N. xelrod, analyst.
35. Magnetite-cummingtonite schist with garnet. Northern part of aksagan Band. M. P. Chinenova, analyst.
36. Magnetite-amphibole schist. Zheltorechenskaya Band. A. N. xelrod, analyst.
37. Magnetite-grunerite-ferrohypersthene quartzite. Zelenovskii chastok. E. V. Romanishina, analyst.
38. Magnetite-cummingtonite schist. Popelnastovskii Uchastok. A. Panchenko, analyst.

As iron increases, there is a decrease in silica and alumina (the ocks have less quartz and more ferruginous silicates). Fe^{2+} exceeds e^{3+} (more ferruginous silicates than magnetite). The Fe^{3+}:Fe^{2+} ratio higher than in garnet-amphibole schists. Al varies from 0.5 to 7 tom per cent; Mg varies from 4 to 9%. Ca, Na, K do not exceed 1 to 2 tom per cent.

Silica increased appreciably in rocks of Group B during the proressive metamorphism, while alumina decreased concurrently. There ere no significant changes in the iron content. It is possible that there as a faint tendency toward higher percentages of iron, because of a ertain decrease in the volume of the rocks during the metamorphism nd because of the relative inertness of iron. There were no variations the Fe^{3+}:Fe^{2+} ratio. Mg content decreased. Ca, K, and Na were ow, even as formerly. As carbonates disappeared from the schists, ere were corresponding decreases in CO_2 content.

GROUP C

ıbgroup. Hematite and Martite-Hematite Quartzites (field 6, Fig. 3)

The least metamorphosed ferruginous quartzites are included in this ıbgroup. They are composed of hematite, quartz, and an almost cometely martitized magnetite. Their high Si and Fe^{3+} and their low ontent of other elements is due to their mineralogic composition.

39. Ferruginous hornfels. Balka (Gulley) Dubovaya.

40. Iron mica jasper. Popelnastovskii Uchastok. S. A. Panchenko, analyst [1].

41. Martite-ironmica jasper. Kremenchug Band.

42. Martite-ironmica jasper. Popelnastovskii Uchastok [1].

43. Martite quartzites (average of $K_2{}^2$ beds). Kremenchug Band [4]

44. Hornfels and martite jaspers (average of 3 analyses). Kremenchug Band.

45. Martite jasper. Popelnastovskii Uchastok. Nadrudnaya ("over-ore") Suite [1].

46. Iron mica jasper. Popelnastovskii Uchastok [1].

47. Martite-ironmica jasper. Popelnastovskii Uchastok [1].

Subgroup. Siderite-Hematite and Siderite-Magnetite-Hematite Quartzites (field 7, Fig. 3)

48. Siderite-magnetite-hematite quartzite (2.85% CaO by weight; a few veinlets of dolomite). Northern part of Saksagan Band. I. V. Aleksandrov, analyst.

49. Siderite-hematite-quartz hornfels. Popelnastovskii Uchastok. S. A. Panchenko, analyst.

50. Siderite-hematite-quartz hornfels. Popelnastovskii Uchastok. S. A. Panchenko, analyst.

51. Siderite-hematite-magnetite quartzite. Northern part of Saksagan Band. I. V. Aleksandrov, analyst.

Four analyses are obviously insufficient for a characterization of this subgroup, especially since they are on rocks in different stages of the metamorphism: Nos. 49 and 50 are the least metamorphosed; Nos. 48 and 51 are metamorphosed to a somewhat greater degree.

The uniform CO_2 content is noticeable in all of the analyses, although this uniformity requires verification, in order to make sure that it is typical of the iron-carbonate quartzites.

Subgroup. Hematite-Magnetite Quartzites (field 8, Fig. 3)

52. Ferruginous hornfels. Right bank of Saksagan River [6].

53. Magnetite quartzites (average of $K_2{}^2$) Kremenchug Band [4].

54. Magnetite-hematite-martite jasper. Zheltianskii Uchastok. P. P. Makhovka, analyst.

55. Martite hornfels. Northern part of Saksagan Band.

56. Magnetite-martite-ferromica jasper. Popelnastovskii Uchastok

The rocks in this subgroup are somewhat more metamorphosed than the hematite quartzites. Magnetite was formed at the expense of hematite, with a concurrent increase in Fe^{2+} and a decrease in Fe^{3+}. Also, in the more thoroughly metamorphosed rocks (Nos. 53 and 55), there is a decrease in Si and an increase in Al and Mg, paralleling the decrease in Fe^{3+}; this is due to a partial replacement of quartz and hematite by micas, chlorite, and possibly amphibole. Small amounts of carbonate are present in some rocks.

Let us pass now to the highly metamorphosed rocks of Group C.

Subgroup. Magnetite-Amphibole Quartzites (field 9, Fig. 3)

57. Mica-magnetite-amphibole quartzite. Zheltorechenskaya Band. A. V. Zmeenkova, analyst.

58. Magnetite-amphibole quartzite. Annovskaya Band.

59. Magnetite amphibole quartzite. Zheltorechenskaya Band. A. V. Zmeenkova, analyst.

60. Ferruginous hornfels. Zheltorechenskaya Band.

61. Amphibole-magnetite hornfels. Zheltorechenskaya Band. A. N. Axelrod and B. S. Kopelevich, analysts.

62. Ferruginous hornfels. Zheltorechenskaya Band.

63. Amphibole-magnetite hornfels (2.23% CaO by weight). Northern part of Saksagan Band. M. P. Chinenova, analyst.

64. Magnetite-amphibole quartzite. Annovskaya Band. A. N. Axelrod, analyst.

65. Amphibole-magnetite-quartz hornfels. Zheltnianskii Uchastok. P. P. Makhovka, analyst.

66. Cummingtonite-magnetite hornfels (2.41% CaO by weight). Northern part of Saksagan Band.

67. Carbonate-amphibole-magnetite quartzite. Northern part of Saksagan Band (little carbonate in the rock, judging by the 0.60% CO_2, by weight).

68. Magnetite hornfels. Zheltorechenskaya Band. M. P. Chinenova, analyst.

As iron increases, there is a noticeable decrease in silica (more magnetite and amphibole; less quartz). There is more Fe^{3+} than Fe^{2+} in the rocks, as the increasing iron content is due chiefly to Fe^{3+}. Al is variable, from zero to 7 atom per cent; Mg varies from 1.5 to 5.5 atom per cent. Magnesium is lower than in magnetite-amphibole schists, because there is less iron silicate in the quartzites. Na, a constituent of the alkali amphiboles, does not exceed 1 to 2%, as a rule. K and Ca are also not over 1 to 2% (except in Nos. 63 and 66 which are somewhat higher in Ca). Some of the rocks in this subgroup contain small amounts of chlorite and carbonate developed during regressive metamorphism.

Subgroup. Amphibole-Pyroxene-Magnetite Quartzites

69. Amphibole-magnetite hornfels with aegirite and alkali amphiboles. Zheltorechenskaya Band. A. N. Axelrod and B. S. Kopelevich, analysts.

70. Amphibole-magnetite hornfels with aegirite. Zheltorechenskaya Band. A. N. Axelrod and B. S. Kopelevich, analysts.

71. Amphibole-magnetite hornfels with alkali amphiboles and aegirite. Zheltorechenskaya Band. A. N. Axelrod and B. S. Kopelevich, analysts.

72. Amphibole-pyroxene-magnetite quartzite. Zelenovskii Uchastok (2.1% CaO by weight). S. A. Panchenko, analyst.

73. Magnetite-amphibole-aegirite-quartz rock. Annovskaya Band. V. M. Kovyazina, analyst.

74. Aegirite-magnetite quartzite. Zelenovskii Uchastok (2.1% CaO by weight). S. A. Panchenko, analyst.

75. Augite-hypersthene-magnetite quartzite. Zelenovskii Uchastok. S. A. Panchenko, analyst [1].

Analyses of amphibole-pyroxene-magnetite quartzites have no independent boundaries in the diagram (Fig. 3). They are distributed among analyses of the most highly ferruginous magnetite-amphibole quartzites.

In rocks of Group C, during progressive metamorphism, while hematite quartzites were undergoing conversion into amphibole-magnetite and amphibole-pyroxene-magnetite quartzites, the Si content decreased and Al content increased, in several instances, alongside a slightly increasing Mg; concurrently, there were no appreciable changes in Fe, although Fe^{2+} tended to increase at the expense of Fe^{3+}. There were no changes in Ca, for all practical purposes, while there was a small increase in Na and K.

CO_2 disappeared in iron-carbonate quartzites, while Si remained essentially unchanged and Na and K were showing a tendency toward a slight increase and the other elements changed in their concentrations very much like in the hematite quartzites.

Let us now compare the behavior of different elements, grouped here under three categories:

a) Elements whose concentration remained practically unchanged during progressive metamorphism. Iron belongs to this category.

b) Elements whose concentration changed during progressive metamorphism, increasing in some rocks, while decreasing in others. Silicon, aluminum, and magnesium are in this category.

c) In contrast with the preceding categories, constituents whose concentrations in the rocks either consistently increased or decreased, without reversals, during the metamorphism. Sodium, potassium, and CO_2 are in this category.

Iron. It is evident from the results shown in Table 2, which are the same as in the diagrams, that the total iron content of these rocks, on the whole, was about the same, regardless of the degree of the metamorphism. As previously stated, it is not easy to ascertain increases or decreases of this element in highly ferruginous rocks. Probably there was neither. There was a partial withdrawal of iron from certain varieties of mica schists.

There was no reduction of Fe^{3+} in schists of Group B. In rocks of Group C where Fe^{3+} content was high, iron was undergoing reduction to a significant extent, but only up to a certain threshold of the Fe^{2+} concentration which was lower than it was in the rocks of Group B.

There were no significant changes in the range of the variation of iron (Table 2). This range was very large, in keeping with the high degree of the differentiation between the rocks with respect to their

Table 1. Chemical Analysis of Rocks, % by Weight

Sample No. Constituent	8	9	11	18	19	20	30	48.	51	57	59
SiO_2	72.40	70.34	61.03	38.74	34.46	24.56	57.72	40.53	31.20	60.62	40.35
TiO_2	0.30	0.55	0.54	0.37	0.32	0.27	0.12	0.08	0.10	0.12	0.08
Al_2O_3	14.88	16.00	16.57	12.05	11.93	6.20	2.27	1.35	0.84	1.59	3.19
Fe_2O_3	1.02	0.84	4.11	7.17	9.00	21.54	7.06	31.22	43.01	17.73	18.83
FeO	2.90	4.01	4.79	26.13	31.33	26.57	25.50	11.88	20.13	14.89	23.92
MnO	0.03	0.02	none	0.02	0.08	0.04	0.01	0.02	0.10	0.01	0.02
MgO	0.07	0.84	2.58	6.91	5.40	6.95	3.65	2.31	0.51	1.57	2.47
CaO	none	none	0.27	0.33	0.50	1.85	none	2.85	0.18	0.07	none
Na_2O	1.90	0.60	2.01	0.55	0.34	0.60	0.56			1.31	0.00
K_2O	4.52	4.81	4.73	none	none	1.10	0.51	0.17	0.18	0.73	0.23
CO_2	—	—	—	—	—	3.99	—	3.75	3.63	—	—
S	0.40	0.81	—	—	—	—	—	—	—	—	—
Loss on ignition	0.33	0.05	3.67	0.56	0.41	0.53	0.72	—	—	0.37	0.53
H_2O	0.99	1.14	—	7.41	6.80	5.66	1.71	0.08	0.06	0.05	1.93
Sum	100.61	100.61	100.30	100.24	100.70	99.86	99.83	100.24	99.94	100.26	100.15

iron content. This was due both to the distribution of iron during the sedimentation and, undoubtedly, to its inertness during the progressive metamorphism.

Silicon. The content of Si in the rocks tended to increase, on the whole, on transition from low to high degree of the metamorphism (Table 2). We must not overlook, however, that, while rocks of Group B were being significantly enriched with respect to Si, the Si enrichment remained negligible in Group A and the ferruginous quartzites of Group C lost silica. The range of Si variation was large and was unaffected, it appears, by progressive metamorphism.

Aluminum. The tendency, on the whole, is toward lower amounts of aluminum. This is especially clear in ferruginous rocks (Table 2). However, while the aluminum content was decreasing substantially in the schists of Group B, there were isolated cases of its increase in the rocks of Group C. The range of aluminum variation is large enough from the start; it tends to grow more narrow during the metamorphism.

Magnesium. Magnesium content of rock in Group B decreased during the metamorphism, while magnesium content of rocks in Group C increased. The range of Mg variation was narrowed in the process from 14 to 8 atom per cent. Mg resembled Al in its behavior.

Thus silicon, aluminum, and magnesium were lost by some rocks of the Middle Suite and were gained concurrently by some others, in the course of the metamorphism.

We observe a tendency, for Si, Al, and Mg, toward a more or less uniform distribution in the rocks of Groups B and C, although the full uniformity is not attained and the distribution process is halted at certain levels which are

Table 2.

Element	Content of Element in Rocks, atom per cent		Range of Variation, atom per cent	
	Relatively weakly metamorphosed rocks	Relatively highly metamorphosed rocks	Relatively weakly metamorphosed rocks	Relatively highly metamorphosed rocks
Iron	4 to 56	3 to 56	52	53
Silicon	27 to 65	37 to 73	38	36
Aluminum	0 to 27	0 to 21	27	21
Aluminum in ferruginous rocks (Groups B and C)	0 to 27	0 to 13	27	13
Magnesium	0 to 14	1 to 9	14	8

pecific for the given kind of rock. These levels are determined by everal factors: chemical and mineralogic composition of the rock; omposition of the solutions (primarily by the amounts of alkalies, arbonic acid, and oxidizing agents); environments of the process emperature, pressure); geologic environments (position of the rock ith respect to other rocks).

No conclusion may be made, to the effect that losses of an element rom a given rock are entirely compensated by gains of the same ele- ent in some other kind of rock. For example, substantial losses of lumina by chlorite schists, and others, in Group B are demonstrable, nd yet there is no evidence of substantial gains of alumina in any ther rock. Minor increases of Al are noticeable in ferruginous uartzites, but we would strain our point excessively, were we to ssume that these gains are compensated by losses of aluminum by chists of Group B.

Sodium, Potassium, and CO_2. CO_2 is withdrawn from the rocks as e carbonates disappear during progressive metamorphism. Insignifi- ant gains of sodium and potassium in some rocks are recorded in everal cases.

Such were the mineralogic and the chemical changes in the compo- ition of the rocks in the course of the progressive metamorphism. he migration of substance on the scale here examined could have aken place only in solutions. The movement of the solutions was ainly lateral, bed-by-bed and horizon-by-horizon, as long as the beds nd the horizons were undisturbed. There was also some migration cross beds and a measure of mixing of the solutions of unlike compo- ition along the contacts of beds and horizons of different kinds, which as conducive to the averaging of Si, Al, and Mg concentrations in the ocks, as already discussed.

There was a state approaching equilibrium between the rocks and e solutions at some time during the progressive metamorphism. his former relationship makes it possible for us simultaneously to eat rocks from a very extensive area.

As the rocks were changing in their composition, the composition the solutions in the rocks also underwent a change. Inasmuch as onditions resembling equilibrium were effective, solutions developing the rocks of different composition were also different in their com- osition during the progressive metamorphism.

We must make now a few remarks about the diagrams in Figure 3:

a) Our study does not include all of the rock types of the Krivoi Rog eries. The rock types which were not included would have their own roup boundaries.

Boundaries of our groups and subgroups become broader, on plotting rger numbers of the analyses on the diagrams, especially if we in- ude analyses of the rock types representative of the intermediate etamorphic stages.

b) Rocks from other magnetic anomalies in Ukraine have their own ecific characteristics. They require their own diagrams, for that reason, or else a high degree of caution in the use of our diagrams for their interpretation.

In conclusion, we give our thanks to L. V. Dmitriev, A. S. Pavlenko, A. I. Tugarinov, for their comments during the preparation of this paper, and to A. V. Shustrov, for his preparation of the graphs.

Received for publication
July 13, 1957

REFERENCES

1. Semenenko, N. P., N. I. Polovko, G. V. Zhukov, V. D. Ladieva, and A. A. Makukhina. *Petrografiya Zhelezisto-Kremnistykh Formatzii Ukr SSSR* (Petrography of ferruginous quartzite formations of the Ukrainian SSR). Izd. Akad. Nauk Ukr. SSSR, 1956.
2. Belevtsev, Ya. N. *Stratigrafiya i Tektonika Krivorozhskogo Basseina* (Stratigraphy and tectonics of Krivoi Rog Basin). Sov. Geolog., No. 11, 1946.
3. Belevtsev, Ya. N. *K Voprosu o Fazah Formirovaniya Struktur Krivorozhskoi Metamorficheskoi Polosy* (In reference to the phases in formations of structures in the metamorphic belt of Krivoi Rog). Izv. Aka Nauk SSSR, Ser. Geolog., No. 6, 1952.
4. Dobrokhotov, M. N. *O Proiskhozhdenii Bogatykh Zheleznykh Rud Krivorozhskogo Tipa po Dannym Izucheniya Kremenchugskogo Mestorozhdeniya* (About the origin of rich iron ores of the Krivoi Rog type as indicated by studies of the Kremenchug Deposit). Izv. Akad. Nauk SSSR, Ser. Geolog., No. 2, 1955.
5. Anikeeva, N. F. *Evoliutsiya Nekotorykh Metamorficheskikh Gornykh Porc Krivogo Roga* (The evolution of certain metamorphic rocks in Krivc Rog). Petrograf. Sb. (Collected Papers in Petrography). Materialy VSEGEI*, vyp. 4, 1955.
6. Kanibolotskii. *Petrogenezis Porod i Rud Krivorozhskogo Zhelezorudnogo Basseina* (Petrogenesis of rocks and ores in Krivoi Rog basin). Ak Nauk Ukr. SSR, 1946.

---

* VSEsoiuzhi GEologicheskii Institut (The All-Union Institute of Geology).

DISTRIBUTION OF COBALT, NICKEL, AND COPPER IN HYDROTHERMALLY ALTERED ROCKS OF THE PYSHMA-KLYUCHEVSKOE DEPOSIT

L. A. Bakhmutov

V. V. Vakhruschev Mining Institute, Sverdlovsk

Abstract

In natural conditions the mobility of elements as a function of a number of ariables may be determined by the way of a comparative study of the peculiari- ies in their behavior. For the Pyshma-Klyuchevskoe deposit an empirical eries of decreasing hypogene mobility of the elements has been established: S, e, Cu, Ni, Co, Au, Ag.

The distribution of matter in the metasomatose is based on the principle of a ifferential mobility of elements established by D. S. Korshinski (4).

As L. N. Ovchinnikov's (7) investigations have shown this principle applies ven for small amounts of elements introduced by solutions, elements—admix- ures not affecting the course of mineral formation or the arise of paragenetic ssociations.

The less mobile the element, the less constant is its concentration and there- ore we shall be able to detect more frequently and for less distances the alter- tions of the composition caused by the concentration inconstancy of this element. he more mobile the element, the more equalized is its concentration, the more niform is its distribution.

The area of the present study is the central part of the Pyshma- lyuchevskoe deposit. Commercial ores of this deposit contain accumu- tions of cobalt, copper, gold, and silver, and have also some nickel, olybdenum, selenium, and tellurium.

Our main interest, in the course of this investigation, was given to e behavior of cobalt and nickel in the host rocks of the Pyshma- lyuchevskoe, especially to their behavior in hydrothermally altered ocks in proximity to the ores which are widely distributed throughout e ore field.

The appreciable depth of the exploratory boreholes, down to 700 me- ers, the shallow depth of the oxidized zone, the broadly distributed idence of metasomatic phenomena—all of these make the Pyshma- lyuchevskoe deposit an exceptionally interesting area for the study of fferent characteristics of primary hypogene haloes.

This report serves also as an illustration of the application of the nission-spectrographic analysis to the systematic studies of hypogene rimary) dispersion haloes of heavy metals.

GENERAL CHARACTERISTICS OF PYSHMA-KLYUCHEVSKOE DEPOSIT

The mineralized ore field is associated with a band of porphyrites bordering on intrusions of ultrabasic rocks in the east and gabbros in the west. The porphyries have a north-south trend.

Rocks of an effusive complex, represented by porphyrites of differen kinds, are preponderant in the ore body. The mineralized band of porphyrites was subjected to shearing and had preserved indications of intensively active post-magmatic hydrothermal processes which had led to the formation of listvenites and of metamorphic schists of chloritic, carbonate-chloritic, and of other types of composition.

The most common effusive rocks in the ore body are represented by pyroxene, pyroxene-plagioclase, and diabase porphyrites and by amygdaloidal lavas of the same composition. A large proportion of porphyrites next to the ore bodies were transformed into porphyritoids by a severe dynamic and hydrothermal metamorphism, into metamorphosed transitional varieties of the porphyrite-schist series (developed chiefly next to the ore bodies). Porphyrites of different kinds are intermixed in their spatial distribution, without any clearly defined contacts, as they grade one into another.

The Pyshma-Klyuchevskoe ores are represented by sulfide-bearing chlorite schists, carbonate-chlorite schists, and listvenites. Pyrite, chalcopyrite, pyrrhotite, and magnetite are the most common ore minerals.

Cobalt in the ores is associated chiefly with pyrite, to some extent with pyrrhotite, and to a still lesser extent with chalcopyrite. Copper i found chiefly as chalcopyrite.

There was very little oxidation. Primary sulfides may be found already at 20 to 40 meters below the surface.

The Pyshma-Klyuchevskoe deposit is a system of ore-bearing zones showing complex mineralization associated with clearly expressed metasomatic alterations of the host rocks. This fact makes the deposit well suited for studies of relationships involved in the distribution of the primary dispersion haloes of heavy metals and of the characteristics of their behavior.

PROCEDURES

Studies of metasomatic alterations in the vicinity of ore bodies have attracted the attention of investigators for a long time. Metamorphically altered rocks near ores are ores themselves, on many occasions co taining tremendous reserves of metals. It is difficult to overestimate the prospecting importance of altered rocks bordering on the ore—the major indications of blind ore bodies. Study of metamorphism in the vicinities of ores is a subject also of a considerable theoretical interes as was pointed out by Academician S. S. Smirnov on several occasions [8, 9].

Drillcores are the test materials. The cores are sampled systema- cally, on a relatively close grid, concurrently with their examination. he cores are sampled every two meters, if they are chiefly varieties f porphyrites. In the case of carbonate-chlorite rocks, listvenites, and her metasomatic formations, the cores are sampled every meter. 20 ores altogether were examined and sampled systematically for the resent study.

S. S. Smirnov [8] attributes major importance to the spectrographic ethod in studies of rock alterations near the ore. In our numerous nalyses for cobalt and nickel [1], we followed the spectrographic proce- ure suggested by S. A. Borovik [2] with the utilization of the background the spectrograms.

3412 spectrograms were taken in our study. Every sample was an- yzed for cobalt, nickel, and copper. The total number of the analyses as 10,236.

COBALT

Concentrations of cobalt in the samples where it is present vary ithin the range of tenths and hundredths of one per cent. Cobalt peaks e found in the carbonate-chlorite rock zones, as a rule. Series of balt peaks are noted where the thickness of the carbonate-chlorite cks amounts to tens of meters (Figs. 1 and 2).

However, not all of the carbonate-chlorite zones show cobalt peaks. everal metasomatic zones contain no cobalt. An indication of the ab- ence of cobalt in the carbonate-chlorite rocks is found in their visible lative thinness, not exceeding 2 to 5 meters.

Carbonate-chlorite interlayers a few meters thin are generally arked by one or two peaks. Further thinning of the metasomatic rocks associated with qualitative changes in the behavior of cobalt, in the nse that cobalt may be absent from the carbonate-chlorite interlayers, they are only 1, 2, 3, 4, or 5 meters thick.

These facts lead us to the conclusion regarding a selective distribu- on of cobalt in the hydrothermally altered rocks of different thickness. balt is localized, chiefly along the main channels of the hydrothermal lutions, while migrating from the altered rocks into the host rocks, cause of its weak migrating tendencies. These main channels through ich the hydrothermal solutions were passing are now associated with e largest zones of the hydrothermally altered rocks.

The observed facts show the dependence of the distribution of cobalt the size of the hydrothermally altered zones. This relationship is pressed by the presence of cobalt in all of the large metasomatic nes in the rocks and by the tendency of cobalt to disappear where the drothermally altered rocks are thinning out to a few meters.

The idea of the selective distribution of cobalt, nickel, and of other re and dispersed elements, along the principal paths of hydrothermal lutions, was first expressed by L. N. Ovchinnikov [7], on the basis of s detailed studies of a large body of data on the Turinskoe skarn de- sit of copper.

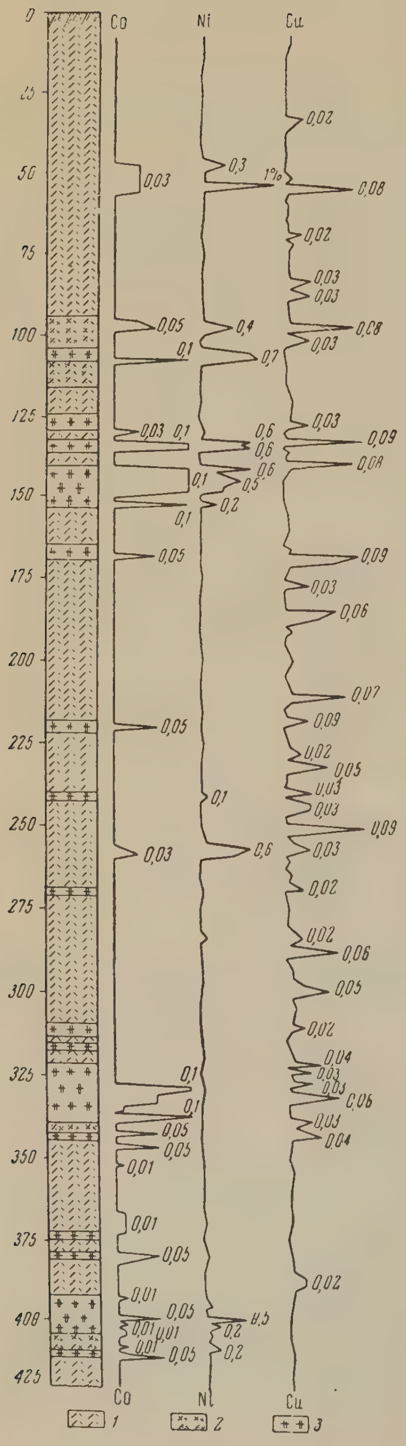

Porphyrite masses of rock, tens of meters thick, contain generally hundredths of one per cent of cobalt, in places where these rocks are in a direct contact with the hydrothermally altered rocks. The same kind of porphyrites at increasing distances from contacts with metasomatic rocks are already cobalt-free.

These facts are indicative of a partial migration of cobalt from the cobalt-bearing metasomatic rocks, containing the sulfide mineralization, into the contact zones of the porphyrites. The enrichment of the porphyrites by cobalt, in their contacts with the zones of hydrothermal metamorphism, was due apparently to a diffusion of some soluble compounds of cobalt, by all evidence.

The relatively low concentrations of cobalt in the hydrotherma solutions, its low mobility, its strong tendency to follow iron, the absence of arsenic (with which both cobalt and nickel are generally associated), the high concentrations of sulfate—all these factors, as a whole, are responsible for the absence of cobalt mineral in the Pyshma-Klyuchevskoe deposit and for settling of cobalt in crystal structures of other minerals. The high geochemical affinit of cobalt and iron, due to the clos resemblance of their electronic shells and to about the same size

Fig. 1. Diagrams of concentrations of cobalt, nickel, and copper in drillcore samples, borehole No. 1132: 1—porphyrites; 2—porphyritoids; 3—carbonate-chlorite rocks.

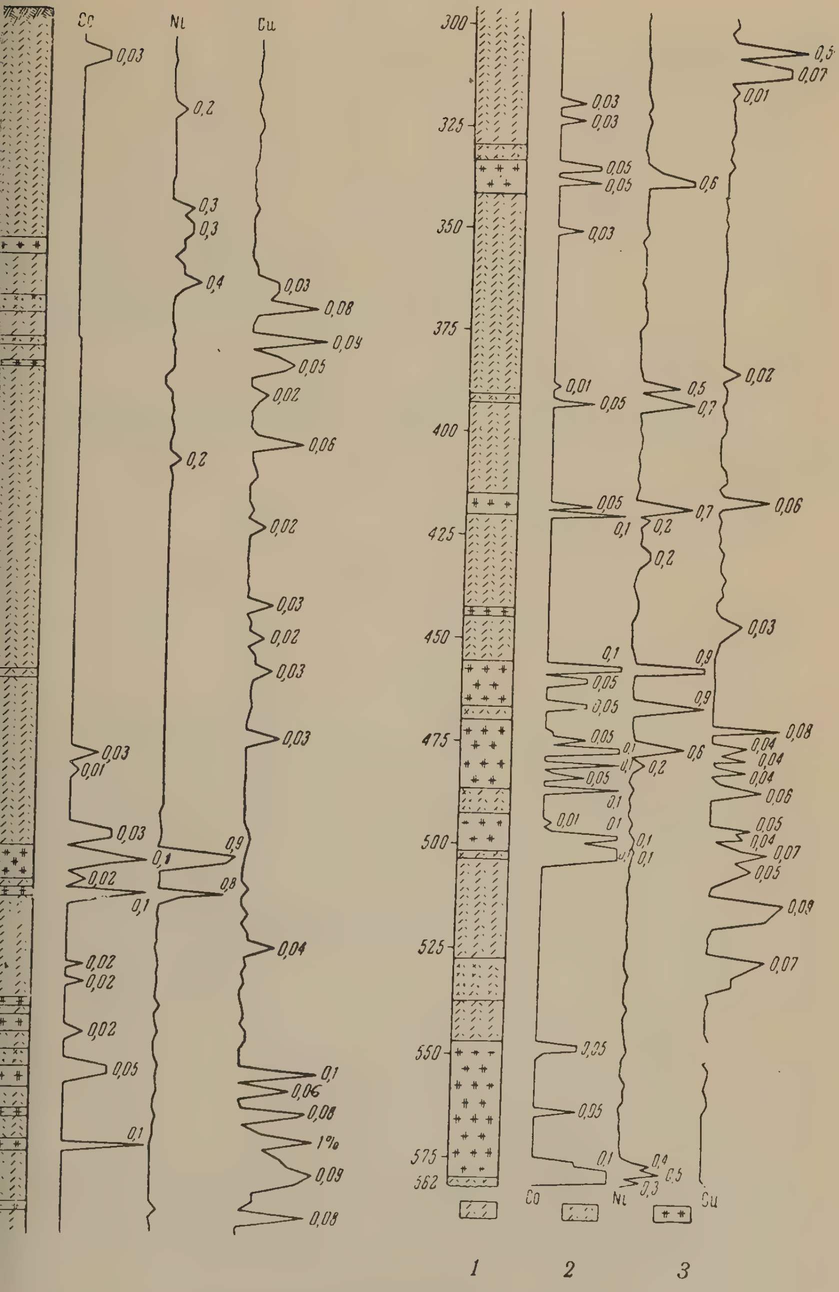

2. Diagrams of concentrations of cobalt, nickel, and copper in drillcore les, borehole No. 646: 1—porphyrites; 2—porphyritoids; 3—carbonate-ite rocks.

of their ionic radii, was responsible for the entry of the bulk of cobalt into the crystal lattice of iron disulfide, the pyrite.

The Pyshma-Klyuchevskoe pyrite is the principal accumulator of cobalt, as had been shown by the experience of many years with the extractions of cobalt.

The irregular distribution of cobalt in thick masses of hydrotherma ly altered rocks is manifested, first of all, both in the presence and in the absence of this element in different parts of the altered zones, in the abrupt variations in the concentrations of cobalt over short distances. This latter feature is evidence of a high concentration gradien of the soluble cobalt compounds and of the low mobility of cobalt in the hydrothermal solutions by which the sulfides were laid down in the Pyshma-Klyuchevskoe deposit.

The irregular distribution of cobalt and the discontinuity of its concentrations are characteristic not only of the hydrothermally altered rocks but of the mineralized zones, as a whole, and even of the isolate ore bodies.

The irregular distribution of cobalt, as a whole, is a major feature of its behavior. This peculiarity is characteristic not merely of the Pyshma-Klyuchevskoe deposit but is manifested in all economic deposits of cobalt of hypogene origin [6], more or less clearly.

NICKEL

The behavior of nickel is similar to the behavior of cobalt. Concen trations of nickel in the basic effusives and in the products of their hy drothermal metamorphism—the host rocks of the deposit—fluctuate within hundredths and tenths of one per cent. Moreover, the hundredt of one per cent represent the ordinary levels of the nickel content, while the tenths are already anomalous and are evidence of the accessions of this metal from the hydrothermal solutions.

The nickel concentration curves, as against the cobalt curves, have fewer peaks and have a smoothness over considerable intervals of the depths amounting to tens and even hundreds of meters. The smaller number of nickel pits is the effect of a higher mobility of nickel, in comparison with cobalt. The higher mobility of nickel is conducive to a more rapid dispersion of this metal, to a partial averaging of its co centrations over considerable distances.

In our view, the higher mobility of nickel, in reference to cobalt, is due to higher concentrations of nickel in the solutions. As was shown by D. S. Korzhinskii [5], concentration of the element in solutions is one of the independent parameters by which mobility of the constituen is determined. Mobility of elements increases at increasing concentrations in the vast majority of the cases.

The concentration of nickel is nearly ten times as high as the concentration of cobalt. This major difference could not help but have a effect on their relative mobility.

There are enough empirical data to show that most of the nickel peaks are seconded by the cobalt peaks.

Inasmuch as both cobalt and nickel were present in the solutions at same time, and to the extent of the higher mobility of nickel than of alt, one may be led to believe that if it is impossible for the mobile kel to come to some more or less uniform concentration in some ticular part of the rock, there is even less chance for the less mo- e cobalt to become dispersed in the same part of the rock. These as- ts of the behavior of cobalt and nickel are the probable causes of the kel peaks being seconded by the cobalt peaks on the concentration ves. Absence of cobalt is the only reason why cobalt peaks are not ociated with nickel peaks on the curves, wherever this is the case.

In such manner, the differences between the distribution of cobalt nickel are due chiefly to the differences between the mobilities of se two elements. Although most of the higher concentrations of nick- re associated with the carbonate-chlorite rocks, some isolated peaks ickel are found also in the porphyrites. These higher concentrations ickel in the porphyrites are apparently not of the primary magmatic gin but are due to some effects of the hydrothermal solutions.

COPPER

The concentrations of copper have a tendency to variation within a er range embracing tenths, hundredths, and thousandths of one per t. As to the copper peaks—it is not always possible to see the order- ss in their distribution which is so clear-cut in the case of cobalt nickel. Most of the copper peaks are associated with rocks in the rothermally altered zones.

The wide range of variations in the concentration of copper suggests copper is more mobile than cobalt or nickel. The greater mobility opper may have been one of the causes responsible for the migration opper into the host rocks and for the consequent copper ''highs'' in porphyrites. There is no observable connection between the copper ks and the peaks of cobalt or nickel. Copper behaves independently n cobalt and nickel.

RELATION OF HYDROTHERMALLY ALTERED ZONES TO MINERALIZATION

The ore-bearing zones show a close genetic relationship to the car- ate-chlorite rocks [3], chlorite schists, listvenites and, to a lesser ree, to other rocks of the metamorphic complex, products of a hy- hermal re-working of the porphyrites. The entire complex of the bearing zones and of the associated hydrothermally altered rocks nds in a north-south direction. The preponderant dip of the rocks the west. Chlorite schists and carbonate-chlorite rocks of differ- kinds are succeeded by porphyritoids, as one moves away from the eralized zones, and, still farther away, by porphyrites. As a rule, ore-bearing zones are represented, to the extent of 80%, by vein

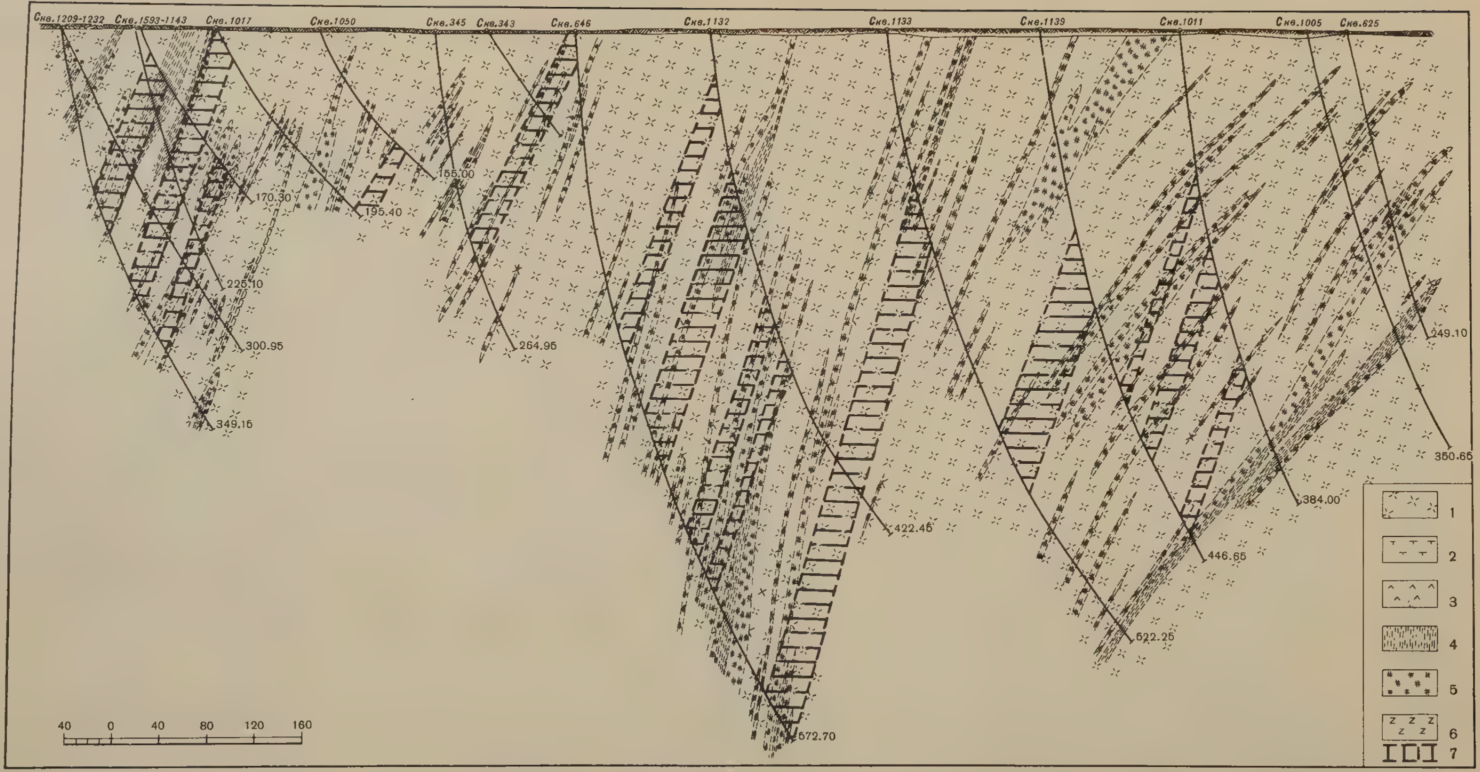

Fig. 3. Distribution of cobalt and nickel in vertical projection of profile: 1—porphyrites; 2—diorites; 3—diabases; 4—schists; 5—chlorite-carbonate rocks; 6—listvenites; 7—zones mineralized by cobalt.

inerals; chlorite, carbonates, quartz, and others. The ore-bearing
nes are 200 to 2,000 meters long, with an average thickness of about
meter.

A vertical projection of the metal concentrations in the profile rep-
esented by 10 boreholes (Fig. 3) was drawn in order to ascertain the
aracteristics of the spatial distribution of cobalt. In constructing the
rtical projection of every one of the boreholes, the cobalt-bearing
rizons were noted, whereupon such horizons were combined into zones,
the directions of the principal developments of the structures. The
sulting pattern has led us to the conclusion that the distribution of co-
lt is determined by the zones of the most intensive hydrothermal al-
ration of the rocks. Figure 3 shows still another major detail: cobalt
es not disappear in depth, while the character of its distribution, as
whole, indicates a real possibility of its further expressions at greater
pths. Analogous projections were drawn for nickel (Fig. 3). Their re-
lts indicate that the distribution pattern of nickel coincides exactly
th the pattern for cobalt. A coincidence of this sort is an indication
itself that nickel and cobalt were migrating through the same chan-
ls, possibly even in the same solutions.

METALS IN THE MAGMATIC COMPLEX AND IN ITS DERIVATIVES

With an appreciable number of the analyses at our disposal, we made
attempt at an estimation of the average concentrations of cobalt,
ckel, and copper in different parts of the ore field. These concentra-
ns were determined as arithmetical averages of many analyses. The
sults are shown in the following tabulation:

em	Rocks	Number of Analyses	Co %	Ni %	Cu %
	Ultrabasic	134	0.12	0.33	0.017
	Gabbros	42	0.007	0.14	0.024
	Porphyrites	1586	0.004	0.06	0.008
	Porphyritoids	502	0.009	0.07	0.008
	Carbonate-chlorite	800	0.015	0.10	0.008
	Listvenites	100	0.006	0.04	0.004

A. E. Fersman [10] and A. P. Vinogradov [11] give the following
erages for cobalt, nickel, and copper in the earth's crust:

	Co %	Ni %	Cu %
Fersman, 1939	0.002	0.02	0.01
Vinogradov, 1949	0.003	0.008	0.01

The average concentrations of cobalt and nickel in the rocks of the ore field are invariably higher than their clarkes, as may be seen in the foregoing comparison. The average copper in the porphyries, 0.008%, is close to its clarke in the earth's crust.

The concentration of cobalt in the ultrabasic rocks is conspicuously high. It is possible that the ultrabasic rocks, by virtue of their relatively high content of cobalt, were enabled somehow to control the cobalt mineralization. The established fact of the more intensive copper-cobal mineralization of the ore-bearing zones, with their decreasing distance from the eastern contact of the effusives with the ultrabasic rocks, acquires a new shade of meaning, in this connection. Also, the special analysis of the variations of the metal content in the 10-borehole profile (Fig. 3) showed marked increases in nickel—whose relatively high amounts in ultrabasic rocks is a generally known fact—in individual boreholes eastward. The ultrabasic rock effects on the mineralization may have been manifested in places where they were at the least distance from the ore zones. There is also a possibility that the hydrothermal solutions, on their way from their source, were becoming enriched by nickel and cobalt on their contacts with the ultrabasic rocks. These comparisons suggest that the underlying ultrabasic rocks played some definite part in the mineralization and an opinion may be in order, to the effect that they exercised a definite control over the mineralization itself.

Comparisons between the behavior of a series of elements, based on a large number of spectrographic analyses, enable us to evaluate the copper-cobalt haloes which are much broader than was believed previously, on the basis of the mine workings. The proved facts of the spontaneous migration of heavy metals into rocks of the hanging wall reveal some real possibilities in the prospecting and in the discovery of blind ore bodies, permitting the advancement of the geochemical method as the means of the preliminary appraisal of economic reserves of the zones containing sulfide mineralization.

Only the geochemical (metallometric) method may be considered efficient in prospecting for blind ore bodies, whose profiles may be projected in most curious directions, geologically. The recommended spacing between samples is 1 meter. Wherever the concentration of cobalt is at least twice its background in the profile, further studies are required, in our opinion.

CONCLUSIONS

Mobility of chemical elements in natural environments, as a function of a series of variables, may be ascertained by comparative studies of the characteristics of its behavior. In the case of the Pyshma-Klyuchevskoe deposit, we have the following empirically established series, in the order of decreasing mobility of the elements: S, Fe, Cu, Ni, Co, Au, Ag.

The principle of differential mobility of the elements, established by

). S. Korzhinskii [3], is based on the distribution of substance in the netasomatic process.

As shown by L. N. Ovchinnikov [7], this principle is valid also for lements brought by the solutions in very small quantities, the admixure-elements, which have no effect on the formation of minerals or on he development of paragenetic associations of different kinds.

The less mobile the element—the more constant is its concentration. onsequently, any change in the composition due to irregularities of the oncentration of such elements is that much more easily detectable, and ver shorter distances. The more mobile the element—the more uniorm its concentration, the more gentle is the slope of its distribution urve, the more uniform is its distribution the smaller is the amplitude f fluctuations of its concentration.

The role of diffusion in metasomatic processes was made manifest n its entirety by the studies of D. S. Korzhinskii, who introduced the oncept of the differential mobility of elements and who developed the heory of metasomatic zonations.

It is possible that the orderly distribution of the admixture elements n ore deposits, as governed by their differential mobility, may have a niversal validity.

Received for publication
August 26, 1957

REFERENCES

Bakhmutov, L. A. *Analiticheskie Spektralnye Linii Kobal'ta v Prisutstvii v Probe Zheleza i Nikelya* (Analytical spectrographic lines of cobalt in the presence of iron and nickel in the samples). Zavodsk. Lab., No. 11, 1956.

Borovik, S. A. *Ispol'zovanie Fona pri Kolichestvennykh Spektral'nykh Analizah Mineral'ogo Syr'ya* (Utilization of the background in quantitative spectrographic analysis of mineral raw materials). Doklady Akad. Nauk SSSR, 36, No. 6, 1942.

Zavaritskii, A. N. *Geologicheskii Ocherk Mestorozhdenii Mednykh Rud na Urale* (Geologic outline of copper ore deposits of Ural). Trudy Geolkoma* 1927.

Korzhinskii, D. S. *Podvizhnost' i Inertnost' Komponentov pri Metasomatoze* (Mobility and inertness of constituents during metasomatic process). Izv. Akad. Nauk SSSR, Ser. Geol., No. 1, 1955.

Korzhinskii, D. S. *Ocherk Metasomaticheskikh Protzessov* (Outline of metasomatic processes). Sb Pamyati Akad. S. S. Smirnova (Papers Collected in Memory of S. S. Smirnov, Member of the Academy). Akad. Nauk SSSR, 1955.

Krutov, G. A. *Kobal't* (Cobalt). Gosgeolizdat, 1952.

Ovchinnikov, L. N. *O Raspredelenii Elementov-Primesei v Metasomaticheskikh Mestorozhdeniyah* (On the distribution of the admixture elements in metasomatic deposits). Izv. Akad. Nauk SSSR, Ser Geol., No. 1, 1948.

Smirnov, S. S. *Nekotorye Obshchie Voprosy Izucheniya Rudnykh Mestorozhdenii* (Certain general problems in studies of ore deposits). Izv. Akad. Nauk SSSR, Ser. Geol., No. 5, 1946.

9. Smirnov, S. S. *O Sovremennom Sostoyanii Teorii Obrazovaniya Magmatogennykh Rudnykh Mestorozhdenii* (On the present state of the theor of origin of magmatic ore deposits). Zap. Mineralog. Obsch., Vyp. 1 1947.
10. Fersman, A. N. *Geokhimiya Kobal'ta* (Geochemistry of cobalt). Izv. Akad. Nauk, Ser. Geol., No. 3, 1939.
11. Vinogradov, A. P. *Predislovic Redaktora K Spravochniku po Fizicheskim Konstantam. Berg, Sherer, Spaiser* (Editor's Preface to the Handbook of Physical Constants by Birch, Schairer, and Spicer). 1949.

EXPERIMENTAL STUDIES IN OXIDATION OF COBALT AND NICKEL ARSENIDES IN SOLUTIONS CONTAINING OXYGEN AND CARBONIC ACID

L. K. Yakhontova

Chair of Mineralogy, M. V. Lomonosov Moscow State University

Abstract

Leaching experiments were carried out on a series of arsenides, smaltite, rammelsbergite, safflorite and niccolite using a carbonic acid solution (pH 3.7) and an oxygen-carbonic acid solution (pH 4.5). Arsenic was the element most easily leached out of the arsenides. In the order of increasing losses of arsenic by leaching, the minerals form the series: safflorite-niccolite-rammelsbergite-smaltite. Iron, cobalt and nickel were very inert to the leaching solutions as compared with arsenic.

Results of laboratory studies of the oxidation of smaltite, rammelsbergite, niccolite, and safflorite, involving a slow seepage of carbonate and oxygen-bearing solutions through pulverized minerals, as here reported, are a continuation of our earlier work [1, 2].

Our objective here was a procurement of quantitative data that would aid our understanding of the leaching of the elements from their minerals—the arsenides—and also of the formation of the secondary minerals, products of oxidation, deposited on the surfaces of the primary minerals.

EXPERIMENTAL CONDITIONS

Single-mineral samples of the arsenides were used in our work, 1 gram aliquots of the 0.25 mm fraction. The minerals were analyzed chemically* prior to the experiments and the results, expressed as formulas, were found to be as follows:

Smaltite, $(Ni_{0.66}Co_{0.28}Fe_{0.06})As_{2.88}$	As	77.68%
	Ni	14.19%
	Co	5.49%
	Fe	1.26%
Safflorite, $(Co_{0.6}Fe_{0.4})As_{1.7}$	As	68.11%
	Co	18.55%
	Fe	12.13%
Rammelsbergite, $(Ni_{0.5}Co_{0.4}Fe_{0.1})As_2$	As	72.36%
	Ni	14.15%

---

*A. N. Bukina, Analyst, Laboratory of the Chair of Mineralogy, Moscow State University.

- Co - 10.51%
- Fe - 2.98%

Niccolite, NiAs - - - - - - - - - - - - - - - As - 43.58%
- Ni - 55.14%

Weighed arsenide powders were placed in glass crucibles with porcelain filter bottoms. Solutions at constant concentrations of CO_2 and oxygen were allowed to drip onto the filters continuously from dropping funnels, 24 hours a day. The percolate was collected in receiving flasks. The experiments were at room temperature (20° ± 2°C).

There were eight experiments altogether: four with the oxidizing solvent, the aqueous solution containing carbonic acid (pH 3.7—the "minus-oxygen series"), and four in which the dissolving-oxidizing function was performed by dissolved CO_2 and oxygen (pH 4.5—"oxygen series").*

Our choice of the pH was determined by two considerations: a) The pH range here used was close to the pH of sulfuric acid solutions whose effects on the minerals were studied by us previously in a similar manner [2], and b) some purely technical aspects of the experiments, as it was established empirically that the pH levels here reported remain constant for a long time, if the distilled water in the 200 mls dropping funnels is treated with CO_2 or oxygen for 30 minutes twice a day.

Duration of every one of our experiments was 120 days. The leachings collected in the receiving flasks were analyzed every ten days. As, Co, Ni, and Fe were determined in these leachings.

The experiments were terminated when the secondary substances (chiefly arsenates) would form a coating over the powdered arsenides, and the solution-oxidation of the primary minerals would change its character entirely. The leaching of some elements (Ni and Co) from the arsenides, at this stage, would be either retarded or inhibited entirely.

The residual arsenides, together with the secondary substances, were treated at once with 3% hot HCL so as to dissolve the secondary substances in order to determine their composition. The arsenides remained on the filters, by virtue of their insolubility under such conditions. A preliminary treatment of the crucibles with boiling water on a stem bath, before the acid treatment, was employed occasionally, as the means of a confirmatory isolation and determination of the arsenolite which was formed under the experimental conditions. Amounts of the arsenolite were determined by calculation from the acid extract analyses, with microscopic control.†

---

*Ordinary distilled water at pH 6.8 as the solvent. Its CO_2 and O_2 content were determined and the expression "minus-oxygen series" is used arbitrarily, here and later on, in the sense that no oxygen was added to the water.

†Chemical analyses by L. S. Abramova and V. V. Bon, Laboratory of the Chair of Mineralogy, Moscow State University.

RESULTS

The following phenomena were taking place in our 120 day experiments:

a) Leaching of the elements from the minerals and their accumulation in the filtrates.

b) Formation of secondary compounds at the surfaces of the arsenide particles undergoing oxidation.

Behavior of the arsenide constituents in the leaching process, their amounts in the leachates, and composition and properties of the residual products accumulated during 120 days of the leaching-oxidation were ascertained by chemical analysis of samples of the leachates and of the residues (analyses of aqueous and acid extracts) at ten-day intervals.

The analytical results on the leachates are shown diagrammatically as weights and atomic quantities (times 10^4) in Figure 1.

It is evident from Figure 1 that arsenic is the principal one among the leached-out elements, in all cases, and that the arsenic content of the leachates in the receiving flasks exceeds significantly the sum of the other elements (Co, Ni, and Fe). The final ratio of arsenic to the sum of the cations is as follows:

Mineral	pH of Leaching Solution	
	3.7	4.5
	As: (Co Ni Fe)	
Rammelsbergite	8:1	17:1
Niccolite	1:1	1.5:1
Smaltite	33:1	15:1
Safflorite	3:1	no As removed by leaching

Only niccolite showed mutually comparable rates of leaching for As and Ni, already outside the equilibrium at pH 4.5, and also safflorite, from which practically no arsenic was migrating outside the boundaries of the mineral, at the same pH level.

Changes in the pH of the environment had a strong effect on the mobility of arsenic, in the case of smaltite and safflorite: the leaching of arsenic was accelerated by the increase in the pH in the former but was practically arrested in the latter case.

The highest absolute amounts of arsenic in solutions, under the experimental conditions, in the smaltite test, were observed when the pH of the solvent was 4.5, although the proportions of this element, with respect to the other solute, were greatest in the presence of the excess of carbonic acid in the solvent (pH 3.7). Arsenates of different kinds, with cations captured from the environment (Cu, Ca, Mg, Mn, etc.) may be formed in both cases outside the borders of the arsenide.

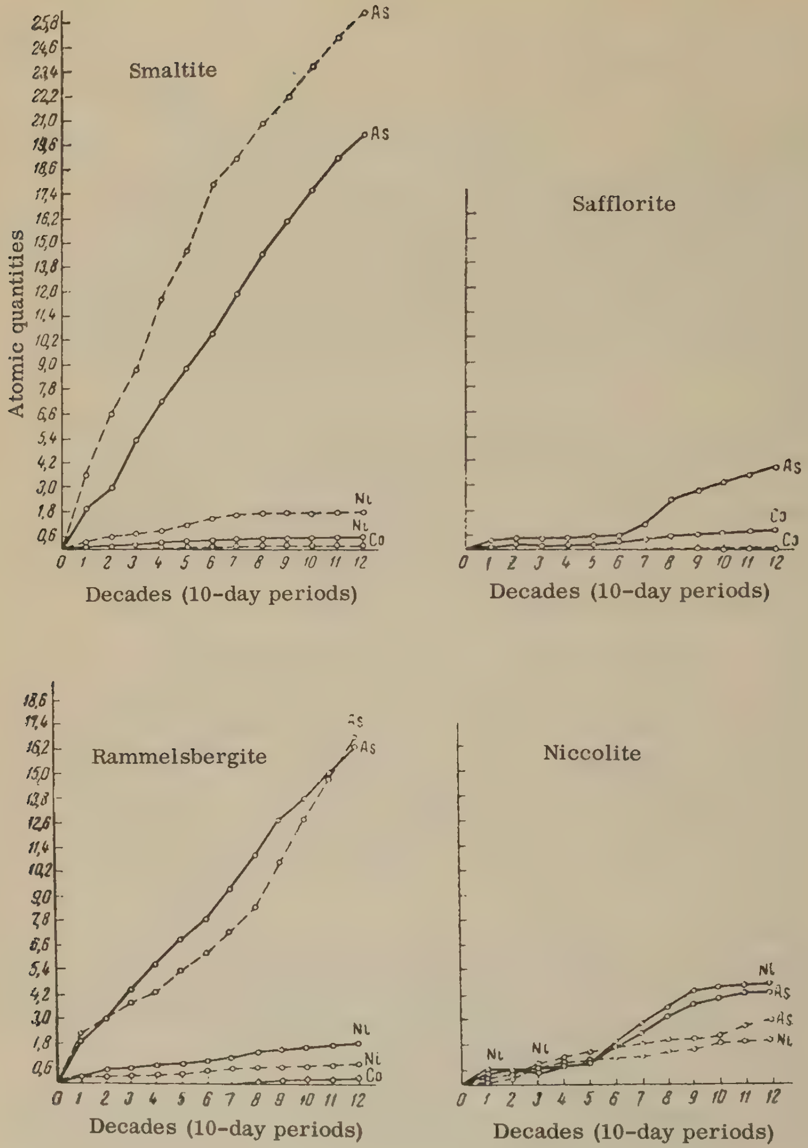

Fig. 1. Leaching curves for arsenide constituents. Solid lines—carbonic acid solutions (pH 3.7); dotted lines—oxygen-carbonic acid solutions (pH 4.5).

Behavior of arsenic in the leaching of smaltite resembles that of rammelsbergite, in both solvents, with the mobility of arsenic being about the same for both minerals, although the proportions of arsenic are not quite the same in the leachates, on account of the differences in the rates of extraction of Co and Ni.

While the arsenic of smaltite and rammelsbergite was leached inensively even during the first ten days of the experiments, and there as no change in its solubility rates on further leaching, the arsenic of iccolite and safflorite (pH 3.7) was not released for a long time (50-0 days) by these minerals into the percolating solutions.

Later on, although the arsenic-leaching curves showed breaks, inicative of the increasing mobility of arsenic, neither the relative nor e absolute amounts of arsenic leached from niccolite and safflorite ere in excess of the corresponding amounts observed for smaltite and ammelsbergite. The solutions at pH 4.5 remained inactive with repect to safflorite for all practical purposes (the total solubility of the rsenide was only 0.1%, attributable to the leaching of cobalt).

Behavior of the cations—nickel, cobalt, and iron—during the solution f the arsenides was especially interesting. Iron was not observed in ny one of the filtrates, i.e. there was no leaching of iron throughout e experiments.

The leaching of cobalt resembled the leaching of iron. There was ractically no cobalt in the filtrates at pH 3.7 and very little cobalt in e oxygen-carbonic acid solutions obtained from rammelsbergite and afflorite.

Next to arsenic, nickel proved to be the most mobile one of the lements. The amounts of nickel leached out of niccolite were almost f the same magnitude as the amounts of arsenic. Smaltite and ramelsbergite resembled each other, with respect to the leaching of ickel and to the behavior of arsenic. Smaltite was different from ramelsbergite, as formerly, by the higher mobility of its nickel at pH 4.5.

In such manner, the cation-leaching curves show two maxima: the ckel peak for niccolite (in both environments) and the cobalt peak for afflorite (in the oxygen-carbonic acid environment). If the loss in eight by the arsenides, due to the passage of their constituents into e percolating solutions, is taken as the criterion of their solubility, e may arrange the four arsenides in the following sequence, in the rder of their increasing solubility at both pH levels of our experients: safflorite - niccolite - rammelsbergite - smaltite.

Certain general and seemingly natural relationships are represented the leaching curves: increased solubility of the constituents at the wer pH of the solvent; the precipitation of smaltite whose constituents ecome less soluble at a higher acidity of the solution.

The peculiar behavior of smaltite which is expressed not only in its eparture from the general rule, as here illustrated, but also in the eater solubility of its arsenic during the oxidation is due probably to rtain complicated and still unknown features of its structure.

Alongside the withdrawal of substance from the powdered arsenides, ere is a gradual accumulation of the secondary end-products on the senide surfaces. These products were examined by us microscopilly and chemically.

Rammelsbergite, in both environments, became thoroughly coated an apple-green crust consisting chiefly of annabergite. Small crusts of white crystalline arsenolite were also present, locally (especially on materials treated by carbonic acid waters).

Smaltite "bloomed" in clusters of pale-pink erythrite associated with white octahedral arsenolite, creeping upwards along the walls of the filters, and with a yellowish-brown arsenate, seemingly of a ferruginous composition. The latter was more abundant under the action of the carbonic acid solutions.

Niccolite remained fresh for a long time (about 50 days), in both cases. Later on, black soot-like spots began to develop in its cracks and on the surface of its grains. The sooty spots were becoming coated by the green films of annabergite. The oxidation of niccolite accompanied by the formation of the secondary compounds was noticeably more rapid in carbonic acid waters (pH 3.7).

Safflorite, like niccolite, was oxidizing very slowly during the first 60 days of the experiments and was developing violet streaks only locally. Later on, the following compounds began to form from the secondary products: bright-pink erythrite, small crusts of brown ferruginous substances, and clusters of grains or crystals of a white arsenolite.

As previously stated, the powdered arsenides were treated with 3% HCl after 120 days of the experiments, in order to isolate the oxidation products. Analyses of the acid extracts, together with the calculations, are presented in Table 1.

We determined the total amounts of the arsenide constituents in the oxidized materials, as indicators of the oxidizability of the arsenides. The results showed that the changes in the pH of the environment, within the chosen range (3.7 to 4.5), had an appreciable effect on the solubility of most of the primary minerals, but very little effect on their susceptibility to oxidation. The only significant effects, in this connection, were manifested only by rammelsbergite.

Comparisons between the amounts of the dissolved arsenide substance, for every mineral, and the amounts of this substance converted into the secondary products of the oxidation showed that, for rammelsbergite, the oxidizability is practically the same as solubility and that oxidizability of safflorite is higher than its solubility, while the reverse is the case for niccolite and smaltite. The oxidizability series here suggested (niccolite - safflorite - smaltite - rammelsbergite) do not parallel the solubility series.

Figures 2 and 3 are special diagrams built on the coordinates of the composition of arsenides (As, Ni, Co, Fe) and representing quantitative relationships between the elements that were leached-out of the primary minerals and had entered the secondary products of the oxidation during 120 days of the experiments. The content of these elements in the arsenides is indicated by magnitudes of the coordinate section.

All of the previously reported regularities in the solubility of the arsenides (the negligible solubility of safflorite at pH 4.5; the nearly equal amounts of As and Ni derived from the solubility of niccolite; the extensive leaching of arsenic out of smaltite and rammelsbergite;

Table 1 (Part 1). Chemical Analyses of Acid Extracts and Calculations

	pH 3.7					
Element	Amount of the Element grams	% of Arsenide	Amounts of As_2O_5 and $R^{++}O$ grams	As Arsenate of the Erythrite Series grams	As Arsenolite grams As	Excess of Cations grams
			Rammelsbergite			
As	0.0538	7.0	0.0823	0.0807	0.0010	----
Co	0.0105	10.0	----	----	----	----
Ni	0.0491	34.0	0.0790	0.0790	----	----
Fe	0.0026	9.0	----	----	----	----
Sum	0.1150	----	----	----	----	----
% oxidizability of arsenide		----	11.6	----	----	----
			Niccolite			
As	0.0035	0.8	0.0053	0.0053	----	----
Ni	0.0154	3.0	0.0195	0.0051	----	0.0113
Sum	0.0187	----	----	----	----	----
% oxidizability of arsenide		----	1.9	----	----	----
			Smaltite			
As	0.0460	6	0.0703	0.0688	0.0010	----
Co	0.0184	33	----	----	----	----
Ni	0.0272	19	0.0673	0.0673	----	----
Fe	0.0074	60	----	----	----	----
Sum	0.0990	----	----	----	----	----
% oxidizability of arsenide		----	9.9	----	----	----
			Safflorite			
As	0.0295	4.3	0.0451	0.0396	0.0036	----
Co	0.0091	5	0.0387	0.0387	----	----
Ni	0.0214	17	----	----	----	----
Sum	0.0600	----	----	----	----	----
% oxidizability of arsenide		----	6.0	----	----	----

e insignificant withdrawals of cobalt) are reflected with a remarkble clarity in the forms of the appropriate diagrams, most of which re elongated appreciably along the "As" axis. Diagrams of the second roup, representing susceptibility of the arsenides to oxidation, are enerally cut short on the arsenic axis, but are markedly elongated in e "cation" directions.

We should note the behavior of iron, the large amounts of which are ccumulated in the secondary products (9 to 22% on rammelsbergite, Table 1 (Part 2). Chemical Analyses of Acid Extracts and Calculations

	pH 4.5					
Element	Amount of the Element grams	% of Arsenide	Amounts of As_2O_5 and $R^{++}O$ grams	As Arsenate of the Erythrite Series grams	As Arsenolite grams As	Excess of Cations grams
		Rammelsbergite				
As	0.0678	9.3	0.1037	0.1037	----	----
Co	0.0117	11.0	----	----	----	----
Ni	0.0618	43.0	0.1015	0.1015	----	----
Fe	0.0064	22.0	----	----	----	----
Sum	0.1477	----	----	----	----	----
% oxidizability of arsenide		----	14.7	----	----	----
		Niccolite				
As	0.0057	1.3	0.0087	0.0087	----	----
Ni	0.0130	2.3	0.0165	0.0085	----	0.0062
Sum	0.0187	----	----	----	----	----
% oxidizability of arsenide		----	1.9	----	----	----
		Smaltite				
As	0.0532	7	0.0814	0.0609	0.0134	----
Co	0.0111	20	----	----	----	----
Ni	0.0310	22	0.0596	0.0596	----	----
Fe	0.0048	38	----	----	----	----
Sum	0.1001	----	----	----	----	----
% oxidizability of arsenide		----	10.0	----	----	----
		Safflorite				
As	0.0259	3.8	0.0396	0.0349	0.0031	----
Co	0.0074	4	0.0342	0.0342	----	----
Ni	0.0195	16	----	----	----	----
Sum	0.0528					
% oxidizability of arsenide		----	5.3	----	----	----

38 to 60% on smaltite, up to 17% on safflorite, as of the iron-content of the original materials). Moreover, a shift of the pH to the acid side (3.7) reduced the iron-content 2.5 times in the secondary products on rammelsbergite but nearly doubled the amount of iron in the substances derived from the oxidation of smaltite.

As shown by the diagrams, the oxidation of smaltite and particularly of rammelsbergite causes a build-up of high concentrations of nickel, in place (as annabergite and as nickeliferous erythrite). A decrease

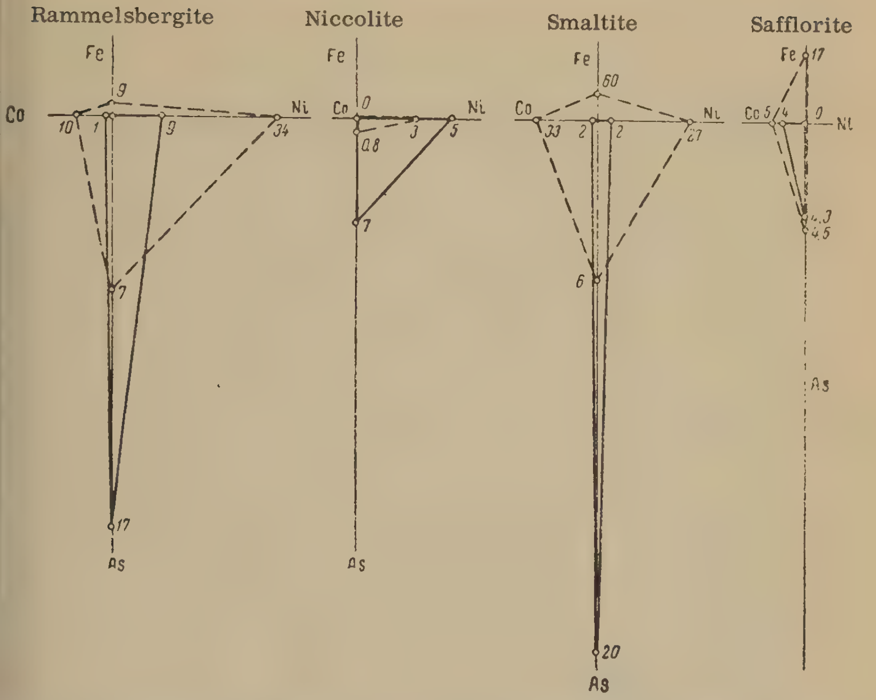

Fig. 2. Diagram showing quantitative ratios between leached elements (solid ines) and elements entering composition of secondary products of oxidation (dotted lines) on treatment of arsenides by carbonic acid waters (pH 3.7).

the acidity (in the environment of the carbonic acid solutions con- ining free oxygen) causes a relative increase in the nickel content of e secondary substances, while the proportions of cobalt are either changed (rammelsbergite) or diminished (smaltite).

In the instance of niccolite, there is an intensive enrichment of the xidized substances by nickel alongside a very small accession of rsenic. Nickel is accumulated apparently in the black, soot-like films ating the nickeline grains and associating with relatively small antities of annabergite.

Cobalt, under the experimental conditions, was pretty nearly absent the solutions percolating through powdered arsenides, although there as an appreciable accumulation of this element in the secondary prod- ts, especially on smaltite under the carbonic acid-water treatment.

On the whole, during the leaching of the elements out of the arsen- es, with the concurrent fixation of some of them by the secondary oducts, there was a marked difference in the behavior of arsenic and the cations: if most of the arsenic was removed from the arsenides leaching and was carried out of the system in the percolate, the tions tended to accumulate in place, as combinations with oxygen, ter, and, to some extent, with arsenic and other anions. Hence the

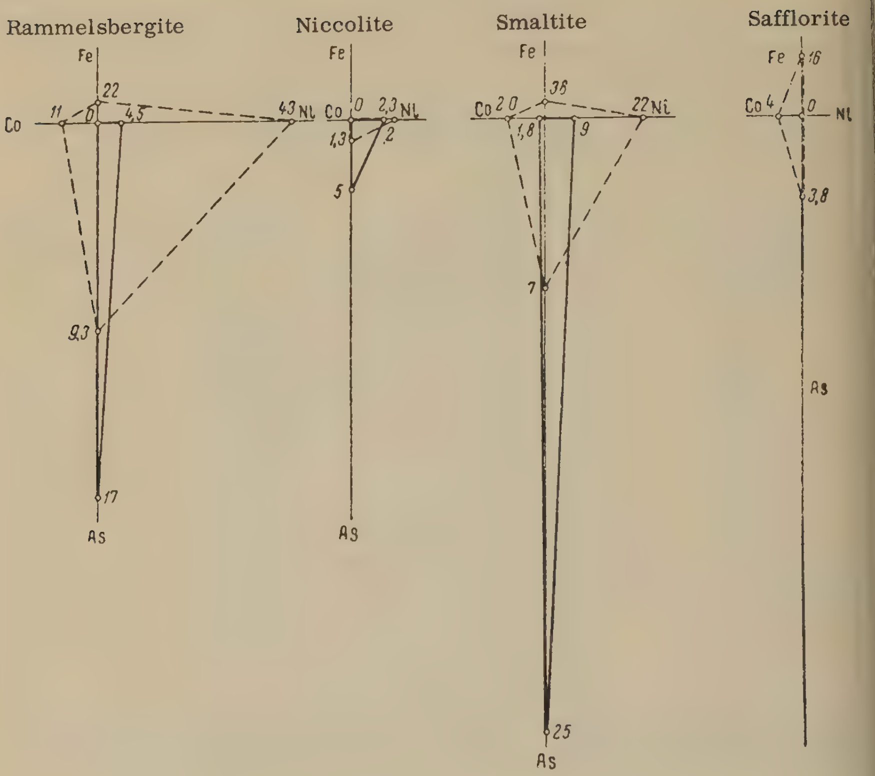
Rammelsbergite Niccolite Smaltite Safflorite

Fig. 3. Diagrams showing quantitative ratios between leached elements (solid lines) and elements entering composition of secondary products of oxidation (dotted lines) on treatment of arsenides by oxygen-carbonic acid waters (pH 4.5).

accumulation of the hydrated arsenates (erythrite and annabergite) and of basic arsenates, oxy-arsenates (smol'ianinovite), carbonates (spherocobaltite), and other substances on the surfaces of the materials.

Optical studies of the secondary substances formed on the arsenides established the presence of the following minerals: erythrite (smaltite and safflorite), annabergite (rammelsbergite and niccolite), ferruginous arsenates of the simplesite type, smol'ianinovite, minerals resembling those that are found in nature on safflorite (smaltite and safflorite), arsenolite (rammelsbergite, smaltite, and safflorite), and black soot-like films (niccolite).

Because of the preponderance of the erythrite-annabergite series, analyses of the acid extracts were expressed as arsenate with the general formula $R_3(AsO_4)_2nH_2O$ (R is the sum of Co, Ni, and Fe) and with the $RO:As_2O_5$ ratio as 3:1, and the residues were assigned either arsenolite or to the soot-like substances (niccolite). The immer- on measurements were used as controls in all instances.

The results of these conversions (Table 1) proved to be fairly close the results of optical and microscopic studies. For example, the ot-like substances were formed, together with annabergite on the idation of niccolite, but no arsenolite could be detected among the condary products. According to our calculations, in this particular se, the products were annabergite and a large residue of nickel. he latter was apparently one of the main constituents of the soot-like lms in which it was present in a combination with water, oxygen, or O_2 (possibly the films were a hydrated form of nickel oxide—the culiar product of the zone of secondary enrichment).

The high concentrations of arsenolite were found to be characteris- c for the smaltite undergoing oxidation in the oxygen-carbonic acid vironment (pH 4.5), which is confirmed also by calculations from the emical analyses.

The content of arsenolite in the secondary substances is a subject some interest. In one of the earlier experimental studies [1] deal- g with the susceptibility of arsenides to oxidation, in the course of days, without the removal of the substances beyond the confines of e minerals, it was established that the amounts of arsenolite were reponderant among the products of rammelsbergite and smaltite, hile they notably were small in the products of safflorite and nickel- e. Moreover, "embryos" of erythrite and annabergite crystals in e arsenolite matrix were also noted, i.e. a gradual decrease of the ncombined arsenide anhydride in the course of progressive oxidation.

The former arsenide oxidation series (rammelsbergite-smaltite- fflorite-niccolite) were modified, as the result of our studies, so at rammeslbergite had to be moved from the first place to the third. he abrupt decrease of the rammelsbergite content of the secondary bstances on rammelsbergite was due evidently to an intensive ar- enitization of the arsenide anhydride produced in large amounts in the rst stage of the oxidation of arsenide. Hence the conclusion regard- g the importance of time in the mineral-forming processes which ay develop in entirely opposite directions.

The optimum conditions for the accumulation of arsenolite, as we ow definitely at this time, are as follows:

1. Smaltite as the original material, 2. Oxygen-carbonic acid aters at pH 4.5.

Calculations based on the analysis of the acid extracts made it also ssible for us to determine the Ni:Co and the Fe:(Co + Ni) ratios in condary arsenates (Table 2).

Our data and the characteristic ratios for the original arsenides— mmelsbergite, smaltite, and safflorite—are shown in Figure 4.

The results, as shown in Figure 4, proved to be as follows: 1) The :Co ratio in arsenates formed on smaltite and rammelsbergite tends decrease at an increasing acidity, i.e. the relative amount of Co nds to increase. 2) On the oxidation of smaltite with the relatively

Table 2. Cation Ratios in Secondary Arsenates

Arsenide	pH 3.7		pH 4.5	
	Ni:Co	Fe:(Co + Ni)	Ni:Co	Fe:(Co + Ni)
Rammelsbergite	4.6:1	1:25	5.2:1	1:11
Smaltite	1.5:1	1:6	3:1	1:9
Safflorite	---	1:4	---	1:3

high original Ni:Co ratio, the proportions of Ni and Co in the secondary substances (arsenates) are either the same as in the original mineral or are shifted in favor of Co, whereupon the role of Co is materially increased. 3) In arsenates developing on rammelsbergite with the originally high concentration of cobalt, nickel is noticeably preponderant over cobalt.

Figure 4 also shows a relatively high content of iron in arsenates derived from the iron-low smaltite and, conversely, a low content of iron in the secondary products of rammelsbergite. Safflorite, as a cobalt-iron arsenide, is characterized by the highest concentration of iron in its arsenate. However, in this latter case, the role of iron, as against cobalt, is likewise not very appreciable.

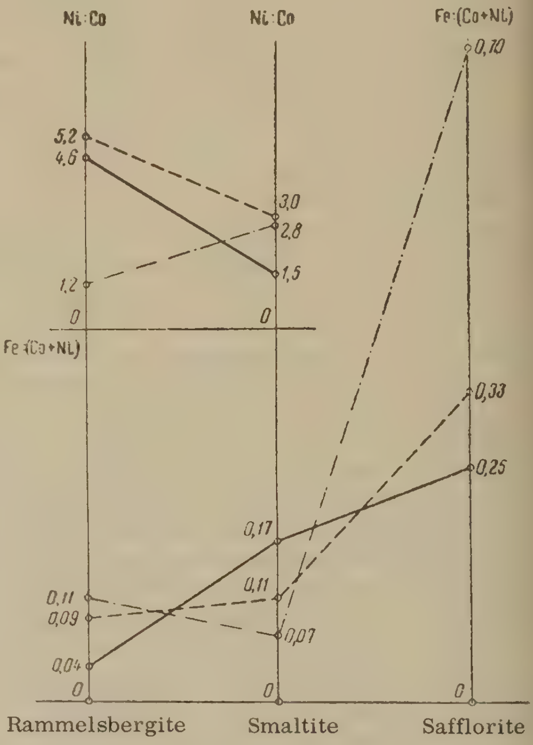

Fig. 4. Diagram of Ni:Co and Fe:(Co - Ni) ratios in original arsenides (dotted-point lines) and in secondary arsenates at pH 3.7 (solid lines) and at pH 4.5 (dotted lines).

CONCLUSIONS

We are enabled to draw the following conclusions on the basis of our quantitative studies of the ratios between the elements leached out of the arsenides (solubility of arsenides) and the elements entering the composition of the secondary products (susceptibility of arsenides to oxidation), in the course of the treatments of smaltite, rammelsbergite, safflorite, and niccolite by carbonic acid (pH 3.7) and oxygen-carbonic acid waters (pH 4.5).

1. Arsenic is among the elements that are most easily leached out of the arsenides here investigated, and in large quantities. In the order of the increasing losses of arsenic by leaching, the minerals form the following series: safflorite - niccolite - rammelsbergite - smaltite.

The pH change (of the leaching solutions, VPS) from 3.7 to 4.5 had practically no effect on the leaching of arsenic from niccolite and rammelsbergite but had a pronounced effect on the leaching of arsenic out of safflorite and smaltite.

2. Fe, Co, and Ni are very inert, in comparison with As, and appear in the leachates only in negligible quantities. This is particularly the case for Fe and Co. Cobalt is noticeably mobile only in the oxidation of safflorite. Nickel is leached out of the arsenides more intensively than Fe and Co and, in the instance of niccolite, in quantities comparable to the quantities of arsenic. Mobility of nickel is diminished at the lower acidity (pH 4.5) of the leaching solution.

The relative inertness of the cations in the weathering of nickel-ron-cobalt arsenides, as indicated by the rates of their leaching from he primary minerals, has its expression in the fact that the cation fraction of the arsenates developing at some distance from an ore body is determined, in its composition, not by the composition of the arsen-des, but of the minerals encountered by arsenic in the paths of its migration (arsenates of Ca, Mg, Cu, Zn). Cobalt and nickel may be found in these minerals in subordinate quantities. Niccolite is a kind of an exception, inasmuch as annabergite may be among the supergenetic products of this mineral, especially if the leaching solutions were empoverished with respect to oxygen.

3. In the instance of rammelsbergite, quantities of the arsenide substance removed from the powdered mineral are nearly the same as he quantities found in the secondary products of the oxidation develop-ng at the surface of the primary mineral. In the instance of smaltite and niccolite, there was more of the arsenide substance removed than was deposited on the arsenides. Consequently, a niccolite-smaltite ore body must lose both volume and weight, during its oxidation, because of the leaching of its constituents into its host rock. Numbers and size of pores and cavities must increase concurrently in the ore body and these pores and cavities must be subjected to filling by the secondary products, to a certain extent.

4. The cations of nickel, cobalt, and iron are accumulated intensively in the secondary products on the arsenides, while arsenic is not concurrently accumulated. The deficiency of arsenic is compensated by other anions: OH^-, O^{--}, CO_3^{--}, etc.

The optimum conditions for the accumulation of the cations in place, at both pH levels, are as follows:

for Fe - a saffloritic or a smaltitic composition of the ore;
for Co - a smaltitic composition of the ore;
for Ni - rammelsbergitic and smaltitic ores.

5. Arsenates of Co, Ni, and Fe were demonstrated to be present among the secondary products developing on the arsenides. These arsenates are chiefly of the erythrite-annabergite series; the secondary products include arsenolite. Smaltite ores and oxygen-carbonic acid solutions at pH 4.5 are especially conducive to the accumulation of arsenolite.

Arsenates developing on smaltite and rammelsbergite have their Ni:Co ratio subject to a lowering at an increasing acidity, i.e. a ratio in which the role of Ni may be tending to be made less important. The arsenates associated with the oxidation of rammelsbergite (even of a Co-rich rammelsbergite) are characterized by the relative prominence of nickel (annabergite is formed). Smaltite has the opposite characteristics: its secondary minerals tend to accumulate cobalt and, to a lesser extent, nickel (erythrite is formed).

6. Despite the low iron content of smaltite, the secondary products of this arsenide are characterized by their relatively high iron, i.e. minerals of the simplesite and the smol'ianinovite types may indeed be formed by the oxidation of smaltite.

7. During the oxidation of niccolite, there is an intensive enrichment of the supergene materials by nickel, because of the major disproportion between the fixable arsenic and the arsenic removed from the system by leaching (4 to 8 times, depending on the pH).

Consequently, alongside annabergite, in this particular case, there may be a formation of oxygen and of hydroxide compounds of nickel—typical products of the zone of the secondary enrichment. These latter compounds, poorly known as they are even to this time, are commonly seen in an association with the oxidation of nickel ores.

Received for publication
September 21, 1958

REFERENCES

1. Yakhontova, L. K., and P. A. Raudonis. Geokhimiya, No. 8, 10, 1955.
2. Yakhontova, L. K., A. N. Bukina, et al. Trudy Mineralog. Mus. Akad. Nauk SSSR, t. 8, 1956.

RHENIUM IN MOLYBDENITES OF THE TYRNY-AUZ DEPOSIT

Z. V. Studenikova and V. A. Zolotareva

V. I. Vernadskii Institute of Geochemistry and Analytical
Chemistry, Academy of Sciences, USSR, Moscow

Abstract

Rhenium contents in molybdenites from various geological formations of the
rny-Auz deposit range from $1 \cdot 10^{-5}$ to $1.4 \cdot 10^{-3}$%.

While engaged in their studies of the distribution of rhenium in the
rth's crust and in meteorites, I. and W. Noddack [1] came to the conclu-
on that the high degree of the dispersion of this element in nature is
mparable only to the dispersion of the short-lived radioactive ele-
ents [2].

Having examined a large number (1,600) of minerals of all classes, a
ixture of 110 samples of igneous rocks, as well as meteorites, the
oddacks had obtained certain data on the rhenium content of these
aterials (Table 1):

Table 1

Materials	Rhenium, %
Mixture of 110 samples of igneous rocks	1×10^{-7}
Meteorites	3.6×10^{-7}
Primary sulfides	2.6×10^{-6}

As to the studies of minerals other than sulfides, it was found [1, 2]
at 1×10^{-6} to 1×10^{-4} % rhenium is found in alvite, gadolinite, orangite,
hortveitite), and zircon. No rhenium whatsoever could be detected in
rbonates, nitrates, and halogen salts.

Rhenium does not form independent minerals, by virtue of its proper-
es, and does not appear as the major constituent in any of the minerals
re enumerated. Consequently, studies of minerals containing appre-
able accumulations of rhenium become a subject of interest.

Rhenium has the same ionic radius as molybdenum (0.68 Å), resem-
es molybdenum in many of its chemical properties, and follows molyb-

denum in the processes of the deposition of sulfides. From these points of view, molybdenite is particularly important.

It is known from the literature [1, 3] that the rhenium content of molybdenites varies from 5×10^{-5} to 2×10^{-3}%. The available data [3] on rhenium in foreign molybdenites are presented in Table 2.

Table 2

Source	Rhenium, %
Lier, Norway*	2×10^{-4}
Drammen, Norway	7.5×10^{-4}
Bandkeli, Norway*	1.2×10^{-4}
Moos, Norway*	6×10^{-5}
Knaben, Norway*	1.4×10^{-4}
Telemark, Norway	2×10^{-3}
Japan	1×10^{-3}
Colorado, USA	1.8×10^{-4}
New South Wales, Australia †	2.5×10^{-4}
Bolivia	5×10^{-6}
Siberia	6×10^{-5}

*Spelling uncertain; not found in available indices. VPS

†In the original "England". VPS

Analyses of molybdenites from our country were made later. Their results [3, 4] are presented in Table 3.

For our studies of the accumulation of rhenium in the Tyrny-Auz molybdenites, samples of molybdenite were collected from different geologic formations. As is known, the Tyrny-Auz molybdenite is localized not only within the boundaries of the main skarn ore body but also in the biotitic hornfels in the hanging wall of the deposit and in the leucocratic granites that outcrop as stocks in the core of the anticlinal fold, in the central part of the deposit. Molybdenite is found in all of the rocks here enumerated, both as finely disseminated inclusions and as discrete accumulations in the numerous veinlets of different composition within the rocks. All three types of the molybdenite-bearing host rocks (skarns, biotitic hornfels, and leucocratic granites) are commercial molybdenum ores.

We took samples of the finely disseminated molybdenite from all of the rock types here listed, as well as samples of molybdenite from the veinlets of different composition.

We also took samples of molybdenite from the fine single-mineral veinlets in the post-ore El'dzhurtinsk biotite granites.

Determinations of rhenium in molybdenites were done colorimetrically, by the method based on the capacity of rhenium to form a colored thiocyanate complex, with stannous chloride as the reducer of rhenium,

Table 3

Molybdenum concentrates and ores	Description	Rhenium, %
Kounrad (concentrate below specifications)*	1941 sample	1.5×10^{-2}
"	Oct. 1943 sample from the Molybdenum Section of the Balkhash Plant; 12.05% Mo	1×10^{-2}
"	October 1944 sample containing 10.11% Mo	1×10^{-2}
Tyrny-Auz concentrate	1939 sample	1×10^{-3}
Unenriched ore (Tyrny-Auz)	1939 sample	2×10^{-4}
Chikoi, concentrate	Sample of the concentrate; 46.16% Mo	1.2×10^{-4}
Umal'ta, concentrate	—	5×10^{-4}

*''Nekonditzionnyi'' may mean ''below specifications'', as it probably means here and also ''non-standard'', in the broad sense. VPS

2N hydrochloric acid solutions. Molybdenum also forms a similar llow-green complex under the same conditions. It was necessary erefore to remove molybdenum quantitatively prior to the extraction the rhenium thiocyanate complex, by the extraction with ether in the esence of added mercury, the reducing agent, and of potassium thio- anate. This method was developed by A. N. Grunina at the Chemical boratory of the Irkutsk Giredmet* [5].

Reliability of the method is 10%; sensitivity 0.1 micrograms per mil- iter.

Upon examination of our results (Table 4), we came to the conclusion at the average rhenium content of the skarns is 3.89×10^{-4}%. The ghest amounts of rhenium (up to 8×10^{-4}%) were found in molybdenites om pyroxene-vesuvianite and garnet-pyroxene skarns that were formed om marbles. The rhenium content of molybdenites from the other pes of the skarns is characteristically smaller.

The average rhenium content of finely disseminated molybdenites in ucocratic granites is characterized by its extremely low magnitudes $\times 10^{-5}$%) and rhenium may be absent entirely, in some isolated cases.

As to the rhenium in molybdenites from the veinlets of different nds, our results were found to be as follows:

In quartz veinlets as a whole, the average rhenium in the molybden- s is 2.63×10^{-4}% and, moreover:

Gornyi Institut Redkih Metallov'', Mining Institute of Rare Metals. VPS

Table 4

Sample No.	Source of molybdenite collected for* the determination of rhenium	Rhenium, %
	I. SKARNS	
0245	Pyroxene-garnet-vesuvianite	1.3×10^{-5}
0201	Garnet-pyroxene	1.5×10^{-4}
0228	Pyroxene, in contact with marbles	2×10^{-4}
0222	Pyroxene-garnet, in contact with leucocratic granites	2×10^{-4}
0305-0306	Pyroxene, from sulfide zone	2×10^{-4}
0217	Garnet-pyroxene, in contact with leucocratic granites	3.5×10^{-4}
0208	Garnet-pyroxene, with relicts of biotite hornfels	3.5×10^{-4}
0366	Pyroxene-vesuvianite	4×10^{-4}
0365	Pyroxene-vesuvianite	6×10^{-4}
0227	Pyroxene, in contact with marbles	6×10^{-4}
0216	Garnet-pyroxene, in contact with leucocratic granites	6×10^{-4}
0433	Sulfide, in contact with marbles	6×10^{-4}
0361	Pyroxene-vesuvianite	8×10^{-4}
	II. LEUCOCRATIC GRANITES	
0352	Leucocratic granites with MoS_2 inclusion	none
0376	" " " " "	none
0353	" " " " "	ca. 1×10^{-5}
0268	" " " " "	" 1×10^{-5}
0269	" " " " "	" 1×10^{-5}
0272	" " " " "	" 1×10^{-5}
	III. QUARTZ VEINLETS	
0520	(a) In biotite hornfels	2×10^{-4}
0511	" "	3×10^{-4}
0497	" "	3×10^{-4}
0505	" "	3.5×10^{-4}
0497a	" "	3.5×10^{-4}
0518	" "	4×10^{-4}
0507	At contacts of biotite hornfels and leucocratic granites	5×10^{-4}

0358-0359	(b) In leucocratic granites	1.8×10^{-4}
0254	(c) In skarns: pyroxene	none
0403	pyroxene	1.5×10^{-4}
0343	pyroxene-garnet	2.5×10^{-4}
0400	pyroxene	4.7×10^{-4}
0377	pyroxene-garnet	8×10^{-4}
0345	garnet-pyroxene	2×10^{-4}
0368	pyroxene-vesuvianite	none

IV. QUARTZ-FELDSPAR VEINLETS

0506	In biotite hornfels	1×10^{-4}
0504	" " "	1.4×10^{-4}
0517	" " "	2×10^{-4}
0503	" " "	2×10^{-4}
0513	" " "	3.25×10^{-4}
0519	" " "	3.5×10^{-4}

V. SKARN VEINLETS

0209	In marbles	none
0412	At contact of biotite hornfels and pyroxene skarns	none
0270-0271	In leucocratic granites	3.5×10^{-4}
0273	" " "	1.5×10^{-4}
0382	" " "	1.8×10^{-4}
0437	In marbles	4×10^{-4}
0440	" "	6×10^{-4}
0439 (1)	" "	6×10^{-4}
0438	" "	7×10^{-4}
0439	" "	7×10^{-4}

VI. QUARTZ-GARNET VEINLETS

0275	In leucocratic granites	none
0281	" " "	none
0277	" " "	2×10^{-4}
0278	" " "	2×10^{-4}
0276	" " "	3×10^{-4}
0284	" " "	3×10^{-4}
0283	" " "	4×10^{-4}
0280	" " "	6×10^{-4}

0294	In pyroxene hornfels	none
0442	In marbles	6×10^{-4}
0429	In pyroxene skarn	7×10^{-4}
0430	In pyroxene skarn	3.5×10^{-4}
0265	In vesuvianite-wollastonite skarn	4×10^{-4}
0431	In pyroxene skarn	1.6×10^{-4}
0258-0259	In pyroxene skarn	5×10^{-4}
0251	" " "	6×10^{-4}
0262	In vesuvianite-wollastonite skarn	7.5×10^{-4}
0250	In pyroxene-garnet-vesuvianite skarn	8×10^{-4}

(a) 3.43×10^{-4}%, in the quartz veinlets in biotite hornfels;
(b) 1.8×10^{-4}%, in the quartz veinlets in leucrocratic granites;
(c) 2.68×10^{-4}%, in the quartz veinlets in skarns.

The average rhenium content in molybdenites from the quartz-feldspar veinlets (the most extensively distributed kind) in biotite hornfels is 2.19×10^{-4}%.

Molybdenites from skarn veinlets, that permeate the skarns as well as the granites and the biotite hornfels, contain on the average 3.36×10^{-4}% rhenium.

Molybdenite-bearing quartz-garnet veinlets are characteristic of the deposit as a whole, particularly for the skarn ores. The average of 3.65×10^{-4}% Re is indicated by a large number of analyses of the molybdenite. Moreover, rhenium is significantly lower (2.5×10^{-4}%) in molybdenites from the quartz-garnet veinlets in the leucocratic granites, while the average rhenium content of these same veinlets cutting the skarns is 4.8×10^{-4}%. We assume therefore, taking all of our data into consideration, that the average content of rhenium in the Tyrny-Auz molybdenites is 3.23×10^{-4}% (Table 4).

The foregoing considerations allow us to draw two conclusions: 1) The lowest amounts of rhenium belong characteristically to the molybdenites that are present either as the inclusions or the veinlets in the leucocratic granites, and 2) the highest amounts of rhenium are found characteristically in molybdenites from quartz-garnet veinlets in the skarns. Also, as noted previously, the highest concentrations of rhenium take place in the molybdenites taken from the quartz-garnet veinlets in the pyroxene-vesuvianite-wollastonite skarns (7.5 to 8×10^{-4}%) which were formed metasomatically from the marmorized limestones. The data on rhenium in concentrates from an enrichment plant are cited in Table 5.

The accumulation of rhenium in the molybdenites collected from veinlets in the El'dzhurtinsk granites proved to be the highest of all: 1.4×10^{-3}%.

Table 5

Sample No.	Material	Rhenium, %
401	Primary crude concentrate of MoS_2	1.25×10^{-4}
402	Tailings dumps of the plant	none
404	Copper concentrate	1×10^{-4}
405	Copper purification feed (MoS_2 tailings)	2×10^{-4}

The fluctuations in the concentration of rhenium in the Tyrny-Auz olybdenites collected from ores of different types and from the veints within the confined of the ore field are related apparently to differces in the physico-chemical environments in which this or that kind molybdenite was deposited.

Studies of problems related to our subject are now in progress.

Received for publication
October 1, 1957

REFERENCES

Noddack, I., and W. Noddack. Die Geochemie des Rheniums. Z. physikal. Chemie. Leipzig. 1931. 154.

Noddack, I., and W. Noddack. *Element Renii* (The element rhenium). Uspekhi Khimii 1, Vyp. 4, 699, 1932.

Bibikova, V. I. *Renii v Pyliah Molibdenovogo Tsekha Balkhashskogo Zavoda* (Rhenium in the dusts of the molybdenum section of the Balkhash Plant). Tsvetnye Metally, No. 4, 1946.

Basitova, S. M. K Geokhimii Reniya (On the geochemistry of rhenium). *Dissertatsiya na Soiskanie Uchenoi Stepeni Kandidata Khimicheskikh Nauk* (Thesis in partial fulfillment of the requirements for the Degree of Candidate of Chemical Sciences). Institut Geokhimii i Analiticheskoi Khimii im. V. I. Vernadskogo (V. I. Vernadskii Institute of Geochemistry and Analytical Chemistry). Akad. Nauk, SSSR, 1950.

Grunina, A. M. *Metodika Opredeleniya Reniya v Molibdenitakh* (Methods for determining rhenium in molybdenites). *Sb. Khim., Fix. i Spektrog. Metodov Opredeleniya Redkikh i Rasseyannykh Elementov* (Collected Papers: Chemical, Physical, and Spectrographic Methods of Determination of the Rare and of the Dispersed Elements). Vyp. II. VIMS. 1957.

ZR/HF RATIO IN ZIRCONS IN SOME IGNEOUS ROCKS OF NORTHERN KIRGIZIA

A. V. Kosterin, V. N. Zuev, and I. D. Shevaleevskii

V. I. Vernadskii Institute of Geochemistry and Analytical
Chemistry, Academy of Sciences, USSR, Moscow

Abstract

The change in the Zr/Hf ratio in zircons from various magmatic rocks of North Kirgizia has been studied.

It has been shown that in consequence of magmatic differentiation the Zr/Hf ratio in zircons changes from 71 in gabbro to 36 in alaskite granites and equals 29 in hydrothermal veins related to alaskites.

It has also been shown that the Zr/Hr ratio in Variscan alaskites and in gneissified Proterozoic alaskites is similar.

The elements Zr and Hf are so much alike in their properties that they are found in nature only together with one another. There is tens of times as much zirconium as there is hafnium in the earth's crust and, for this reason, there are no independent minerals of hafnium and insignificant quantities of hafnium are present invariably in zirconium minerals [1].

Zirconium minerals are represented almost entirely by zircon and by its varieties (malacon, cyrtolite, and others) in rocks of the acid series.

Studies of the Zr/Hf in zircon are convenient, inasmuch as this mineral has a wide distribution in practically all types of rocks and contains up to 65% of Zr and Hf dioxides. It is possible accordingly to determine the ratio of these two elements in zircon without any preliminary chemical enrichment of the sample [1, 2]. Morover, the Zr/Hf ratio in rocks is apparently the same as in the zircons isolated from the rocks. Specifically, the available pertinent data by I. M. Lipova, I. D. Shevaleevskii, and A. N. Tuzova [2] show that the Zr/Hf ratio in granites and granodiorites is the same as this ratio in the zircons isolated from the corresponding rocks. Consequently, any regularities in variations of the Zr/Hf ratio in zircons may be expanded to include also the corresponding rocks.

It has been shown by the earlier investigators [2, 3, 4] that there may be variations in the Zr/Hf ratio, depending on origin of the mineral.

The available data in the literature, however, are applicable chiefly to zircons of the acid and of the basic rock series.

Igneous rocks of the southern slopes of Zailiiskii Alatau are of all kinds, from gabbro to alaskite granites.

The present report is concerned, for that reason, with the sequence of variations in the Zr/Hf ratio in zircons from igneous rocks of different composition: basic to acid.

According to N. D. Tikhomirova, Luik, and others, the igneous rocks of the district were formed in the following sequence, from the more ancient to the more recent:

1. The Proterozoic cycle: gneiss-like alaskite granites
2. The Caledonian cycle: gabbro, diorites, granodiorites, porphyry-like biotite-hornblende granites
3. The Variscan cycle: pink hornblende-biotite granites, syenites, alaskite granites

Zirconium-bearing hydrothermal veins are related genetically to the Variscan alaskite granites.

Beginning with gabbro, the succession of the rocks in the district becomes progressively more acidic. For this reason, the rocks presently to be discussed are regarded by us tentatively as members of a single series of magmatic differentiations.

The Zr Hf ratio in zircons from different rocks of the district and from the hydrothermal veins is shown in the Table. Zr and Hf were determined by the x-ray spectrographic procedure. The relative error of the Zr/Hf determinations was ± 5%.

Comparisons of the average Zr/Hf ratios in zircons from different kinds of rock are represented in the Figure.

It is evident from the Table that the Zr/Hf ratio is the same both in the Variscan and in the Proterozoic alaskite granites. The Zr/Hf ratio in zircons from rocks of identical composition belonging to different magmatic epochs is conspicuously the same. This conclusion is in agreement with the conclusion that was made for the granites of Central Ural and of Eastern Kazakhstan [3].

Inasmuch as the available data show that variations in the Zr/Hf are not dependent on the age of the intrusion, let us examine these variations entirely in reference to the variations in composition of the rocks in the course of the magmatic differentiation.

As may be seen from the averages in the Table, the Zr/Hf ratio in zircons changes from 71 for gabbro to 46 for porphyry-like granites and then to 36 in alaskites and to 29 in hydrothermal veins.

Significant changes in the Zr Hf ratio in zircons are taking place accordingly, in the course of the magmatic differentiation, from gabbro

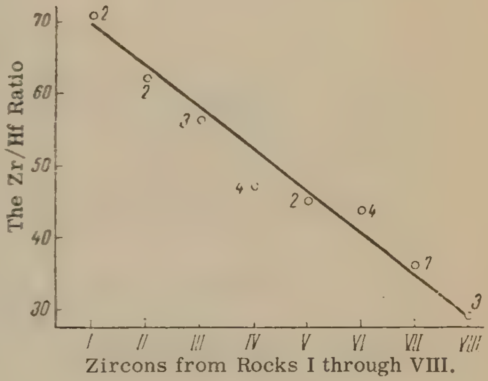

Figure. Variations in Zr/Hf ratio in zircons during magmatic differentiation of rocks.

0 - average Zr/Hf in the rock (the figures show the number of zircon samples examined); I - gabbro; II - diorites; III - granodiorites; IV - porphyry-like biotite-hornblende granites; V - pink hornblende-biotite granites; VI - syenites; VII - alaskites; VIII - hydrothermal veins.

The Zr/Hf Ratio in Zircons from Some Igneous Rocks of Northern Kirgizia

Intrusive cycle	Rock	Sample No.	Zr/Hf in zircons	Average
Proterozoic	Gneiss-like alaskite granites	84	26	
		99	36	36
		80	46	
	Gabbros	90	59	71
		75	83	
	Diorites	69	54	62
		72	70	
Caledonian	Granodiorites	101	50	
		79	50	58
		71	73	
	Porphyry-like biotite-hornblende granites	77	38	
		81	46	46
		68	46	
		96	52	
Variscan	Pink hornblende-biotite granites	85	42	45
		70	48	
	Syenites	82	37	
		86	39	44
		76	47	
		105	54	
	Alaskite granites	18-21	27	
		98	30	
		89	33	
		106	36	36
		22-25	38	
		42	39	
		91	46	
	Hydrothermal veins	200	23	
		201	24	29
		202	40	

to alaskite and to hydrothermal veins, with the shift to the higher Hf toward the end of the magmatic differentiation.

Concurrently with the observed general trend toward the increase in Hf in different rock bodies of identical composition, there are also appreciable fluctuations in the Zr/Hf ratio and an overlapping of this ratio in zircons from rocks that are close one to another in the magmatic differentiation series. For example, the Zr/Hf ratio in zircons from syenites fluctuates between 37 and 54, while the fluctuation range is 38 to

52 in zircons from porphyry-like granites, i.e. within the syenite range, which precede syenites in the magmatic differentiation series.

Consequently, as a rule, one must not try to determine the type of rock, which is represented by zircon, on the basis of a single analysis of the zircon for the Zr/Hf ratio.

As long as we have only a small number of the Zr/Hf analyses of zircons, our conclusions should be taken only a preliminary.

CONCLUSIONS

1. The Zr/Hf ratio equals 36 and is the same in zircons from the Variscan and from the Proterozoic alaskite granites.
2. A general progressive decrease in the Zr/Hf ratio, from 71 in gabbro to 36 in alaskites and to 29 in hydrothermal veins associated with alaskites, may be observed in the course of the magmatic differentiation of the rocks.
3. There are some fluctuations of the Zr/Hf ratio in zircons from rocks of identical composition. Concurrently there is some overlapping between the Zr/Hf ratios in zircons from rocks of unlike composition close to each other in their positions in the magmatic differentiation series.

Received for publication
October 10, 1957

REFERENCES

1. Rankama, K., and Th. G. Sahama. Geochemistry, 1949, 557.
2. Tugarinov, A. I., E. E. Vainshtein, and I. D. Shevaleevskii. Geokhimiya, No. 4, 28, 1956.
3. Lipova, I. M., I. D. Shevaleevskii, and A. M. Tuzova. Geokhimiya, No. 2, 133, 1957.
4. Pavlenka, A. S., E. E. Vainshtein, and I. D. Shevaleevskii. Geokhimiya, No. 5, 532, 1957.

A CONTRIBUTION TO GEOCHEMISTRY OF TITANIUM IN INTRUSIVE PROCESS OF GRANITIC SERIES

E. B. Znamenskii

V. I. Vernadskii Institute of Geochemistry and Analytical Chemistry, Academy of Sciences, USSR, Moscow

Abstract

Titanium content in the intrusive phases of the Kalba granite batholith of Variscan age in eastern Kazakhstan shows serial change. From oldest to youngest, the first intrusive granite phase (porphyritic fine-grained biotite granite) contains 0.80 per cent TiO_2; the second phase (coarse-grained potassium biotite granite) contains 0.25 per cent TiO_2; the third phase (fine-grained granitic dike rocks) 0.09 per cent; and finally pegmatites 0.02 per cent TiO_2. These Ti contents are typical of the listed phases and facies. Assimilation of Ti-rich shale may account for the high Ti content in the ''apical'' facies. In the consolidation and subsequent fractionation of these granitic intrusives, there is enrichment of Ti in the earlier phases and resulting in a Ti-impoverished pegmatite phase. Biotite and ilmenite are the host minerals for Ti. The average TiO_2 content of the most abundant and least contaminated granite facies of the Kalba batholith is 0.33 per cent which conforms closely to estimates of R. A. Daly and A. P. Vinogradov.

Progressively more attention is being given now to geochemistry of individual elements. This interest is due significantly to the expansion of petrochemical investigations, including appraisals of their possible use alongside geochemical data in prospecting and exploration for economic mineral raw materials.

Studies of the abundance of chemical elements and of their distribution in different rocks acquire a special importance accordingly.

The average content of TiO_2 in granites of all periods is close to 0.29%*, according to R. A. Daly [1]. Nearly the same magnitude is reported also by A. P. Vinogradov [2].

According to A. E. Fersman [3], the average content of titanium dioxide in granitic pegmatites is 0.06%.

Comparisons of these averages show that granitic pegmatites are nearly 6.5 times as poor in titanium as the parent rocks.

One may suppose therefore that, in the process of the birth and the formation of pegmatitic melts, in the stabilization of intrusives of the acid series, there is a more intensive binding of titanium in the magma during the earlier stages of the crystallization, so that the later product

---

*The percentages are by weight, here and further on in this report.

(pegmatites)[*] are found to be impoverished with respect to this element.[†] One may suppose also that, if a "decontamination" of granitic magma, with respect to titanium, indeed does take place, in the course of the formation of the pegmatitic melt from the granitic magma, it is quite evident that such changes should be reflected somehow in the intermediate products of the crystallization (rocks) which were formed in the interval of the geologic time between the early granites and the pegmatities.

Insofar as the accumulation or the dispersion phenomena for this or that element, including titanium, have a major importance in the stabilization of intrusives preceding the formation of ores and in the petrochemistry of the process as a whole, it becomes evident that, in addition to the relative abundance studies, we must ascertain the character of the distribution of elements in genetically interrelated rocks of individual intrusive complexes. It is evident that, in this case, the geochemical history of the elements may be ascertained more fully, because the initial sorting of the magma was apparently the same for all of the members of the genetic series of this or that intrusive complex.

We undertook accordingly studies of the distribution of titanium in the Kalba Granite Body, Eastern Kazakhstan, whose origin belongs to the Variscan time [5].

On the basis of studies by N. A. Eliseev, V. P. Nekhoroshev, N. K. Morozenko, A. P. Nikol'skii, Zh. A. Aitaliev, G. N. Scherb, and other investigators, and in harmony with the ideas of V. S. Koptev-Dvornikov [6], the following principal intrusive phases may be recognized in the Kalba granitic body,[‡,§] in the order of the sequence of the intrusions:

The first (main) intrusive phase, represented by medium-grained weakly porphyroid and porphyry-like biotite granites of the so-called Kalba Type (more than 65% of the area of the massiv).

The second intrusive phase (phase of supplementary intrusions) represented by coarse-grained essentially potassium biotite granites of the so-called Monastyr Type.

The third intrusive phase (phase of veined rocks) may be subdivided further as follows:

(a) Vein rocks of Stage I (fine-grained veined biotite granites, stocks and dikes; also aplites, pegmatites, granite–porphyries, and quartz-cassiterite veins).

(b) Vein rocks of Stage II: lamprophyres and quartz veins with sulfide minerals.

---

[*] We have in mind the epigenetic pegmatities, in A. I. Ginzburg's terminology [4].

[†] As we know, titanium minerals (ilmenite, rutile, sphene) are very limited in their distribution in typical granitic pegmatites [3].

[‡] Russian "massiv", here translated as "body" is a nonrestricted term and it is used freely, meaning an intrusive body of unknown deposition or shape, a small exposure of the crystalline pediment of a platform, or a poorly articulated upland whose length and width are about the same, etc. The term may be used synonymously with "shield". VPS

[§] According to N. A. Eliseev, – a batholith.

In rocks of the first (main) phase, in addition to its principal facies, the apical facies are clearly recognizable. The latter facies are expressed morphologically by their association with the apical (top) parts of the massiv, where basicity of the granitoids is raised to that of granodiorites and where xenoliths are also present, with occasional hybrids, and the dark minerals are more abundant. Granitoids of the apical facies, the first phase, are present in isolated parts of the massiv and are subordinate to granitoids of the principal facies of the same phase, in respect to the size of the area of their distribution.

The inquiry into the character of the distribution of titanium* was conducted for everyone of the representatives of the intrusive phases, from the granitoids of the first (main) phase through the pegmatites. Moreover, the basic trends in the distribution of titanium in the sequence of the products of the intrusive activity of the Kalba Body were studied in the example of G. Air (Mt. Air) and in the area next to this mountain, where four successive stages of the intrusion are fixed by the geologic cross-penetrations.

The results are presented in Table 1.

Table 1. TiO_2 Content of the Sequence of Granites at Air Mountain (every successive rock cuts through its predecessor)

Sample No.	Granite, Source, Phase	TiO_2, %
114	Medium-grained biotitic granite; (5 km east of Mt. Air); 1st phase	0.45
117a	Coarse-grained biotitic granite; (at Mt. Air); 2nd phase	0.28
117	Fine-grained biotitic granite (stock); same place; 3rd phase	0.16
116	Fine-grained biotitic granite (dike); same place; 3rd phase	0.08

As shown in Table 1, every successive rock (in the intrusion sequence) is characteristically lower in titanium, in comparison with its predecessor.

This tendency is sustained invariably by the distribution of titanium in the granites, in other parts of the body, wherever the host rock (granite) is cut through by a younger granite. The phenomenon is illustrated by Table 2.

Table 2 shows that TiO_2 is 3 to 13 times as low in the younger granites as it is in the host, by comparison of every one of the rock couples (the host and dikes).

In addition, we undertook an extended inquiry into the distribution of

---

*Determinations of titanium were made by the method of A. I. Ponomarev [7].

Table 2. TiO_2 Content of Successively Formed Granites of the Kalba Body

Host Rocks			Rocks Cutting Through Hosts		
ample No.	Granite, Phase, Source	TiO_2, %	Sample No.	Granite, Phase, Source	TiO_2, %
244	Porphyroid biotitic granodiorite; 1st phase, apical facies; Asu-Bulak	0.74	7a	Fine grained granite (dike) with 2 kinds of mica; 3rd phase; same source	0.25
35	Medium-grained biotitic granite; 1st phase (main facies); near Chebyndy-Kul' Lake	0.40	35a	Fine-grained granite (dike); 3rd phase; same source	0.10
235	Coarse-grained biotitic granite; Gora Dungaly	0.13	236	Fine-grained granite (dike); 3rd phase; same source	0.01

anium in the representatives of all phases of the Kalba body intrusions, th the calculation of the average magnitudes.

The results are presented in Table 3.

As we may see in Table 3, the highest average content of titanium oxide, 0.80%, is observed in the granites of the apical facies in the rst phase of the intrusion; then follow (in the decreasing order) gran- s of the main facies of the same phase (0.33%), granites of the second ase (0.25%), granites of the third phase (0.09%), and, finally, pegma- es (0.02%).

Biotite and ilmenite in the rocks are decreasing in the same sequence om the early rocks to the late), as is illustrated in Table 4.

Inasmuch as we had already established that the primary accumula- ns of titanium in Kalba granites are associated with biotite and il- enite [10], with biotite as the principal carrier of this element (up to % of total TiO_2), the distribution of titanium in the intrusive phases of body, as here observed, becomes intelligible. The decrease of this ement in the younger rocks is due partly to the progressive decrease the amounts of biotite and ilmenite in these rocks and partly to the crease of the TiO_2 content of the biotites.

As it may be seen from Table 3, our TiO_2 average (0.33%) for gran- s of the main facies, first intrusive phase, Kalba body, is close to the sults reported by R. A. Daly and A. P. Vinogradov (0.39 to 0.34%) 2]. In regards to the higher amounts of titanium in the granitoid ies of the apical parts of the first phase (0.80%), they may be related the assimilation of sandy-shaly materials of the host rocks, inasmuch TiO_2 is relatively high in the shales, as shown in Table 5 and the anites themselves contain indications of their proximity to the roof d of their reworkings as previously discussed.

Comparisons of the titanium dioxide average in granites of the main ies, first phase (0.33%) with the results obtained for pegmatites 02%) show that nearly a 16-fold impoverishment of these late products k place, with respect to titanium, during the consolidation of the in- sive. Rocks that were intermediate as to the time of their formation anites of the 2nd and of the 3rd phase) are characterized, in turn, by

Table 3. TiO_2 Content of Granitoids and Pegmatites of the Kalba Body (by the intrusion phases)

Sample No.	Source	Phase and Facies	TiO_2, %	Remarks
250	Medium-grained biotitic granodiorite (near Ognevka settlement)	1st phase, apical facies	1.16	
62	Weakly porphyroid biotitic granodiorite (near Bakennoe settlement)	"	0.81	10 to 18% biotite; up to 0.30% ilmenite (rarely higher)
245	Medium-grained biotitic granite (West of Belaia Gora)*	"	0.70	
29	Medium-grained biotitic granite (South of Belaia Gora)	"	0.61	
244	Porphyry-like biotitic granodiorite (Asu-Bulak)	"	0.74	
-	Average for apical facies, first phase		0.80	
260	Porphyry-like biotitic granite (miroliubov Vystup)*	1st phase, main facies	0.35	
35	Medium-grained biotitic granite (near Chebyndy-Kul' Lake)	"	0.40	4 to 8% biotite; up to 0.17% ilmenite
104	Medium-grained biotitic granite (Sorokin Sopka)*	"	0.30	
102	Medium-grained biotitic granite (near Leninka Village)	"	0.25	
113	Medium-grained biotitic granite	"	0.21	
114	Medium-grained biotitic granite (vicinity of Zheltostas Settlement)	"	0.45	
45	Medium-grained biotitic granite	"	0.33	
46	Medium-grained biotitic granite (near Gremiach'e Settlement)	"	0.41	
211	Medium-grained biotitic granite (middle course of Voilochevka River)	"	0.32	
-	Average for main facies, first phase		0.33	

*"Gora" is "mountain"; "vystup" - a protruding flat piece of rock; Sopka - an isolated hill, generally cone-like (in Siberia), a volcano (in Kamchatka), a mud valcano (in Caucasus). The author's usage is Siberian. VPS

Table 3. TiO_2 Content of Granitoids and Pegmatites of the Kalba Body (by the intrusion phases)—continued

Sample No.	Source	Phase and Facies	TiO_2, %	Remarks
-	Coarse-grained biotite granites; mixture of 5 samples; composites of equal weights; (3 samples from Sebinsk body, one from Monastyr, one from Dungaly)*	2nd phase	0.25	3 to 5% biotite; up to 0.05% ilmenite
7a	Fine-grained two-mica granite dike (Asu-Bulak)	3rd phase	0.25	1 to 2% biotite, and less; isolated grains of ilmenite in panned samples
117	Fine-grained biotitic granite stock (Mt. Air)	"	0.16	
116	Fine-grained granite dike (Mt. Air)	"	0.08	
116a	Fine-grained granite dike (Mt. Air)	"	0.06	
35a	Fine-grained granite dike (near Chebyndy-Kul' Lake)	"	0.10	
236	Fine-grained granite dike (Mt. Dungaly)	"	0.01	
123	Granite-porphyry (near Leninka Village)	"	0.01	
-	Average for third phase	"	0.09	
-	Pegmatites from Kalba body (data by S. G. Shavlo [9])	3rd phase	0.02 maximum	Biotite and ilmenite very rare

*The meaning is obscure, possible because the author (or the editor) says: ''v ravnyh vesovyh'' instead of ''v vesovyh srednih''. A ''weighted-mean'' composite sample is meant consisting of 3, 1, and 1 parts of the contributing samples. VPS

the intermediate contents of TiO_2, reflecting thereby, in the sequence of their formation, the progressively decreasing amounts of titanium and constituting, as if it were, a connecting link between the earlier rocks and the pegmatites of Kalba.

Bearing in mind that the apical parts of the intrusive were the first ones to be formed during the consolidation of the intrusion and that the formation of every one of the subsequent products of the intrusion (as attested by the observable geologic cross-intersections) was associated with accessions of fresh intrusive materials from the deeper parts of the magmatic basin, one may be led to the supposition that the inner parts of the intrusive body were progressively being deprived of their titanium, even right up to the horizons of the origins of the pegmatitic melts.

Table 4. TiO_2 Content of Biotites of Kalba Granites

Sample No.	Source	TiO_2 in Biotite, %
244	Porphyry-like biotitic granodiorite, first phase, apical facies	4.00
260	Porphyry-like biotitic granite, first phase, main facies	3.03
246	Coarse-grained biotitic granite, 2nd phase	3.04
235	Coarse-grained biotitic granite, 2nd phase	2.7
236	Fine-grained granite, 3rd phase (dike)	1.4
20	Ak-Kezen' pegmatite	1.0

Table 5. TiO_2 Content of Shales (Takyr Suite)*

Sample No.	Source	TiO_2, %
64	Quartz-feldspar-biotite dark gray shale with coal and ore substance (left bank of Ognevka River, by the brook)	1.11
63	" " " "	1.04
255	Quartz-feldspar-biotite-chlorite-sericite dark gray shale containing coal and ore substance (Chalchin wedge)	1.05
6a	Dark-gray shale of the same composition (left bank of the middle course of Ognevka River)	0.92
	Average	1.03

*Upper Devonian and Lower Carboniferous (named after Takyr River, S. Altai). Black shales up to 1,000 meters thick interbedded with quartz sandstones in their upper parts. VPS

CONCLUSIONS

With the example of the TiO_2 distribution in genetically interrelated rock series in the Kalba granite body, the following was ascertained:

1. On the whole, the distribution of titanium in the rocks of the granite body is irregular, although of the geologically fixed intrusive phases and facies each contains its own characteristic amounts of this element.

2. The highest content of TiO_2 (0.80%) is observed in granitoids of the apical facies of the first intrusive phase; then follow the granites of the main facies of the same phase (0.33%), the granites of the second phase (0.25%), of the third (0.09%), and finally, pegmatites (0.02%). Thus, in the course of the consolidation of intrusives and of the subsequent formation of the rocks composing the granite body, there was an

ntensified binding of titanium (formation of biotite and ilmenite) during he earlier phases of the magmatic activity, in consequence of which the ater phases (pegmatites) became impoverished with respect to this elenent.

3. The granites of the main facies of the first phase, preponderant n the granite body and, at the same time, least affected by the assimilaion, are characterized by their average content of TiO_2 which is very lose to the granite averages reported by R. A. Daly and A. P. Vinoradov.

In conclusion, the author gives his sincere thanks to L. M. Rodionova nd L. P. Timokhova for their aid in his work.

Received for publication
November 15, 1957

REFERENCES

Daly, R. A. *Izverzhennye Porody i Glubiny Zemli* (Igneous rocks and depths of the earth). L.-M. 1936. (English edition, 1933).

Vinogradov, A. P. *Zakonomernost: Raspredeleniya Khimicheskikh Elementov v Zemnoi Kore* (Regularities in the distribution of chemical elements in the earth's crust). Geokhimiya, No. 1, p. 6-52, 1956.

Fersman, A. E. *Pegmatity* (Pegmatites). Leningrad. 1932.

Ginzburg, A. I. In Razvedka Nedr, No. 2, 1952.

Eliseev, N. A. *Petrografiya Rudnogo Altaya i Kalby* (Petrography of Rudnyi Altai and Kalba) Izd. Akad. Nauk SSSR, 1938.

Koptev-Dvornikov, V. S. *K Voprosu o Nekotoryh Zakonomernostyakh Formirovannya Intruzivnykh Kompleksov Granitoidov (na primere Tzentral'nogo Kazakhstana)* (On the subject of certain regularities in the formation of intrusive granitoid complexes (with the example of Central Kazakhstan)). Izv. Akad. Nauk SSSR, Ser. Geol. No. 7, 1952.

Ponomarev, A. I. *Metody Khimicheskogo Analiza Mineralov i Gornykh Porod* (Methods of chemical analysis of minerals and rocks). t. I, 1951; t. II, 1955.

Kupletskii, B. M. *Kolichestvenno-Mineralogicheskii Sostav Granitoidov* (Quantitative mineralogical composition of granitoids). Vopr. Petrogr. i Mineralog. t. I, Akad. Nauk SSSR, 1953.

Shavlo, S. G. *K Geologii Pegmatitov i Gidrotermalitov Kalba-Narymskogo Raiona* (In reference to geology of pegmatites and hydrothermaliths of the Kalba-Narym District) *Trudy Altaiskogo Gorno-Metallurgicheskogo Nauchno-Issledo-vatel'skogo Instituta* (Transactions of the Altai Research Institute of Mining and Metallurgy). t. 3, Akad. Nauk KazSSR, 1956.

Znamenskii, E. B. *O Raspredelenii Titana v Granitakh* (About distribution of titanium in granites). Geokhimiya, No. 2, 1957.

EDITOR'S NOTE:

Comparison of a mafic extrusive series (A) and a calc-alkaline plutonic intrusive series (B) with Znamenskii's data (C) shows a similar trend in late fractionation stages.

Ti ppm

(A) Skaergaard extrusives Wager and Mitchell (1951, Table F)		(B) Caledonian intrusives Nockolds and Mitchell (1948, Table II)		(C) Kalba granites (this paper)	
Earlier olivine gabbro (A')	3300	Ultramafic	4500	First phase	4800* 2000
Hypersthene olivine gabbro (B)	4700	Mafic	5000	Second phase	1500
Fayalite ferrogabbro (F)	14900	Intermediate	7000	Third phase	540
Average acid granophyre (I)	1900	Silicic	3000	Pegmatite	120

*High value because of probable shale assimilation.

The high capacity of biotite for Ti suggests that the valence state of Ti in granitic magma is four. It is tempting to speculate that a serial change in Ti mineralogy occurs with impoverishment of Ti in the melt. Highly silicic residuums would tend to crystallize out titanite in preference to ilmanite. Undersaturated sodic magmas, on the other hand, would preferentially yield melanite and astrophyllite (Goldschmidt, 1954, 417-418).

Goldschmidt, V. M., 1954, Geochemistry: Oxford, Clarendon Press, 730 pages.

Nockolds, S. R. and Mitchell, R. L., 1948. The geochemistry of some Caledonian plutonic rocks: A study in the relationship between the major and trace elements of igneous rocks and their minerals: Trans. Roy. Soc. Edinburgh, v. 61, 533-575.

Wager, L. R. and Mitchell, R. L., 1951. The distribution of trace elements during strong fractionation of basic magma - a further study of the Skaergaard intrusion, East Greenland: Geochim. Cosmochim. Acta. v. 1, 129-208.

(J. G.)

CHRONICLE

International Conference on Interplanetary Substance

The International Conference on Interplanetary Substance took place in Jena, German Democratic Republic, on October 7-12, 1957. The Conference was organized by the German Academy of Sciences. Representatives of 11 countries participated in the Conference: England, Bulgaria, Hungary, German Democratic Republic, Holland, China, Poland, Rumania, Soviet Union, Federated Republic of Germany, and Czechoslovakia. The total number of participants in the sessions was up to 100. The Soviet Delegation was represented as follows:

E. L. Krinov, Scientific Secretary, Committee on Meteorites, Academy of Sciences, U.S.S.R.; L. G. Kvasha, Senior Scientific Associate, the same Committee, and V. S. Safronov, Senior Scientific Associate of the Institute of Physics of the Earth, Academy of Sciences, U.S.S.R.

The Conference was directed by Prof. K. Hoffmeister, Director of the Sonnenberg Astronomic Observatory, with the participation of Prof. F. Heide, Director of Mineralogic Institute, University of Jena, and Dr. I. Hoppe, Dozent of the Institute of Astrophysics of the same University.

This was the first conference in the history of science embracing a wide range of problems, from purely astronomic to mineralogic-geochemical; all of which have a bearing on the highly complex problem of interplanetary substance: zodiacal light and the counter-luminescence, comets, meteors, meteorites. This serves to explain the nature of the Conference in which astronomers, mineralogists, and geochemists took their parts and where they all listened, with equal interest, to all of the reports.

Thirty papers were presented at the Conference, 10 of which were by members of the Soviet delegation, as follows:

Akad. V. G. Fesenkov - On the northern zodiacal light
Akad. V. G. Fesenkov - On the air wave caused by the fall of the Tunguska Meteorite in 1908*
E. L. Krinov - The Tunguska Meteorite
E. L. Krinov - On the mechanisms of destruction of meteoritic bodies in the atmosphere and on their original forms
L. G. Kvasha - On certain types of stony meteorites
B. Yu. Levin - A contribution to the history of variation studies of the numbers of meteors
B. Yu. Levin - On origins of comets and meteorites
Acad. A. P. Vinogradov, I. K. Zadorozhnyi, and K. P. Florenskii - The content of inert gases in the Iron Meteorite Sikhote-Alin'†

---

* This meteorite fell in the basin of Podkamennaya Tunguska (river) at 7 a.m., June 30, 1908. VPS

† A report under the same title was published in Geokhimiya (6) 1957.

N. N. Pariiskii and L. M. Gindilis - Investigation of luminescence of the Green Line 5577 within the counter-luminescence area of nocturnal sky

I. S. Shklovskii - The state of ionization of interplanetary gas and its importance in certain geophysical problems

The following gifts were transmitted by the Soviet Delegation, on behalf of the Academy of Sciences, USSR:

To the German Academy of Sciences - two specimens of the Sikhote-Alin' iron meteoritic shower weighing 9.3 and 8.0 kilograms.

To the Mineralogic Institute of the University of Jena - five specimens of stony meteorites from USSR (chondrites), with the total weight of 379 grams.

To the Institute of Astrophysics, same University - a specimen of meteoric and meteoritic dust from the site of the Sikhote-Alin' meteoritic shower fall.

On the motion by Prof. K. Hoffmeister, the Conference accepted the resolution to publish all of the presented reports in special issues of the following journals: the astronomical subjects - in *Die Sterne*, and the reports on composition of meteorites - in *Chemie der Erde*. Thus everyone who is interested in these topics may have the opportunity to see the full text of the reports.

Interesting and worthwhile excursions to Potsdam, Babelsberg, and Sonnenberg Astronomical Observatories and to the optical and the astronomic plants of the K. Zeiss Enterprises, as well as to certain historic monuments of Weimar were organized for the members of the Conference.

It should be pointed out that, throughout the time of the Conference, the relationships between its participants were warm and friendly and that the entire work of the Conference was in a healthy and businesslike atmosphere.

E. L. Krinov

Geokhimiya began publication in 1956 under the able editorship of A. P. Vinogradov. It is the Soviet counterpart of *Geochimica et Cosmochimica Acta,* having practically identical fields of interest and coverage and publishing approximately the same number of pages per year. With the great increase in geochemical research in the U.S.S.R., there have come into being a variety of highly specialized journals in geochemistry and related fields. It is probably better to begin translating this more general journal first and follow with some of the more specialized ones if interest appears to justify this course of action and if the financial arrangements can be made. It is hoped that there will be sufficient interest in this journal to justify translation and publication (as complete volumes) of the issues for 1957 and 1956. If individuals and organizations who would purchase such translations will write to one of the Editors, the work will be undertaken when enough expressions of interest have been received to justify the expense involved. Prices presumably would be approximately the same as for the 1958 issues.

The National Science Foundation has been most cooperative in this venture. They not only indicated willingness to back it financially but also helped in calculating probable costs and possible subscription income during the first year. It is on these figures, and those for advertising and administration, that the grant is based. It is a pleasure to acknowledge here the advice, assistance and support of the National Science Foundation.

The translation has been done by Dr. V. P. Sokoloff of the U.S. Bureau of Mines. The abstracts are those that appeared with the original articles except where the transliteration was not consistent with the system used in the translation or where minor changes were required for the sake of clarity.

Earl Ingerson
Translation Editor

In matters of subscription for Geokhimiya refer to: Moskva K-104, Pushkinsakaya, 23, Akademkniga. Chief Editor: A. P. Vinogradov. Editorial Council: V. I. Baranov, K. A. Vlasov, V. I. Gerasimovskii, D. S. Korzhinskii, A. A. Saukov, N. I. Khitrov (Responsible Secretary), V. V. Scherbina (Deputy Chief Editor).

Geochemical News is an informal news letter published by the Geochemical Society and sent without charge to all of its members. It contains news of the activities of the Society, such as summaries of Council Meetings, reports of committees and plans for the future. It also includes announcements of forthcoming meetings and symposia of interest to geochemists, personalia, announcements or short reviews of books of geochemical interest, information on translations and translation services, letters and short notes by members, etc.

Thus far it has not been possible to publish *Geochemical News* on a regular schedule, but it is hoped that this can be done in the near future.

Subscriptions are available to institutions at $2.00 per year. Orders should be sent to the Treasurer:

Dr. George T. Faust
U.S. Geological Survey
Washington 25, D.C.

Individuals who wish to receive the *News* should join the Geochemical Society. Application blanks are available on request from the Treasurer. Dues are $2.00 per year.

Geochimica et Cosmochimica Acta is the official journal of the Geochemical Society. It is an international journal interested in the broad aspects of geochemistry, both geographically and subject-wise; articles have been received from contributors from all of the (inhabited) continents.

New chemical data and interpretations involving chemical principles are emphasized. For example, papers in chemical mineralogy, petrology, oceanography and volcanology are acceptable, as are those in the chemistry of meteorites, whereas it would be suggested that those in descriptive mineralogy and volcanology, petrography, physical and biological oceanography and physical meteorites, be sent to other journals specializing in these subjects.

Thus, the subject coverage is closely similar to that of *Geokhimiya*. Also, the number of pages published per year is of the same order of magnitude. Subscription prices are as follows:

To members of the Geochemical Society--$10.00 per year
To other individual subscribers----------$20.00 per year
To libraries, laboratories, and other institutional subscribers
----------$46.50 per year

Orders for subscriptions should be sent to:

Pergamon Press
122 E. 55th Street
New York 19, N. Y.

OR

Pergamon Press, Ltd.
4 Fitzroy Square
London W.1, England